Supporting Information:

Ischemia in tumors induces early and sustained phosphorylation changes in stress kinase pathways but does not affect global protein levels

Philipp Mertins, Feng Yang, Tao Liu, DR Mani, Vladislav A. Petyuk, Michael A. Gillette, Karl R. Clauser, Jana W. Qiao, Marina A. Gritsenko, Ronald J. Moore, Douglas A. Levine, Reid Townsend, Petra Erdmann-Gilmore, Jacqueline E. Snider, Sherri R. Davies, Kelly V. Ruggles, David Fenyo, R. Thomas Kitchens, Shunqiang Li, Narciso Olvera, Fanny Dao, Henry Rodriguez, Daniel W. Chan, Daniel Liebler, Forest White, Karin D. Rodland, Gordon B. Mills, Richard D. Smith, Amanda G. Paulovich, Matthew Ellis and Steven A. Carr

On behalf of the Clinical Proteomic Tumor Analysis Consortium (CPTAC)

SI Materials and Methods:

Preparation of ovarian tumor samples for proteomic analysis:

After obtaining consent to IRB-approved protocols, tissue was collected from four patients with high-grade serous ovarian carcinoma. Each patient was under general anesthesia and had a large midline vertical incision that identified advanced disease (FIGO stage IIIC or IV). Prior to performing primary tumor resection and before any compromise to vascular supply, a portion of ovarian tumor attached to the omentum was rapidly resected using sharp or blunt dissection. The tumor specimen was immediately dissected into four contiguous and adjacent specimens strips each no larger than 10 x 3 x 3 mm. Tumor strips were placed into cryovials and frozen in liquid nitrogen at specified time points. The first specimen was processed as quickly as possible with an elapsed time from resection to freezing of 1 minute or less. The average weight of all tumor specimens was 215 mg. All specimens were then stored at -80 ˚C freezers until shipment to a central processing facility as described below. For pathology review, sections were obtained after the first and third section (0 and 30 min time points) for assessment of tumor content. Each tumor section evaluated contained 80% tumor cell nuclei or greater.

Generation and preparation of xenograft tumor samples for proteomic analysis:

Patient-derived xenograft tumors (PDX tumors) from established basal (WHIM6) and luminal (WHIM20) breast cancer subtypes were raised subcutaneously in 8 week old NOD.Cg-*Prkdc*^{scid} *Il2rg*^{tm1Wjl}/SzJ mice (Jackson Labs, Bar Harbor, Maine) as previously described (22, 23). Tumors from each animal were harvested by surgical excision at approximately 1.5 cm^3, rapidly divided into 4 pieces, and snap-frozen by immersion in a liquid nitrogen bath at times 0 (~ 30 s), 5, 30 and 60 minutes post-excision. The snap frozen tumor tissues for individual time points were then placed in pre-cooled tubes on dry ice and stored at -80 ^{o}C until cryopulverization. Three time course sets from multiple mice (n) were obtained as biological replicates (BR) of both luminal and basal subtypes: basal (BA1 (n=6); BA2 (n=5); BA3 (n=6)) and luminal (LU1 (n=10); Lu2 (n=6); Lu3 (n=6).

Processing of ovarian cancer tumor samples and breast cancer PDX tumor samples by cryopulverization was done centrally at Washington University, St. Louis (Ellis Lab). Tumor pieces were transferred into pre-cooled Covaris Tissue-Tube 1 Extra (TT01xt) bags (Covaris #520007) and processed in a Covaris CP02 Cryoprep device using different impact settings according to the total tumor tissue weight: <250mg=3; 250-350 mg=4; 350-440 mg=5; 440-550 mg=6 . Tissue powder was transferred to an aluminum weighing dish (VWR #1131-436) and the tissue was thoroughly mixed with a metal spatula precooled in liquid nitrogen. The tissue powder was then partitioned (~ 100 mg aliquots) into precooled cryovials (Corning #430487). (Note: Cryopulverized tissue will melt if transferred to a plastic weighing boat). All procedures were carried out on dry ice to maintain tissue in a powdered, frozen state.

RPPA Analysis:

Protein expression or phosphorylation was measured by reverse phase protein arrays (RPPAs) as previously described (9). All Tissue-Tubes were rinsed with 60 µl RPPA Lysis buffer containing: 1 % Triton X-100, 50mM HEPES, pH 7.4, 150 mM NaCl, 1.5 mM MgCl2, 1 mM EGTA, 100 mM NaF, 10 mM Na pyrophosphate, 1 mM Na_3VO_4, 10 % glycerol, containing freshly added protease and phosphatase inhibitors from Roche Applied Science (Cat. # 05056489001 and 04906837001). Samples were extracted using the Barocycler NEP3229 (Pressure Biosciences, Inc.) with the following settings: 35 Kpsi for 30 seconds, then 20 seconds at ambient pressure for 20 cycles. Samples were transferred to a 0.5 mL Eppendorf tube and centrifuged at 16K rcf for 5 minutes to remove particulates. The supernatant was transferred into a new 0.5 mL Eppendorf tube and the protein concentration determined by Advanced protein assay kit (Cytoskeleton, Inc, Denver, Co) on a Biotek Synergy H1M at 590 nm. Samples were adjusted to a final protein concentration of 1-1.5 mg/mL by the addition of RPPA Lysis buffer before the addition of 4X SDS sample buffer without Bromophenol Blue (3 parts of cell lysate plus one part of 4X SDS sample buffer). Samples were boiled for 5 minutes before printing onto nitrocellulose-coated glass slides (FAST Slides, Schleicher & Schuell BioScience, Inc., Keene, NH) with an automated Aushon arrayer (Aushon Biosystems, Burlington, MA) as previously described (42). The 3,3'-diaminobenzidine tetrachloride (DAB)-based DAKO signal amplification system (DAKO, Copenhagen, Denmark) was used to detect and amplify antibody-binding intensity. A biotinylated secondary antibody was used as a starting point for signal amplification. Signal intensity was measured by scanning the slides and quantifying with MicroVigene software (VigeneTech Inc., Carlisle, MA) to generate spot level signal intensity data. The protein concentration levels in the samples were estimated using Supercurve (version 1.5.0) developed by the Department of Bioinfomatics and Computational Biology at the University of Texas MD Anderson Cancer Center, "http://bioinformatics.mdanderson.org/OOMPA"). The program fits a single non-decreasing spline curve using all the dilution series on a slide (hence the name "SuperCurve") with the signal intensity as the response variable and the dilution steps as independent variable (43) to estimate some basic parameters and then estimate the IC50 of each dilution series. All data were then normalized for protein loading by linear transformation using the median expression level across all antibody experiments followed by a Log2 transformation. A total of 40

phosphorylation-site specific antibodies and 87 protein specific antibodies were used in this study for RPPA measurements across all different tumor types (see Table S3).

Protein extraction, digestion, labeling and MS analysis of peptides from patient-derived ovarian tumors (Pacific Northwest National Laboratories)

Protein extraction, digestion and labeling of peptides: The pulverized human ovarian cancer tissue samples (~50 mg tissue weight) were homogenized in 500 µl lysis buffer containing 8 M urea, 75 mM NaCl in 100mM NH_4HCO_3 (pH 7.8), 10 mM NaF, phosphatase inhibitor cocktail 2 (Sigma, P 5726) and cocktail 3 (Sigma, P0044), Complete (Roche, 05 892 791 001). Lysates were precleared by centrifugation at 16,500 g for 5 min and protein concentrations were determined by BCA assay (Pierce). Proteins were reduced with 5 mM dithiothreitol for 1 h at 37°C, and were subsequently alkylated with 10 mM iodoacetamide. Samples were diluted 2-fold with 50 mM NH_4HCO_3 and digested with trypsin (Promega, V5113) at a ratio of 1:50 trypsin:protein (w/w) for 4 h at 37°C, diluted by 4-fold, and subjected to a second treatment with trypsin and incubation at room temperature overnight (~16 h). The digest was acidified with trifluoroacetic acid (TFA) to pH ~2.5. Tryptic peptides were desalted on reversed phase C18 SPE columns (SUPELCO Discovery, 50 mg, 52601-U) and dried using SpeedVac.

Desalted peptides were labeled with 4-plex iTRAQ reagents according to the manufacturer's instructions (AB Sciex, Foster City, CA). For 500 µg peptide from each ovarian cancer time point sample, 5 units of labeling reagent were used. Peptides were dissolved in 150 µL of 0.5 M triethylammonium bicarbonate (TEAB) (pH 8.5) solution and labeling reagent was added in 350 µL of ethanol. After 1 h incubation, 1.5 mL of 0.05% TFA was added to stop the reaction and hydrolyze the unreacted iTRAQ reagents. Differentially labeled peptides were mixed and subsequently desalted on 50 mg C18 SPE columns.

Offline fractionation of peptides and preparation of proteome and phosphoproteome samples:

iTRAQ-labeled peptides from ovarian tissues were separated on a RP XBridge C18 column from Waters (250 mm × 4.6 mm column containing 5 µM particles and a 4.6 mm × 20 mm guard column) using Agilent 1200 HPLC System. The sample loaded onto the C18 column was washed for 9 min with 5% of solvent B (10 mM TEAB, pH 7.5, 90% ACN), followed by 10 min solvent A (10 mM TEAB, pH 7.5) equilibration before an 109 min LC gradient. The LC gradient started with a linear increase of solvent A to 10% B in 3 min, then linearly increased to 30% B in 86 min, 10 min to 42.5% B, 5 min to 55% B and another 5 min to 100% solvent B. The flow rate was 0.5 mL/min. A total of 96 fractions were collected into a 96 well plate through the LC gradient. The high pH RP fractions were combined into 24 fractions using the concatenation strategy reported in our previous study (24). For proteome analysis, ~ 5% of each concatenated fraction was dried down and re-suspended in 0.1% TFA to a peptide concentration of 0.15 µg /µL. The rest of the concatenated fractions (95%) were further concatenated into 12 fractions and subjected to immobilized metal affinity chromatography (IMAC) for phosphopeptide enrichment. Magnetic Fe^{3+}-NTA-agarose beads were prepared using the Ni-NTA-agarose beads (Qiagen, Valencia, CA,) following the protocols reported (44, 45). Briefly, peptides (~100-

150 µg) were reconstituted in 300 µL IMAC binding/wash buffer (80% MeCN, 0.1% TFA) and incubated for 30 min with 75 µL of the 5% bead suspension. After incubation, the beads were washed 4 times each with 300 µL of wash buffer. Phosphorylated peptides were eluted from the beads using 50-75 µL of 1:1 ratio of acetonitrile to 2.5 % ammonia in 2 mM (pH 8) phosphate buffer (v/v) after incubating for 1.5 min. Samples were acidified and concentrated, then were reconstituted to 30 µL with 0.1% TFA for LC-MS/MS analysis.

Mass-spectrometry based analysis of ovarian tumor samples:

All peptide samples were analyzed using an automated home-built constant flow nano LC system (Agilent) coupled to an LTQ Orbitrap Velos mass spectrometer (Thermo Fisher Scientific). Electrospray emitters were custom made using either 360 µm o.d. (phosphoproteomics) or 150 µm (global proteomics) o.d. x 20 µm i.d. chemically etched fused silica (46). The nano LC system for phosphoproteomics analysis has an online 4-cm x 360 µm o.d. x 150 µm i.d. C18 SPE column (5-µm Jupiter C18, Phenomenex, Torrence, CA) to desalt each phosphopeptide sample (20 µL), which is connected to a home-made 60-cm x 360 µm o.d. x 50 µm i.d. capillary column (3-µm Jupiter C18, Phenomenex, Torrence, CA). Mobile phase flow rate was 100 nL/min and consisted of 0.1M acetic acid in water (A) and 0.1M acetic acid in 70:30 (v/v) acetonitrile:water (B) with a gradient profile as follows (min:%B); 0:0, 5:10, 140:35, 160:60, 165:90, 170:90. For global proteome analysis, an on-line 4-cm x 360 µm o.d. x 150 µm i.d. SPE column packed with 3.6-µm Aeris Widepore XB-C18 and a 35-cm x 360 µm o.d. x 75 µm i.d. fused-silica capillary analytical column (3 µm Jupiter C18) were used. Mobile phases consisted of 0.1% formic acid in water (A) and 0.1% formic acid acetonitrile (B) operated at 300 nL/min with a gradient profile as follows (min:%B); 0:5, 2:8, 20:12, 75:35, 97:60, 100: 85.

The LTQ Orbitrap Velos mass spectrometer was operated in the data-dependent mode acquiring higher-energy collisional dissociation (HCD) scans (R=7,500, 5×10^4 target ions) after each full MS scan (R=30,000, 3×10^6 target ions) for the top ten most abundant ions within the mass range of 300 to 1800 *m*/*z*. An isolation window of 2.5 Th was used to isolate ions prior to HCD. All HCD scans used a normalized collision energy of 45 and a maximum inject time of 1000 ms. The dynamic exclusion time was set to 60 s and charge state screening was enabled to reject unassigned and singly charged ions.

Protein extraction, digestion, labeling and MS analysis of peptides from PDX breast cancer tumors (Broad Institute)

Protein extraction, digestion and iTRAQ labeling of peptides:

Cryopulverized xenograft breast cancer tissues (~75 mg tissue weight) were homogenized in 1000 µL lysis buffer containing 8M urea, 75mM NaCl, 1mM EDTA in 50mM Tris HCl (pH 8), 10 mM NaF, phosphatase inhibitor cocktail 2 (1:100; Sigma, P5726) and cocktail 3 (1:100; Sigma, P0044), 2 µg/mL aprotinin (Sigma, A6103), 10 µg/mL Leupeptin (Roche, #11017101001), and 1 mM PMSF (Sigma, 78830). Lysates were centrifuged at 20,000 g for 10 minutes before measuring protein concentration of the clarified lysates by BCA assay (Pierce). Protein lysates were subsequently reduced with 5 mM dithiothreitol (Thermo Scientific, 20291) for 45 minutes at

room temperature, and alkylated with 10 mM iodoacetamide (Sigma, A3221) for 45 minutes. Samples were diluted 4-fold with 50mM Tris HCl (pH 8) prior to digesting them with trypsin (Promega, V511X) at a 1:50 enzyme-to-protein ratio at room temperature overnight on a shaker.

Digested samples were acidified with formic acid (FA; Fluka, 56302) to a final volumetric concentration of 1 % or final pH of ~3-5, and centrifuged at 2,000 g for 5 minutes to clear precipitated urea from peptide lysates. Samples were desalted on tC18 SepPak columns (Waters, 100mg, WAT036820) and 1.5 mg peptide aliquots were dried down using a SpeedVac apparatus.

Desalted peptides were labeled with 4-plex iTRAQ reagents as directed by the manufacturer (AB Sciex, Foster City, CA), where 15 units of labeling reagent were used for each time-point sample. Samples were dissolved in 450uL 0.5M triethylammonium bicarbonate (TEAB; pH 8.5), 15 iTRAQ label units were diluted with ethanol to a final volume of 1.05 mL and immediately added to the peptide sample. After 1 hour, iTRAQ labeling reactions were quenched with 225 µL Tris HCl (pH 8.0). Differently labeled peptides were then mixed to generate a 4-plex iTRAQ sample, and desalted on 500mg tC18 SepPak columns (Waters, 500mg, WAT036790).

Offline fractionation of peptides and preparation of proteome and phosphoproteome samples:

Desalted 4-plex iTRAQ labeled peptides were reconstituted in 900 µL 20mM ammonium formate (pH 10), loaded on a 4.6mm x 250mm column RP Zorbax 300 A ExtendC18 column (Agilent, 3.5 µm bead size), and separated on an Agilent 1100 Series HPLC instrument by basic reversed-phase chromatography. Solvent A (2% acetonitrile, 5 mM ammonium formate, pH 10) and a nonlinear increasing concentration of solvent B (90% acetonitrile, 5 mM ammonium formate, pH 10) were used to separate peptides according to their hydrophobicity. Prior to loading samples, the C18 column was washed for 70 minutes using an LC gradient consisting of two solvent A-to-solvent B washing cycles. The 90 minute separation LC gradient began with 100% solvent A for 9 minutes, then a linear increase in percentage of solvent B to 6% in 4 min, 6% to 28.5% in 50 min, 28.5% to 34% in 5.5 min, 34% to 60% in 13 min, and another 8.5 min at 60% solvent B. The flow rate was 1 mL/min. A total of 84 fractions were collected into a 96 x 2mL well plates (Whatman, #7701-5200), which were combined in a step-wise concatenation strategy as reported previously (24). 5% of the volume of each proteome fraction was allocated for proteome analysis, dried down, and re-suspended in 3% MeCN/0.1% FA to a peptide concentration of 1 µg/uL for LC-MS/MS. The remaining 95% of concatenated fractions were further combined into 12 fractions that were enriched for phosphopeptides using immobilized metal affinity chromatography (IMAC). Ni-NTA agarose beads were used to prepare Fe^{3+}-NTA-agarose beads, following a method adapted from Ficarro et al. (44). In each phosphoproteome fraction, ~500 µg peptides were reconstituted in 1,000 µL 50% MeCN/0.1% TFA solvent and incubated with 10 µL of the IMAC beads for 30 minutes. After incubation, samples were briefly spun down on a tabletop centrifuge, and the clarified peptide flow-through was separated from the beads, and the beads were reconstituted in 150 µL IMAC binding/wash buffer (80 MeCN/0.1% TFA) and loaded on equilibrated Empore C18 silica-packed stage tips (3M, 2315) as described in a previous publication (14). Samples were then washed twice with 50 µL of IMAC binding/wash buffer, once with 100uL 1% FA, then eluted from the IMAC beads to the stage tips with 3 x 70uL washes of 500mM dibasic sodium phosphate (pH 7.0, Sigma S9763). Stage tips were washed once with 100 µL 1%FA and eluted from the stage tips with 60uL 50%

MeCN/0.1% FA. Phosphopeptides were dried down and re-suspended in 9 µL 50% MeCN/0.1%FA for LC-MS/MS analysis.

Mass-spectrometry based analysis of tumor samples

All peptides were separated with an online nanoflow EASY-nLC 1000 UHPLC system (Proxeon, Thermo Fisher Scientific) and analyzed on a benchtop Orbitrap Q Exactive mass spectrometer (Thermo Fisher Scientific) equipped with a nanoflow ionization source (James A. Hill Instrument Services, Arlington, MA). The LC system was connected to a custom-fit tee (360 µm, IDEX Health & Science, UH-753), and columns were heated to 50 ^{o}C using column heater sleeves (Phoenix-ST) to prevent overpressurizing of columns during UHPLC separation. As the implemented IMAC enrichment procedure included an integrated desalting step, phosphoproteome samples were directly loaded onto the nano LC system for analysis. 10% of each global proteome sample, and 50% of each phosphoproteome sample were injected onto an in-house packed 20cm x 75um dia. C18 silica picofrit capillary column (1.9 µm ReproSil-Pur C18-AQ medium, Dr. Maisch GmbH, r119.aq; Picofrit 10um tip opening, New Objective, PF360-75-10-N-5). Mobile phase flow rate was 200 nL/min, comprised of 3% acetonitrile/0.1% formic acid (Solvent A) and 90% acetonitrile /0.1% formic acid (Solvent B), and the 150-minute LC-MS/MS method consisted of a 10-min column-equilibration procedure, 20-min sample-loading procedure, and the following gradient profile: (min:%B) 0:0; 2:6; 84:30; 87:60; 90;90; 105:90; 106:50; 120:50 (last two steps at 500 nL/min flowrate). Data-dependent acquisition was performed using Xcalibur 2.2 software in positive ion mode at a spray voltage of 2.00 kV. MS1 Spectra were measured with a resolution of 70,000, an AGC target of 3e6 and a mass range from 300 to 1800 m/z. Up to 12 MS2 spectra per duty cycle were triggered at a resolution of 17,500, an AGC target of 5e4, an isolation window of 2.5 m/z, a maximum ion time of 120 msec, and a normalized collision energy of 28. Peptides that triggered MS2 scans were dynamically excluded from further MS2 scans for 20 sec. Charge state screening was enabled to reject precursor charge states that were unassigned, 1, or >6. Peptide match was enabled for monoisotopic precursor mass assignment.

All mass spectra, in the original instrument vendor format, contributing to this study may be downloaded from

https://cptac-data-portal.georgetown.edu/cptacPublic/ for the two study names: Time Course Breast Cancer (0,5,30,60) and Time Course Ovarian Cancer (0,5,30,60).

URLs with the web address for annotated MS2-spectra are provided for every identified phosphopeptide in Supplemental Table S2.

Protein identification, phosphosite localization, and quantification

All MS data for ovarian and breast cancer PDX samples were interpreted using the Spectrum Mill software package v4.1 beta (Agilent Technologies, Santa Clara, CA). Similar MS/MS spectra acquired on the same precursor m/z within +/- 60 sec were merged. MS/MS spectra were excluded from searching if they failed the quality filter by not having a sequence tag length > 0 (i.e., minimum of two masses separated by the in-chain mass of an amino acid) or did not have a precursor MH+ in the range of 750-4000. MS/MS spectra from PDX breast cancer

tumors were searched against a RefSeq v37 database containing 32,799 human proteins, 29,617 mouse proteins, and porcine trypsin. The mouse proteins were omitted from the database when searching the MS/MS spectra from human ovarian cancer tumors. Scoring parameters were ESI-QEXACTIVE-HCD-v2, or ESI-ORBITRAP-HCD-v2 for whole proteome datasets from PDX and ovarian tumors respectively. ESI-QEXACTIVE-HCD-v3 parameters were used for all phosphoproteome datasets. All spectra were allowed +/- 20 ppm mass tolerance for precursor and product ions, 40% minimum matched peak intensity, and trypsin allow P enzyme specificity with up to 4 missed cleavages. Carbamidomethylation at cysteine and iTRAQ at N-termini and lysine were fixed modifications. Allowed variable modifications for whole proteome samples were oxidized methionine, deamidation of asparagine, and pyro-glutamic acid modification at N-terminal glutamine with a precursor MH+ shift range of -18 to 64 Da. For phosphoproteome samples the allowed variable modifications for whole proteome samples were oxidized methionine, acetylation of protein N-termini, and phosphorylation of serine, threonine, and tyrosine with a precursor MH+ shift range of 0 to 272 Da. Identities interpreted for individual spectra were automatically designated as confidently assigned using the Spectrum Mill autovalidation module to apply target-decoy based false-discovery rate (FDR) scoring threshold criteria via a two-step auto threshold strategy at the spectral and protein levels. For phosphoproteome samples the second step was omitted. First, peptide mode was set to allow automatic variable range precursor mass filtering with score thresholds optimized to yield a spectral level FDR of <1.2% for each precursor charge state in each LC-MS/MS run. Second, protein mode was applied to further filter all the peptide-level validated spectra combined from all LC-MS/MS runs derived from a single tumor sample using a maximum protein-level FDR of zero. The protein level step filters the results so that each identified protein is comprised of multiple peptides unless a single excellent scoring peptide was the sole match. For the whole proteome samples the above criteria yielded false discovery rates (FDR) of <1.1% for each sample at the peptide-spectrum match level and <2.0 % at the distinct peptide level as estimated by target-decoy-based searches using reversed sequences. For the phosphoproteome samples the FDR was <1.1% at the spectrum level and <2.3% at the distinct peptide level.

In calculating scores at the protein level and reporting the identified proteins, redundancy is addressed in the following manner: the protein score is the sum of the scores of distinct peptides. A distinct peptide is the single highest scoring instance of a peptide detected through an MS/MS spectrum. MS/MS spectra for a particular peptide may have been recorded multiple times, (i.e. as different precursor charge states, in adjacent bRP fractions, modified by deamidation at Asn or oxidation of Met, or different phosphosite localization) but are still counted as a single distinct peptide. When a peptide sequence >8 residues long is contained in multiple protein entries in the sequence database, the proteins are grouped together and the highest scoring one and its accession number are reported. In some cases when the protein sequences are grouped in this manner there are distinct peptides which uniquely represent a lower scoring member of the group (isoforms, family members, and different species). Each of these instances spawns a subgroup and multiple subgroups are reported and counted towards the total number of proteins in SI Table S1. The reporting of peptides contributing to each subgroup can be altered by enabling the subgroup-specific option in Spectrum Mill. This was done for the whole proteome PDX datasets primarily to include only species-specific peptides

for quantification, and thus exclude peptides found in both the human and mouse proteomes. This approach allowed us to distinguish mouse from human orthologs. Interestingly, human versions of the plasma proteins ceruloplasmin and serotransferrin were observed in the basal xenograft breast cancer samples with 10 and 3 ortholog-specific peptides, respectively. None of these human proteins were observed in the luminal breast cancer tumors. Both proteins are not exclusively plasma-specific proteins and can be expressed also in non-blood related tissues and cells (see www.genecards.org). Since gene expression is often deregulated in cancer it is not entirely surprising to detect these proteins at low levels in the basal breast cancer samples.

For each of the phosphoproteome samples 55 to 59% of all identified phosphopeptide MS/MS spectra yield fully localized phosphosites. The phosphosite tables organized across all the samples combine into a single row all non-conflicting observations of a particular phosphosite (i.e. different missed cleavage forms, different precursor charges, confident and ambiguous localizations, different sample handling modfications). The peptide form with the best localization score becomes the displayed representative of the combination. For a single peptide neither observations with a different number of phosphosites nor different confident localizations are allowed to be combined. While the Spectrum Mill identification score is based on the number of matching peaks, their ion type assignment, and the relative height of unmatched peaks, the phosphosite localization score is the difference in identification score between the top two localizations. The score threshold for confident localization (>1.1), essentially corresponds to at least 1 b or y ion located between two candidate sites that has a peak height 10% of the tallest fragment ion (neutral losses of phosphate from the precursor and related ions as well as immonium and iTRAQ reporter ions are excluded from the relative height calculation). The ion type scores for b-H_3PO_4, y-H_3PO_4, b-H_2O, and y-H_2O ion types are all set to 0.5. This prevents inappropriate confident localization assignment when a spectrum lacks primary b or y ions between two possible sites but contains ions that can be assigned as either phosphate loss ions for one localization or water loss ions for another localization.

Relative abundances of proteins and phosphosites were determined using iTRAQ reporter ion intensity ratios from each MS/MS spectrum. The median ratio is calculated from all MS/MS spectra contributing to a protein subgroup in whole proteome samples or to a phosphosite in the phosphoproteome samples. To account for differences in total protein amount in between single time point samples within one iTRAQ 4-plex experiment, all iTRAQ time point ratios in the proteome as well as phosphoproteome datasets were normalized for the global population median in the corresponding proteome datasets. It is important to note that protein and phosphosite abundance ratios measured with iTRAQ quantification can be compressed by a factor of 20-30% due to co-isolation interference and that real effect sizes might be larger than what was measured (11, 47). In the final report of the phosphosite table only phosphosites are shown that have a positive maximum forward-reverse Spectrum Mill score across all experiments to remove reversed-decoy database hits. In addition only phosphosites are shown that contain iTRAQ ratio information for at least one experiment.

Kinetic model of statistical data analysis:

This model assumes that changes observed within a reasonably short period of time (1 hour at most) following perturbation (cold ischemia) can be described by the law of unidirectional chemical reaction (eq 1).

$$\log(Y) = \log(B + (A - B)e^{-kt}) + \varepsilon \quad \text{(eq 1)}$$

Where Y is the measured relative protein concentration or abundance, A – starting concentration, B – final concentration, k – rate constant, t – time and ε is the normally distributed measurement error. To infer the A, B and k parameters we applied constrained Nelder-Mead optimization that minimizes the sum of squared errors. The imposed constrains are along the lines of chemical kinetic principles. A > 0, B > 0 as the concentrations cannot be negative. k>0 since no species can be exponentially growing. The statistical significance of chemical kinetic model was tested against null hypothesis model that assumes that there is not any change in the data associated with timepoints (eq 2).

$$\log(Y) = \log(C) + \varepsilon \quad \text{(eq 2)}$$

Where C is the constant proteins abundance or concentration value. The fit of null hypothesis model is represented by a flat line. The statistical significance of the alternative model can be assessed using F-statistic that looks at the ratio of the sums of squared errors residuals taking into account the degrees of freedom of the alternative and null hypothesis models.

Statistical analysis using the moderated F-test:

Protein and phosphopeptide quantification tables from Spectrum Mill, with Log_2 ratios normalized as specified above, are used for the statistical analysis. Each cold ischemia time point is treated as an independent group in an ANOVA analysis, with statistical significance being assessed using an F-test based on the ratio of between group to within group variability. This allowed capturing trends that are not unidirectional. To leverage information across observed proteins or phosphopeptides for more robust estimation of variance, we employed an empirical Bayes approach implemented as a moderated F-test in the Bioconductor “limma” package (48). The resulting p-values were adjusted for multiple testing using the Benjamini-Hochberg method (49).

Supporting Information References:

42. Neeley ES, Baggerly KA, & Kornblau SM (2012) Surface Adjustment of Reverse Phase Protein Arrays using Positive Control Spots. *Cancer Inform* 11:77-86.
43. Hu J*, et al.* (2007) Non-parametric quantification of protein lysate arrays. *Bioinformatics* 23(15):1986-1994.
44. Ficarro SB*, et al.* (2009) Magnetic bead processor for rapid evaluation and optimization of parameters for phosphopeptide enrichment. *Anal Chem* 81(11):4566-4575.
45. Nguyen TH*, et al.* (2012) Quantitative phosphoproteomic analysis of soybean root hairs inoculated with Bradyrhizobium japonicum. *Mol Cell Proteomics* 11(11):1140-1155.
46. Kelly RT*, et al.* (2006) Chemically etched open tubular and monolithic emitters for nanoelectrospray ionization mass spectrometry. *Anal Chem* 78(22):7796-7801.
47. Ow SY*, et al.* (2009) iTRAQ underestimation in simple and complex mixtures: "the good, the bad and the ugly". *Journal of proteome research* 8(11):5347-5355.
48. Smyth GK (2004) Linear models and empirical bayes methods for assessing differential expression in microarray experiments. *Stat Appl Genet Mol Biol* 3:Article3.
49. Benjamini Y & Hochberg Y (1995) Controlling the False Discovery Rate: A Practical and Powerful Approach to Multiple Testing. *Journal of the Royal Statistical Society. Series B (Methodological)* 57(1):289-300.
50. Kelder T*, et al.* (2012) WikiPathways: building research communities on biological pathways. *Nucleic Acids Res* 40(Database issue):D1301-1307.
51. van Iersel MP*, et al.* (2008) Presenting and exploring biological pathways with PathVisio. *BMC Bioinformatics* 9:399.

Supporting Information Table legends:

Table S1: Lists of all quantified proteins in ovarian cancer, and luminal/basal breast cancer samples.

Table S2: Merged list of all quantified phosphorylation-sites in ovarian cancer, and luminal/basal breast cancer samples.

Table S3: Comparison of cold ischemia time point data for phosphorylation-sites and proteins analyzed by RPPA and mass spectrometry (ovarian, luminal/basal breast cancer). Tabs indicated with "pSTY" contain annotation and quantification information for MS and RPPA data for all three tumor types. Tabs indicated with "protein" contain the corresponding information for proteins analyzed by MS or RPPA.

Supporting Information Figure legends:

Figure S1: Comparison of moderated F test and first-order kinetic modeling as statistical tests to identify regulated phosphosites. Scatter plots showing the Benjamini-Hochberg corrected p-values for all quantified phosphosites. Axes are Log_{10} scale and dashed lines indicate a p-value of 0.01.

Figure S2: Inter-tumor differences in the kinetics of protein phosphorylation changes for kinases that were regulated by cold ischemia in all analyzed tumor types. Up-regulated (U1-3; panel A) and down-regulated (D1-3; panel B) fuzzy c-means clusters are shown for the global phosphoproteome data. T ½ denotes the median half activation/decrease time for all phosphosites in each cluster. Kinase phophosites with membership values $\alpha > 0.7$ are marked with “X” for ovarian cancer (OC) or basal-like (BA) and luminal (LU) breast cancers.

Figure S3: Hierarchical clustering of all phosphosites that were identified in all analyzed tumor types and also regulated in at least one of the tumor types. Phosphosites that were quantified in all tumors and for which a cold ischemia regulation p-value <0.01 was observed in at least one of the tumor types were analyzed by hierarchical clustering using Gene-E (http://www.broadinstitute.org/cancer/software/GENE-E). Phosphosite rows were clustered with an euclidean distance metric. A global color scheme was used to display phosphosite ratios.

Figure S4: Gene enrichment analysis of KEGG pathways enriched among cold-ischemia regulated phosphoproteins in ovarian tumors, basal-like or luminal breast tumors. We used DAVID Bioinformatics Resources 6.7 (http://david.abcc.ncifcrf.gov/) (39) to test for enrichment of KEGG pathways in the up- and down-regulated phosphoproteome for each cancer type using a modified Fisher’s exact test (EASE score). KEGG pathways with $p<0.01$ and a minimum occurrence of ≥10 genes/proteins were called significant. P-values were $–Log_{10}$ transformed and the transformed values for each pathway were plotted as a heat map in Gene-E (http://www.broadinstitute.org/cancer/software/GENE-E).

Figure S5: Regulated phosphoproteins in the JNK/p38 MAP kinase pathway. Phosphoproteins with at least one ischemia-regulated phosphosite in the ovarian or breast tumors were mapped onto a modified version of the WikiPathways MAPK signaling pathway (http://www.wikipathways.org/index.php/Pathway:WP382) (50) using PathVisio (www.pathvisio.org) (51).

Figure S6: Comparison of RPPA versus mass spectrometry for the small subset of overlapping phosphosites. Averaged cold ischemia time point ratios quantified by mass spectrometry (iTRAQ) or reversed-phase protein arrays (RPPA) were plotted for ovarian cancer and basal-like/luminal breast cancers. Pearson correlation coefficients (r) were calculated for each tumor type to compare quantification results obtained by mass spectrometry and RPPA.

Figure S7: Annotated MS2-spectra of phosphopeptides for all 158 commonly cold ischemia-regulated phosphosites. The highest scoring MS2 spectra for each phosphosite are shown.

Figure S1:

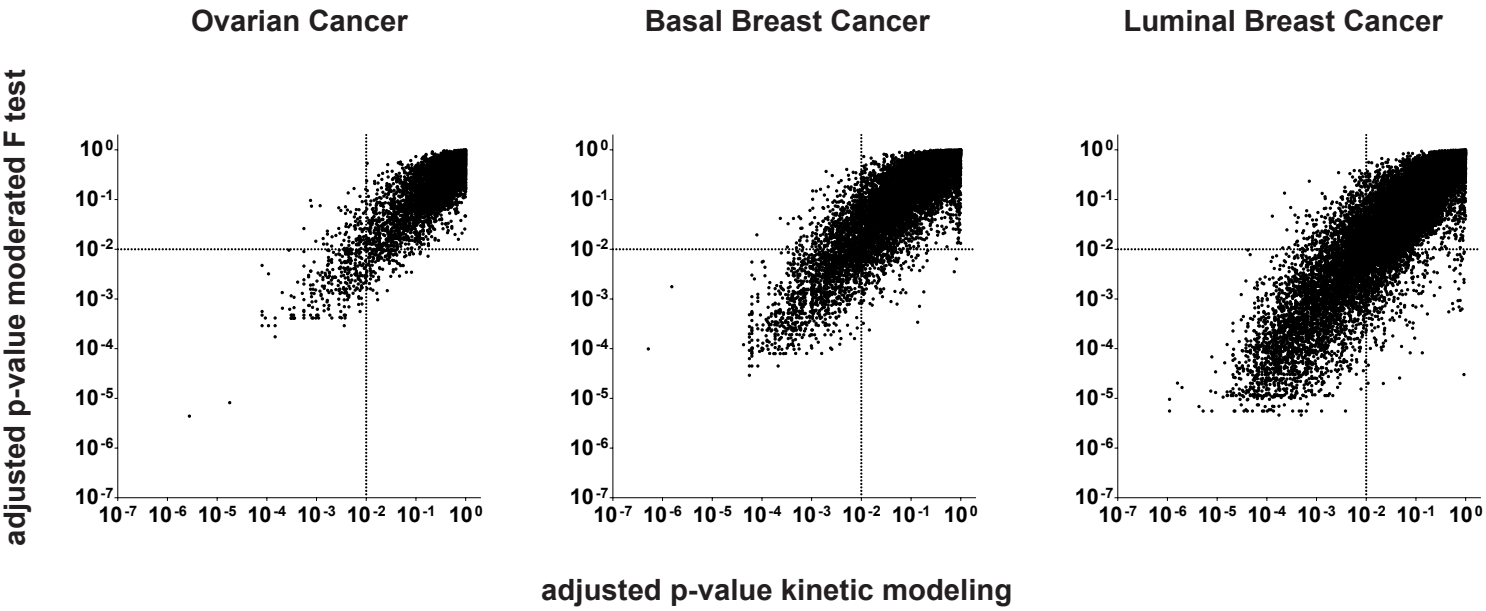
Ovarian Cancer
Basal Breast Cancer
Luminal Breast Cancer
adjusted p-value moderated F test
adjusted p-value kinetic modeling
10^0
10^-1
10^-2
10^-3
10^-4
10^-5
10^-6
10^-7

Figure S2:

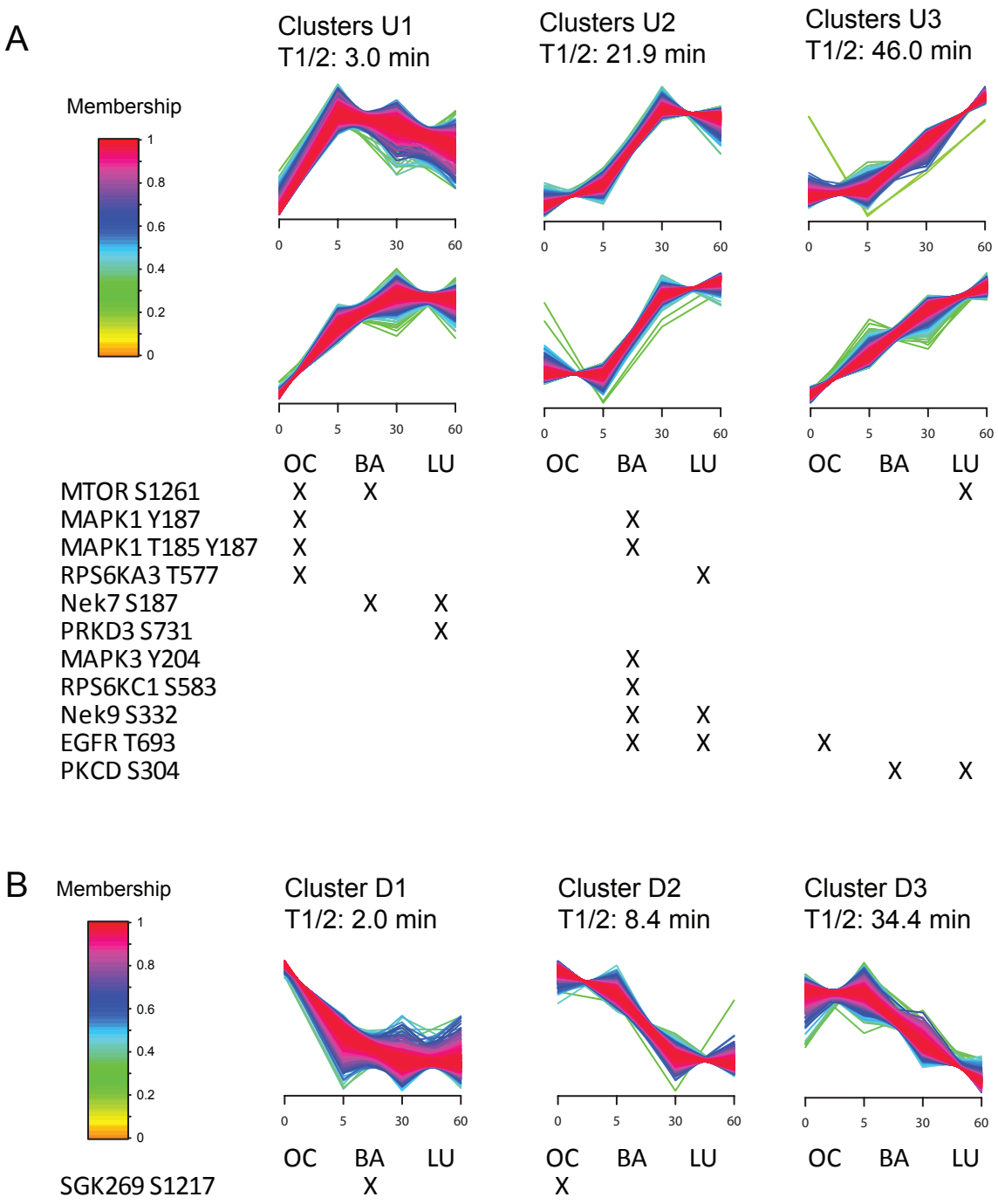
A
Membership
1
0.8
0.6
0.4
0.2
0
Clusters U1
T1/2: 3.0 min
Clusters U2
T1/2: 21.9 min
Clusters U3
T1/2: 46.0 min
0
5
30
60
OC
BA
LU
MTOR S1261
MAPK1 Y187
MAPK1 T185 Y187
RPS6KA3 T577
Nek7 S187
PRKD3 S731
MAPK3 Y204
RPS6KC1 S583
Nek9 S332
EGFR T693
PKCD S304
B
Membership
Cluster D1
T1/2: 2.0 min
Cluster D2
T1/2: 8.4 min
Cluster D3
T1/2: 34.4 min
SGK269 S1217

Figure S3:

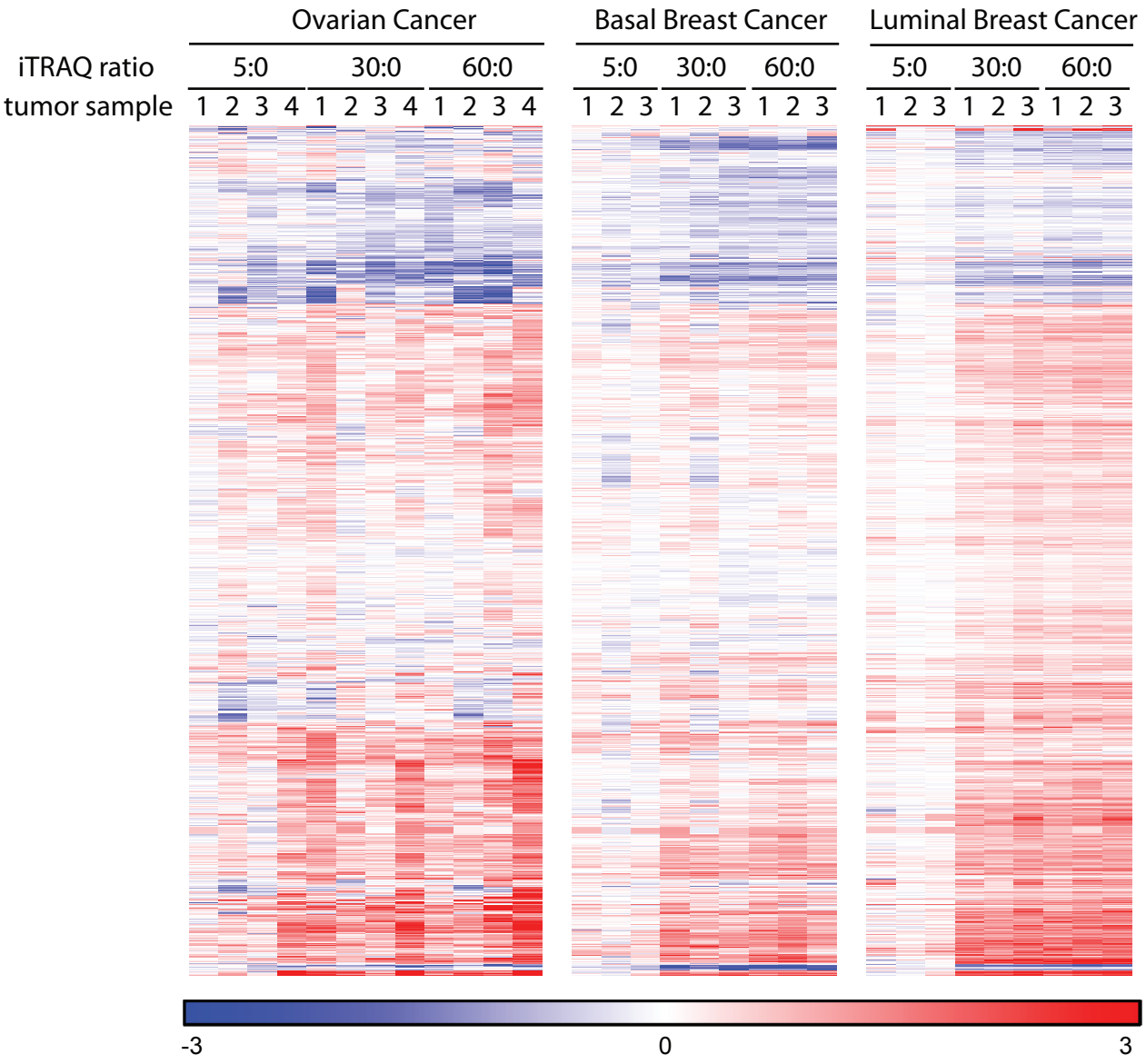
Ovarian Cancer
Basal Breast Cancer
Luminal Breast Cancer
iTRAQ ratio
5:0
30:0
60:0
tumor sample
1 2 3 4 1 2 3 4 1 2 3 4
1 2 3 1 2 3 1 2 3
1 2 3 1 2 3 1 2 3
-3
0
3

Figure S4:

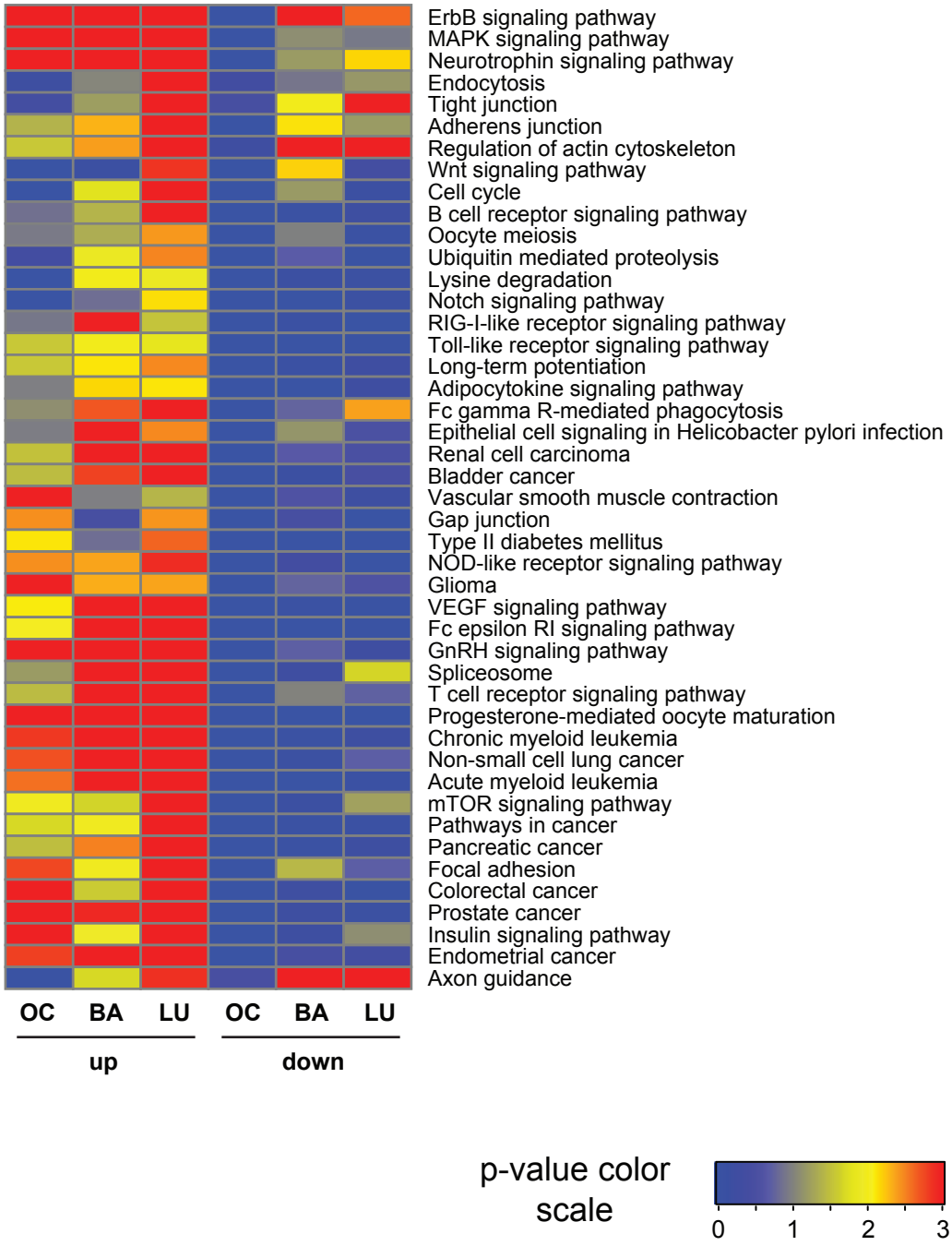
ErbB signaling pathway
MAPK signaling pathway
Neurotrophin signaling pathway
Endocytosis
Tight junction
Adherens junction
Regulation of actin cytoskeleton
Wnt signaling pathway
Cell cycle
B cell receptor signaling pathway
Oocyte meiosis
Ubiquitin mediated proteolysis
Lysine degradation
Notch signaling pathway
RIG-I-like receptor signaling pathway
Toll-like receptor signaling pathway
Long-term potentiation
Adipocytokine signaling pathway
Fc gamma R-mediated phagocytosis
Epithelial cell signaling in Helicobacter pylori infection
Renal cell carcinoma
Bladder cancer
Vascular smooth muscle contraction
Gap junction
Type II diabetes mellitus
NOD-like receptor signaling pathway
Glioma
VEGF signaling pathway
Fc epsilon RI signaling pathway
GnRH signaling pathway
Spliceosome
T cell receptor signaling pathway
Progesterone-mediated oocyte maturation
Chronic myeloid leukemia
Non-small cell lung cancer
Acute myeloid leukemia
mTOR signaling pathway
Pathways in cancer
Pancreatic cancer
Focal adhesion
Colorectal cancer
Prostate cancer
Insulin signaling pathway
Endometrial cancer
Axon guidance
OC BA LU OC BA LU
up
down
p-value color scale
0 1 2 3

Figure S5:

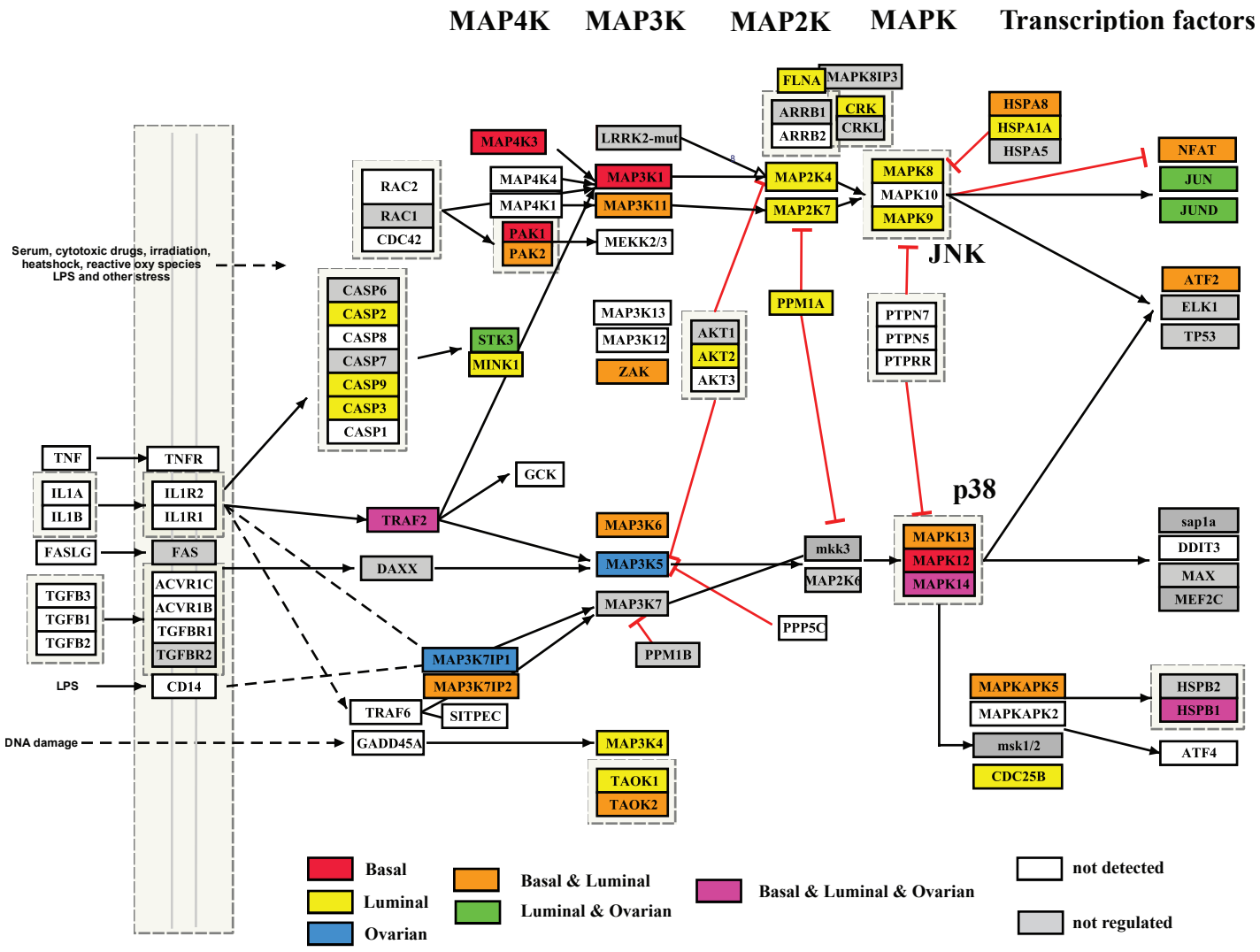
JNK & p38 MAP kinase pathway
MAP4K
MAP3K
MAP2K
MAPK
Transcription factors
Serum, cytotoxic drugs, irradiation, heatshock, reactive oxy species LPS and other stress
LPS
DNA damage
TNF
TNFR
IL1A
IL1B
IL1R2
IL1R1
FASLG
FAS
TGFB3
TGFB1
TGFB2
ACVR1C
ACVR1B
TGFBR1
TGFBR2
CD14
RAC2
RAC1
CDC42
CASP6
CASP2
CASP8
CASP7
CASP9
CASP3
CASP1
MAP4K3
MAP4K4
MAP4K1
PAK1
PAK2
STK3
MINK1
GCK
TRAF2
DAXX
TRAF6
GADD45A
MAP3K7IP1
MAP3K7IP2
SITPEC
LRRK2-mut
MAP3K1
MAP3K11
MEKK2/3
MAP3K13
MAP3K12
ZAK
MAP3K6
MAP3K5
MAP3K7
PPM1B
MAP3K4
TAOK1
TAOK2
FLNA
MAPK8IP3
ARRB1
ARRB2
CRK
CRKL
MAP2K4
MAP2K7
AKT1
AKT2
AKT3
PPM1A
PPP5C
mkk3
MAP2K6
MAPK8
MAPK10
MAPK9
JNK
PTPN7
PTPN5
PTPRR
p38
MAPK13
MAPK12
MAPK14
MAPKAPK5
MAPKAPK2
msk1/2
CDC25B
HSPA8
HSPA1A
HSPA5
NFAT
JUN
JUND
ATF2
ELK1
TP53
sap1a
DDIT3
MAX
MEF2C
HSPB2
HSPB1
ATF4
Basal
Luminal
Ovarian
Basal & Luminal
Luminal & Ovarian
Basal & Luminal & Ovarian
not detected
not regulated

Figure S6:

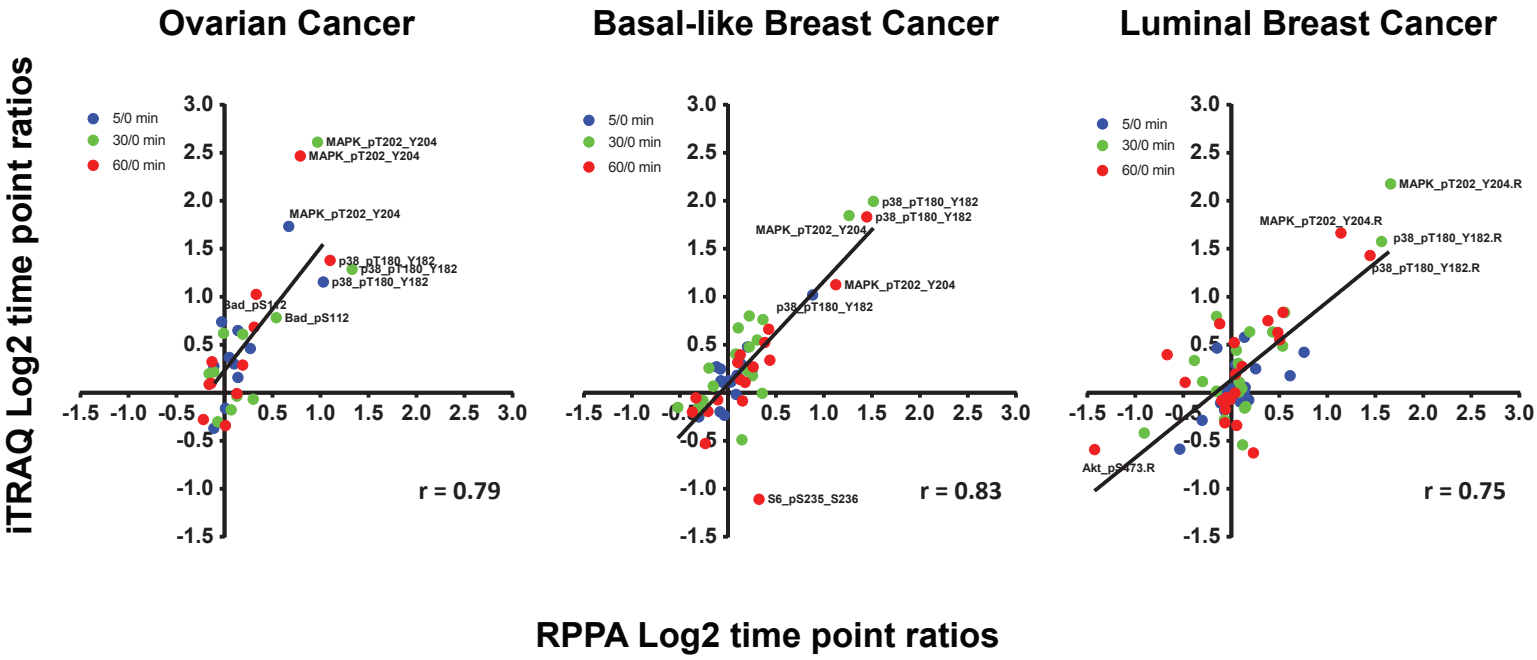
Ovarian Cancer
Basal-like Breast Cancer
Luminal Breast Cancer
iTRAQ Log2 time point ratios
RPPA Log2 time point ratios
5/0 min
30/0 min
60/0 min
MAPK_pT202_Y204
MAPK_pT202_Y204
MAPK_pT202_Y204
p38_pT180_Y182
p38_pT180_Y182
p38_pT180_Y182
Bad_pS112
Bad_pS112
r = 0.79
p38_pT180_Y182
p38_pT180_Y182
MAPK_pT202_Y204
MAPK_pT202_Y204
p38_pT180_Y182
S6_pS235_S236
r = 0.83
MAPK_pT202_Y204.R
MAPK_pT202_Y204.R
p38_pT180_Y182.R
p38_pT180_Y182.R
Akt_pS473.R
r = 0.75

Figure S7:

GI-number	Protein name	Gene name	Phosphosite	Sequence
87299628	Biorientation of chromosomes in cell division protein 1-like	BOD1L	S800	KLsVLGK

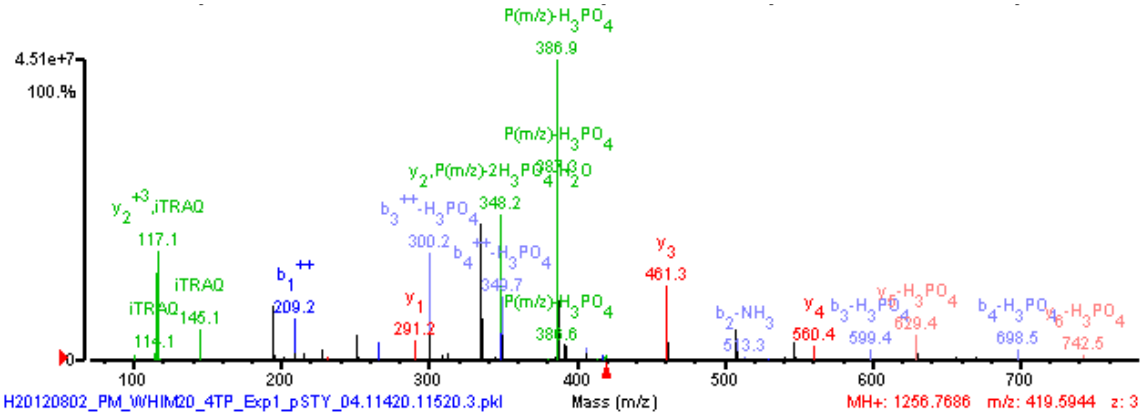

GI-number	Protein name	Gene name	Phosphosite	Sequence
4504517	Heat shock protein beta-1	HSPBL2	S15	GPsWDPFR

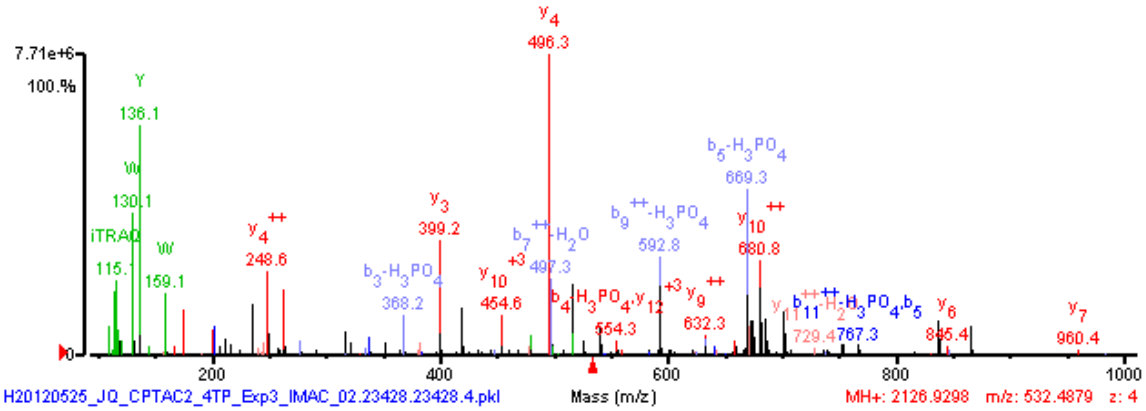

GI-number	Protein name	Gene name	Phosphosite	Sequence
61743954	Neuroblast differentiation - associated protein AHNAK	AHNAK	S3426	VSMPDVELNLKsPK

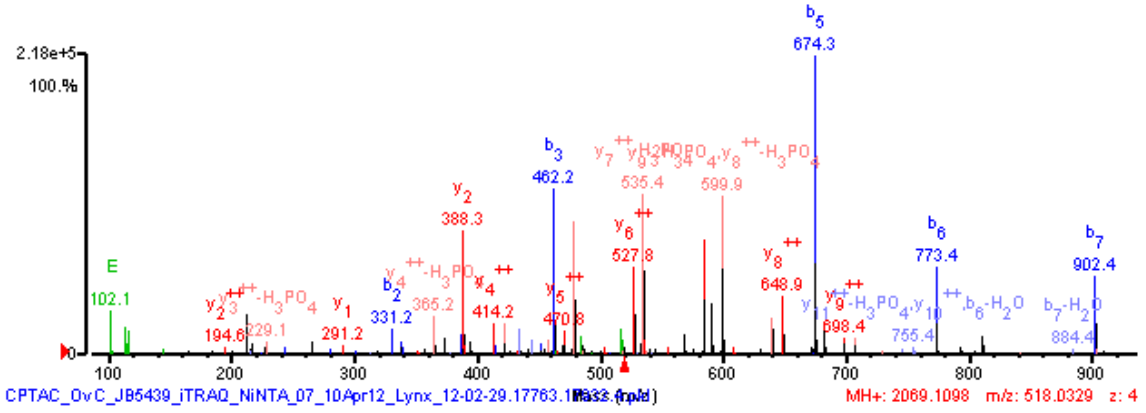

GI-number	Protein name	Gene name	Phosphosite	Sequence
48255933	Non-histone chromosomal protein HMG-14	HMGN1	S7	RKVsSAEGAAKEEPK

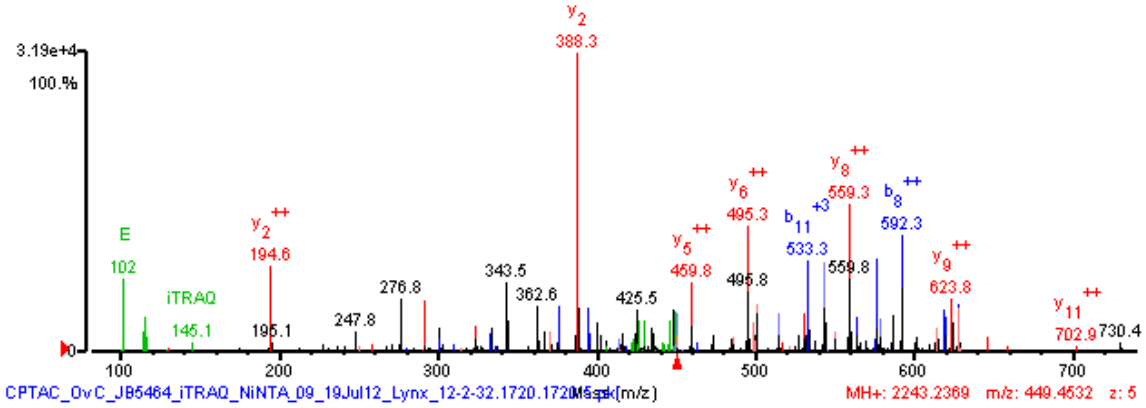

GI-number	Protein name	Gene name	Phosphosite	Sequence
192807323	Transcription activator BRG1 isoform A	SMARCA4	S1382	EVDYSDsLTEKQWLK

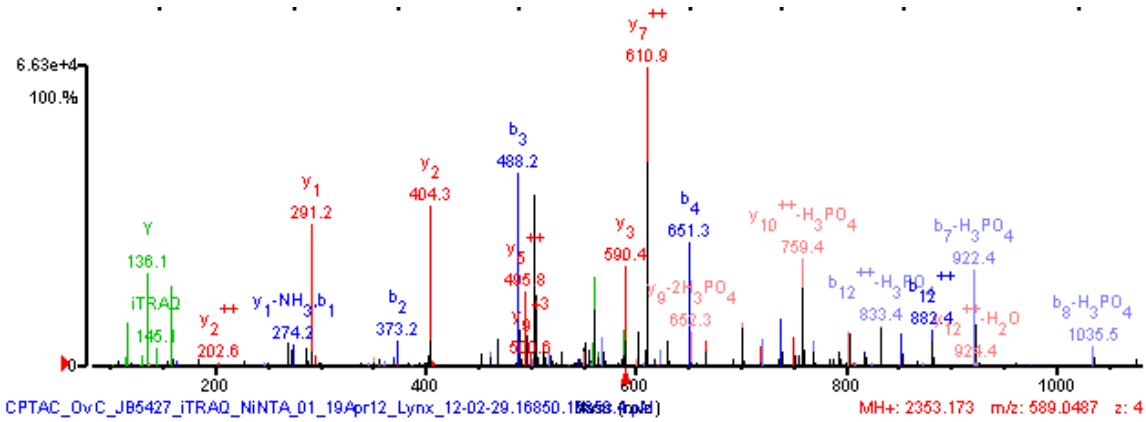

GI-number	Protein name	Gene name	Phosphosite	Sequence
223555917	Protein LYRIC	MTDH	S298	LSSQIsAGEEK

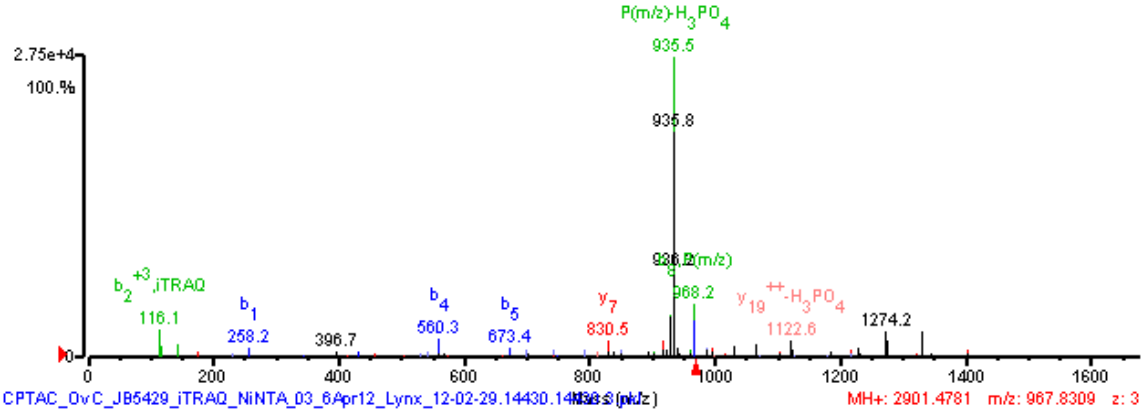

GI-number	Protein name	Gene name	Phosphosite	Sequence
5032179	Transcription intermediary factor 1-beta	TRIM28	S489	KVPRVsLER

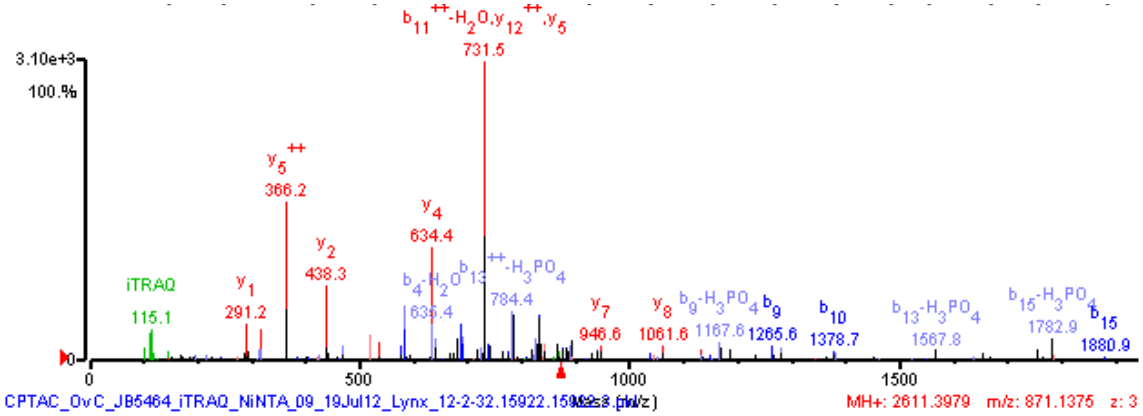

GI-number	Protein name	Gene name	Phosphosite	Sequence
14670350	General transcription factor II-I isoform 1	GTF2I	S722	GREFsFEAWNAK

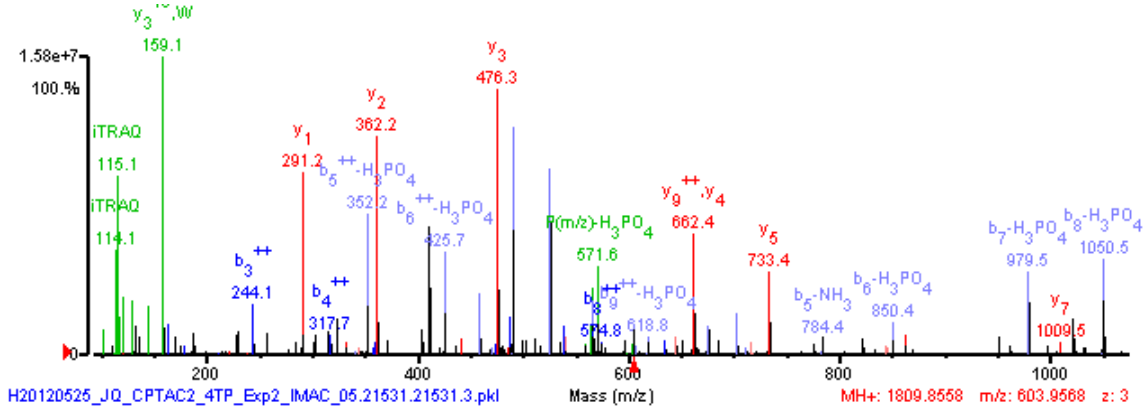

GI-number	Protein name	Gene name	Phosphosite	Sequence
259906018	Apoptotic chromatin condensation inducer in the nucleus isoform 2	ACIN1	S864	KPSIsITTESLK

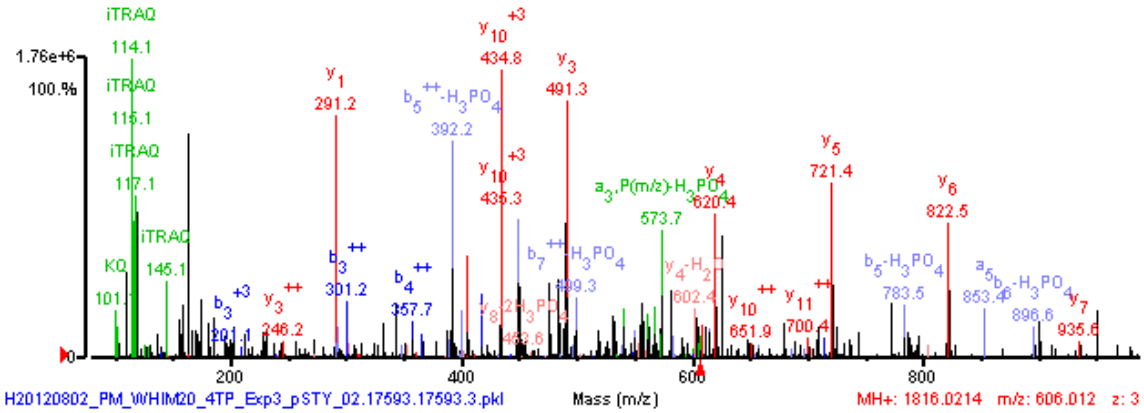

GI-number	Protein name	Gene name	Phosphosite	Sequence
37577122	Ubiquitin-conjugating enzyme E2 J1	UBE2J1	S184	QIsFKAEVNSSGK

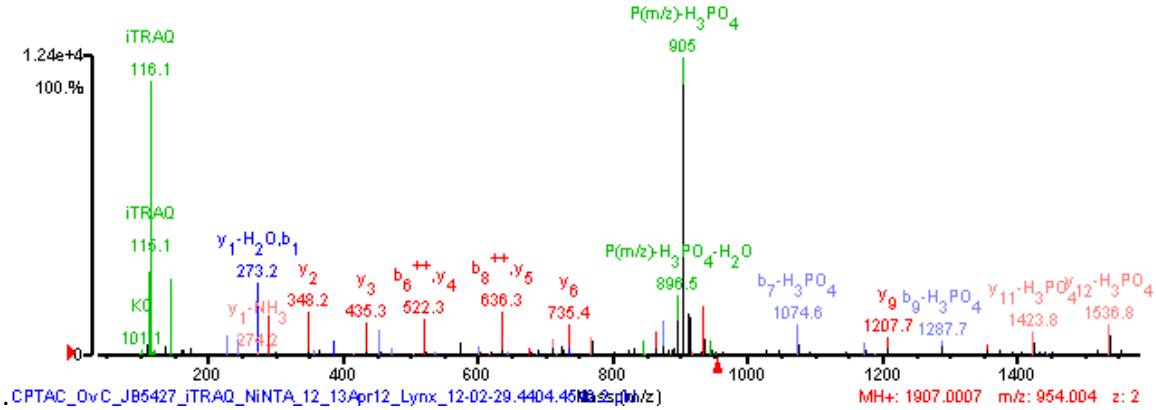

GI-number	Protein name	Gene name	Phosphosite	Sequence
20357552	Src substrate cortactin isoform a	CTTN	S432	AELsYRGPVSGTEPEPVYSMEAADYR

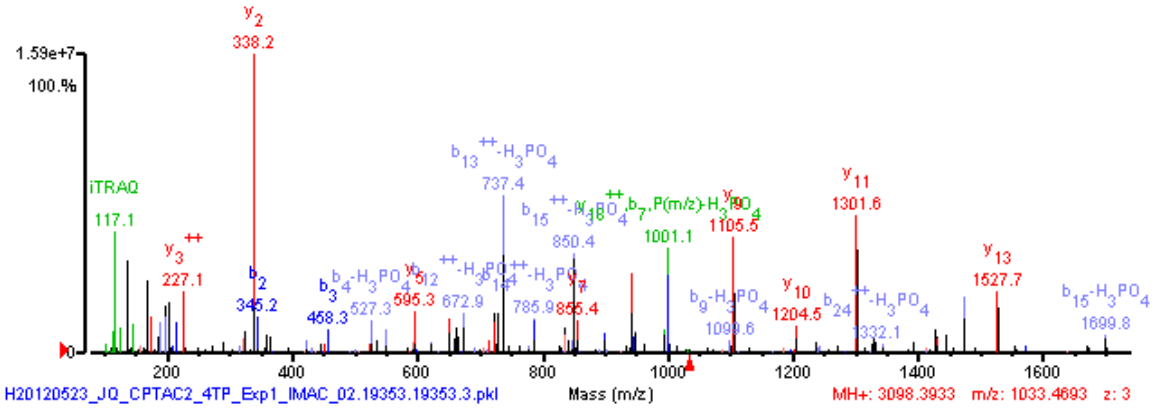

GI-number	Protein name	Gene name	Phosphosite	Sequence
38372909	Lysine-specific demethylase 3B	KDM3B	S798	RFsLDER

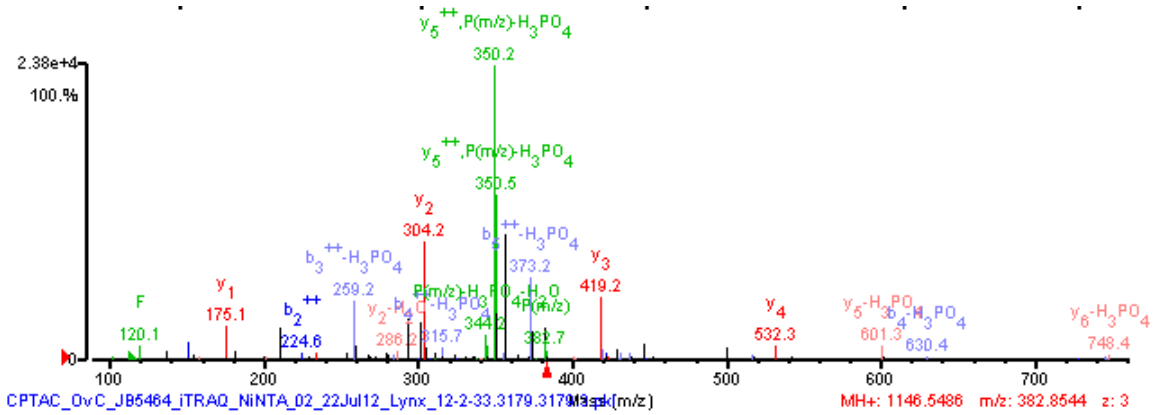

GI-number	Protein name	Gene name	Phosphosite	Sequence
14670350	General transcription factor II-I isoform 1	GTF2I	S103	MsVDAVEIETLRK

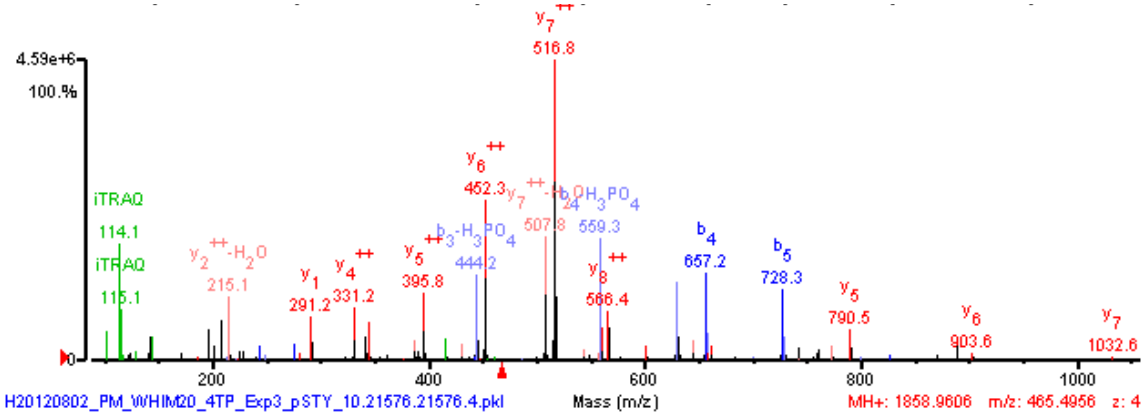

GI-number	Protein name	Gene name	Phosphosite	Sequence
82659109	E3 ubiquitin-protein ligase UBR4	UBR4	S1760	HAsTSSPADKAK

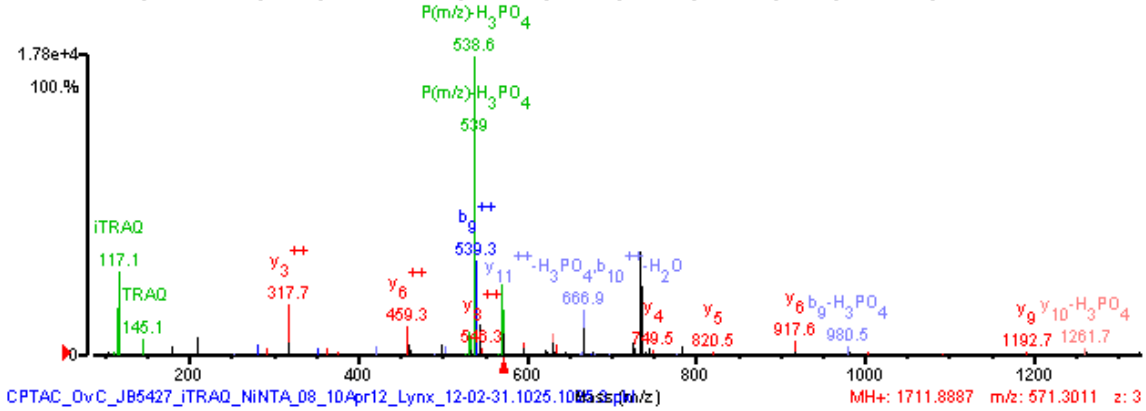

GI-number	Protein name	Gene name	Phosphosite	Sequence
193083183	Synaptopodin-2 isoform a	SYNPO2	S1091	SLsLPGR

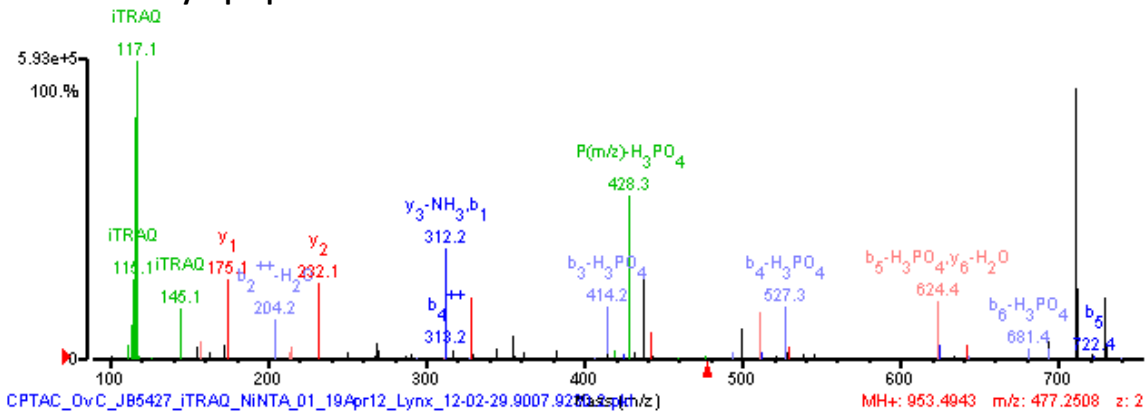

GI-number	Protein name	Gene name	Phosphosite	Sequence
114842410	Zinc finger CCCH domain-containing protein 11A	ZC3H11A	S290	RKFsAGGDSDPPLKR

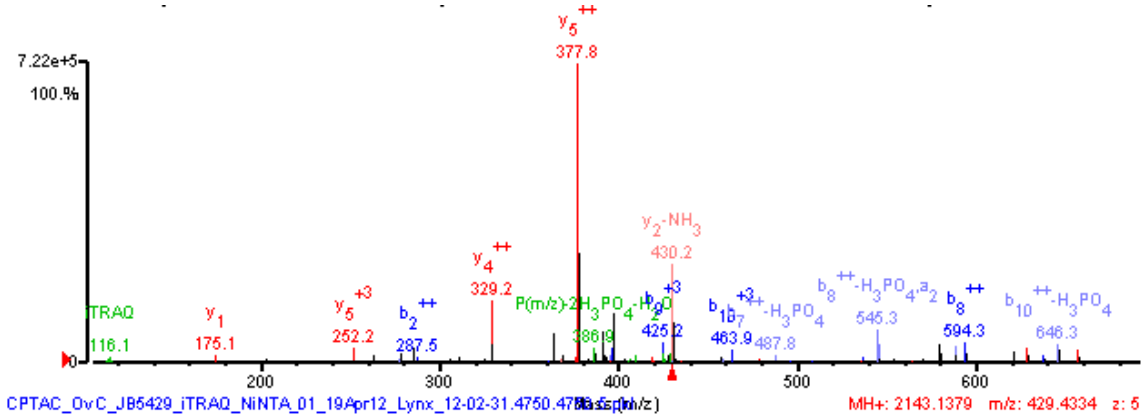

GI-number	Protein name	Gene name	Phosphosite	Sequence
9994185	RNA-binding protein 7	RBM7	S204	MNsYPYLADR

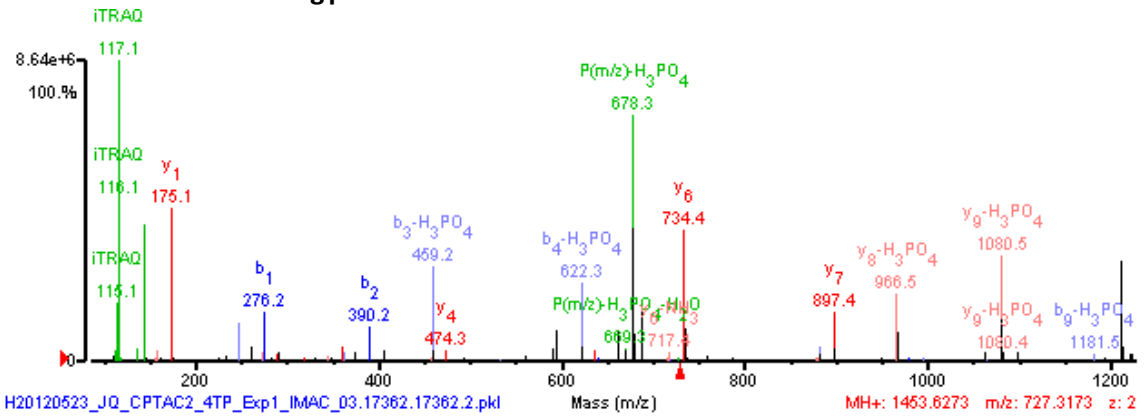

GI-number	Protein name	Gene name	Phosphosite	Sequence
40556376	Putative oxidoreductase GLYR1	GLYR1	S130	RKLsLSEGK

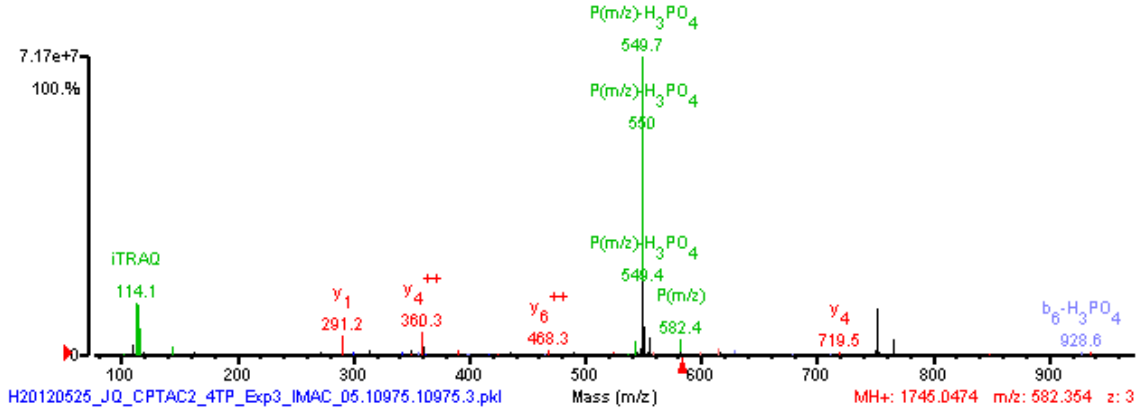

GI-number	Protein name	Gene name	Phosphosite	Sequence
281182404	Gamma-taxilin isoform 1	CXORF15	S105	NLVSPAYCT*QEs*REEIPGGEAR

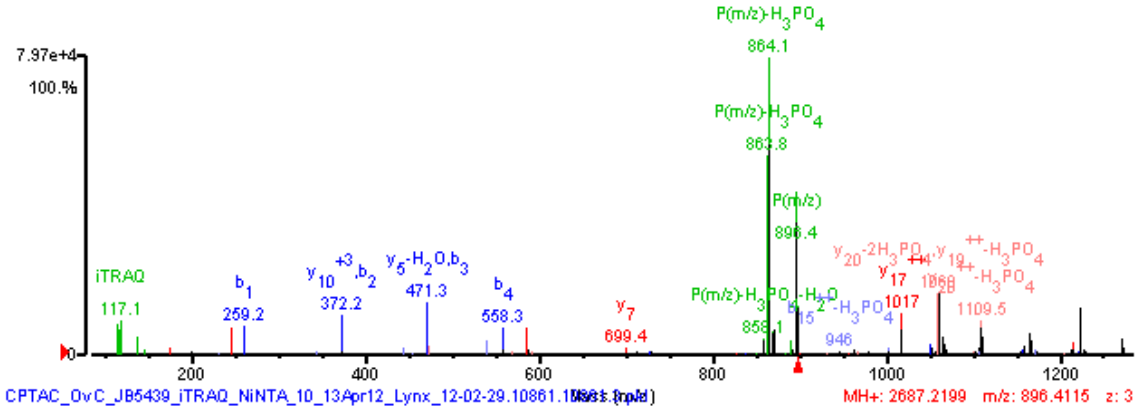

GI-number	Protein name	Gene name	Phosphosite	Sequence
4507691	Transformation/transcription domain-associated protein	TRRAP	S2033	RGLsVDSAQEVKR

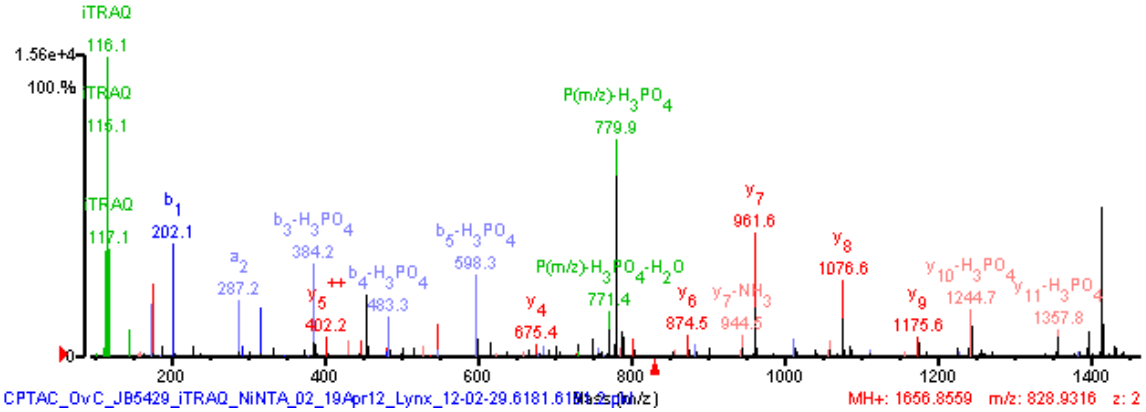

GI-number	Protein name	Gene name	Phosphosite	Sequence
41281917	Protein polybromo-1 isoform 4	PBRM1	S948	TYsQDCSFK

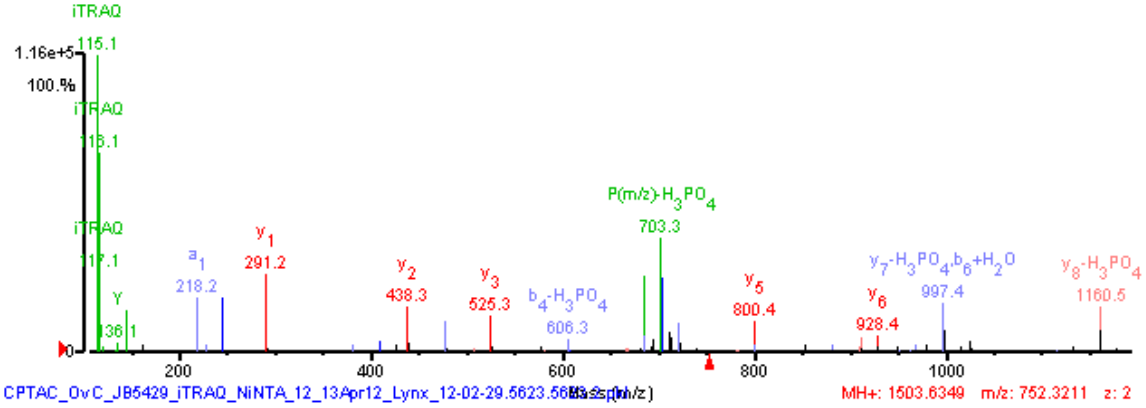

GI-number	Protein name	Gene name	Phosphosite	Sequence
33356174	Pinin	PNN	S66	RGFsDSGGGPPAK

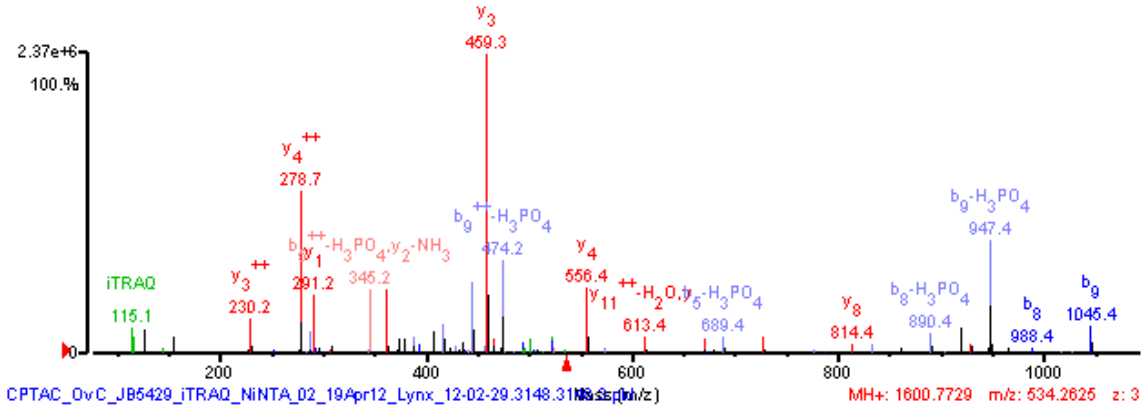

GI-number	Protein name	Gene name	Phosphosite	Sequence
4502193	Serine/threonine-protein kinase A-Raf	ARAF	T181 S186	QHEAPSNRPLNELLtPQGPsPR

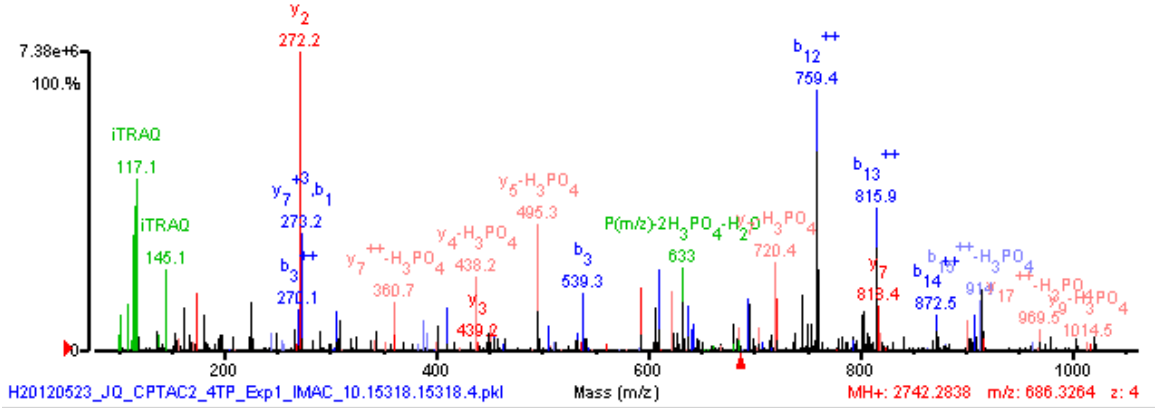

GI-number	Protein name	Gene name	Phosphosite	Sequence
112421108	Protein capicua homolog	CIC	S1389	AILGsYR

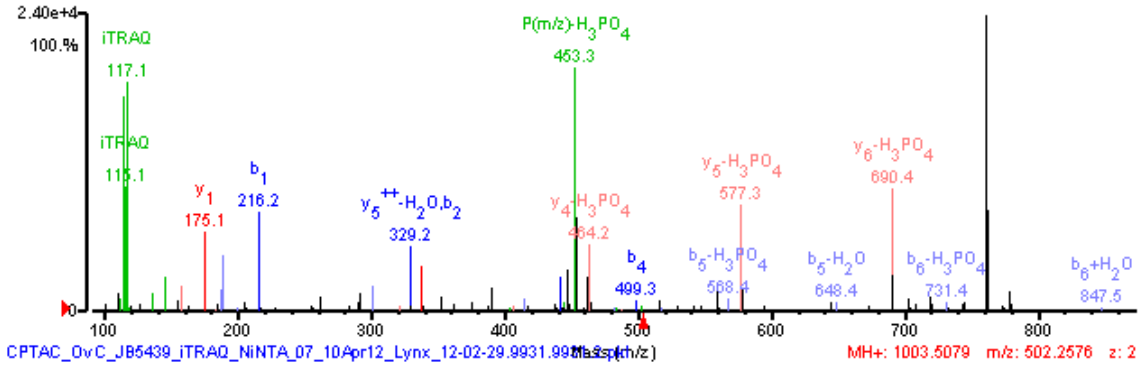

GI-number	Protein name	Gene name	Phosphosite	Sequence
21626468	Zinc finger protein 638	ZNF638	S383	NYQSQADIPIRsPFGIVK

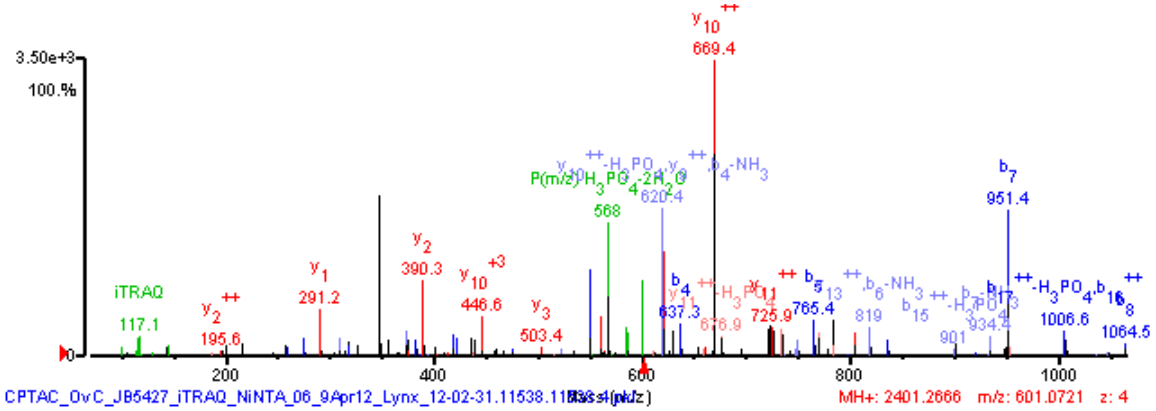

GI-number	Protein name	Gene name	Phosphosite	Sequence
61743954	Neuroblast differentiation-associated protein AHNAK	AHNAK	S3411	FKMPFLSIsSPK

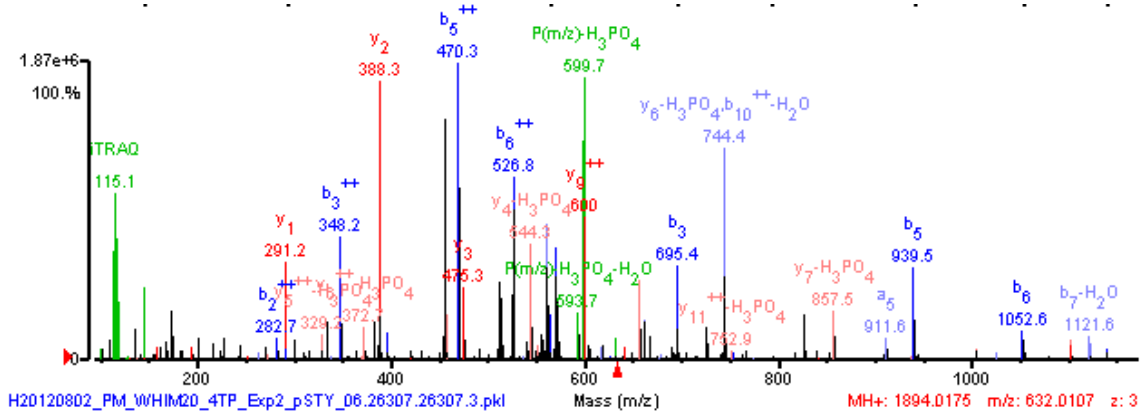

GI-number	Protein name	Gene name	Phosphosite	Sequence
9994185	RNA-binding protein 7	RBM7	S136	SFsSPENFQR

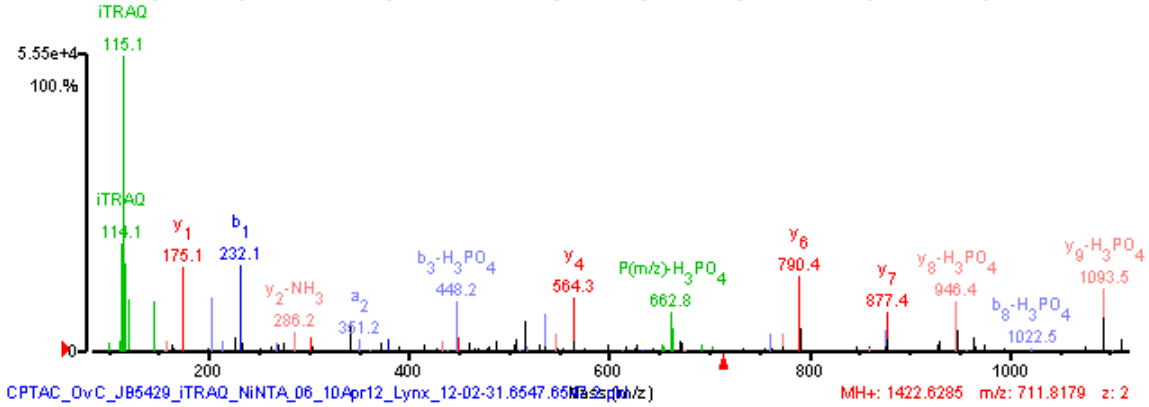

GI-number	Protein name	Gene name	Phosphosite	Sequence
34996489	PH-interacting protein	PHIP	S1315	AQsYDIQAWKK

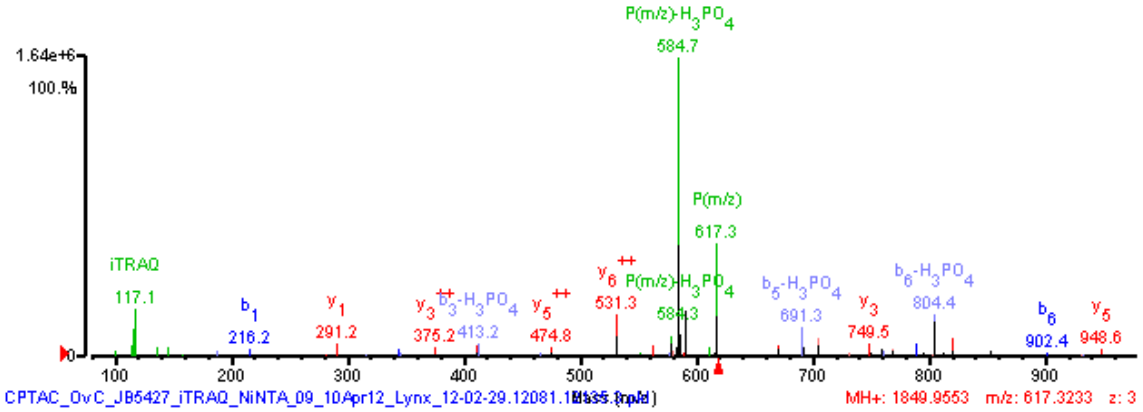

GI-number	Protein name	Gene name	Phosphosite	Sequence
5174545	Myocyte-specific enhancer factor 2D	MEF2D	S121	RAsEELDGLFR

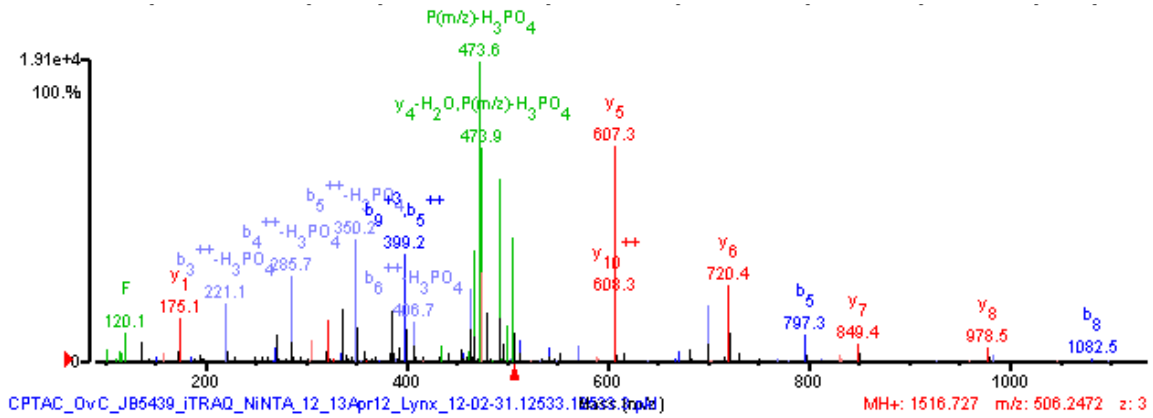

GI-number	Protein name	Gene name	Phosphosite	Sequence
28872725	26S proteasome non-ATPase regulatory subunit 11	PSMD11	S14	AQsLLSTDREASIDILHSIVKR

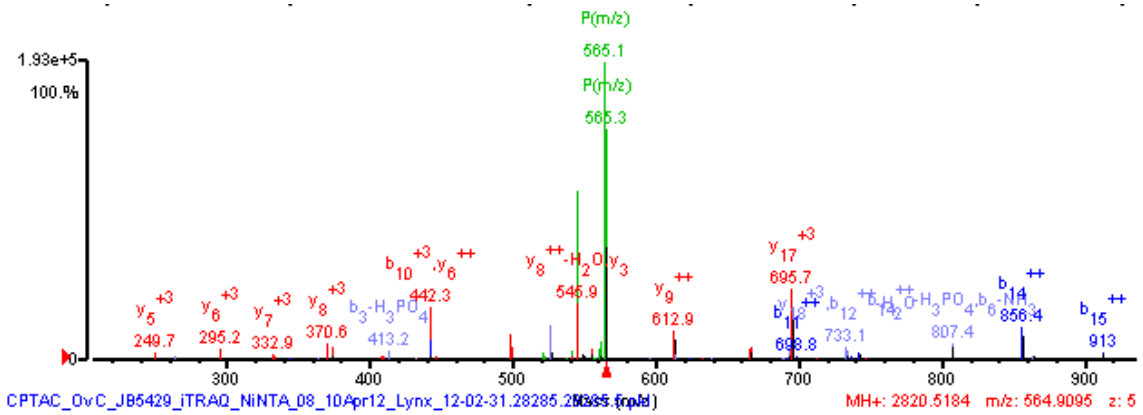

GI-number	Protein name	Gene name	Phosphosite	Sequence
20986514	Mitogen-activated protein kinase 14 isoform 3	MAPK14	Y182	HTDDEmTGyVATR

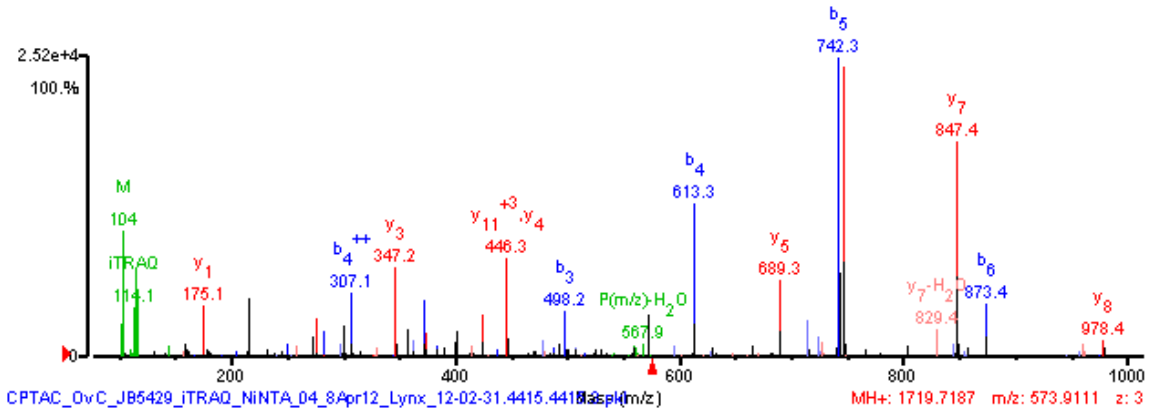

GI-number	Protein name	Gene name	Phosphosite	Sequence
7662238	Apoptotic chromatin condensation inducer in the nucleus isoform 1	ACIN1	S825	KIsVVSATK

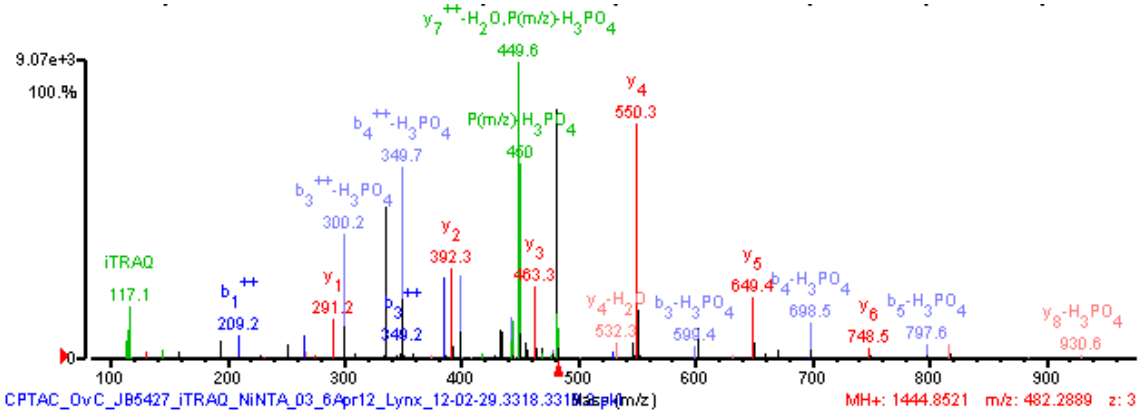

GI-number	Protein name	Gene name	Phosphosite	Sequence
65288071	Tensin-3	TNS3	S1154	ASEAASPLPDsPGDKLVIVK

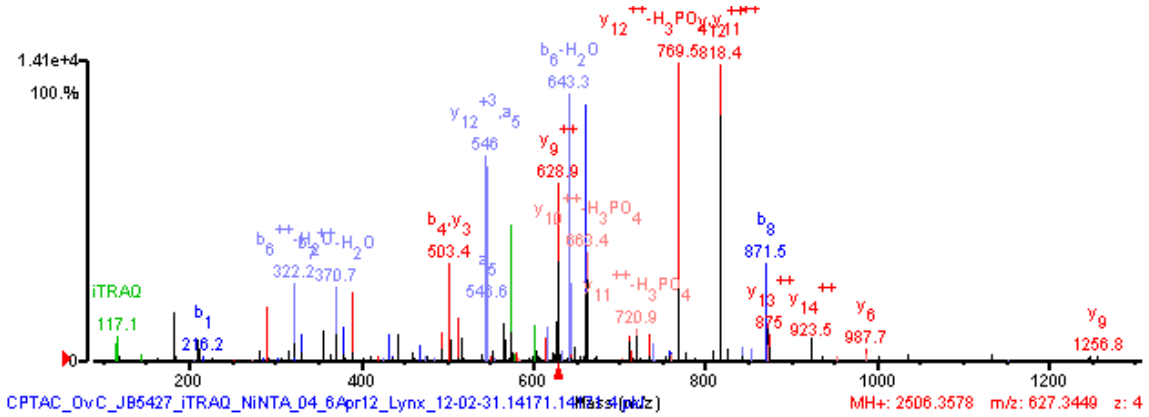

GI-number	Protein name	Gene name	Phosphosite	Sequence
14670268	Negative elongation factor E	RDBP	S51	SLsEQPVMDTATATEQAK

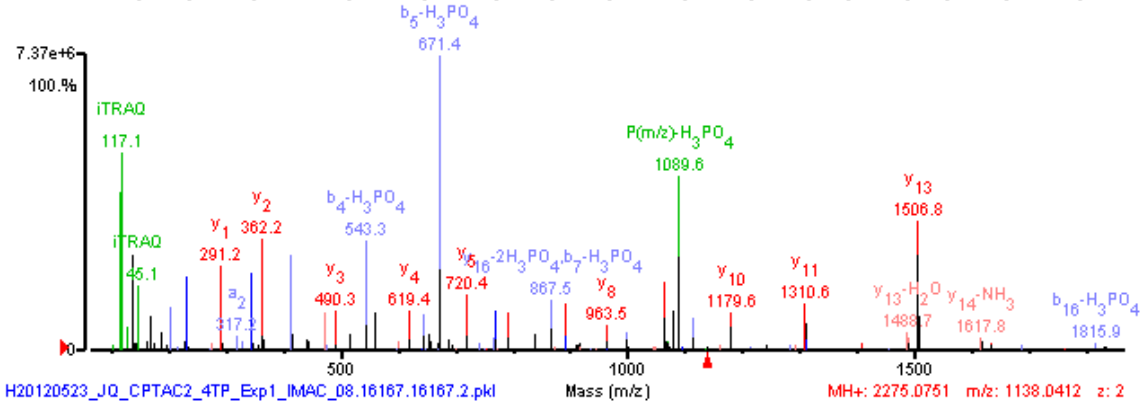

GI-number	Protein name	Gene name	Phosphosite	Sequence
61676188	E3 ubiquitin-protein ligase HUWE1	HUWE1	S2593	LLGPSAAADILQLsSSLPLQSR

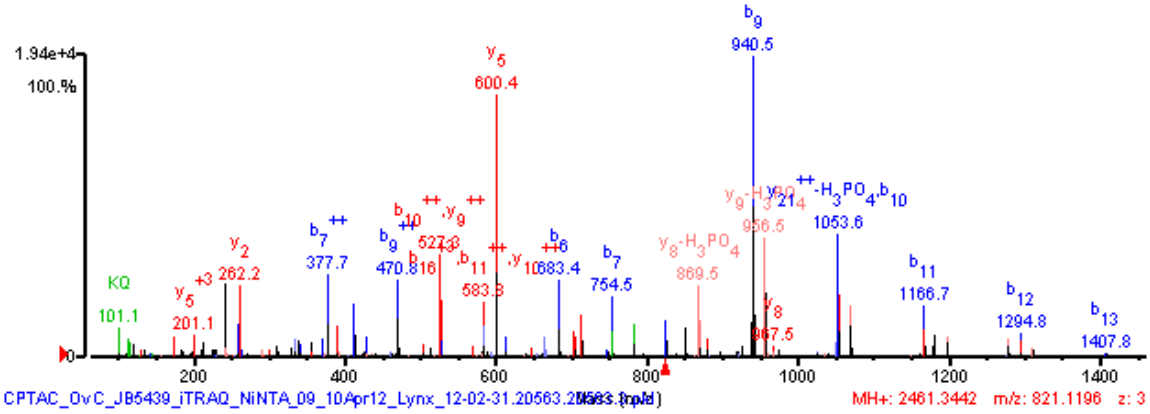

GI-number	Protein name	Gene name	Phosphosite	Sequence
190886437	RalBP1-associated Eps domain-containing protein 1 isoform b	REPS1	S272 S273	RQs*s*S*Y*DDPW KITDEQR

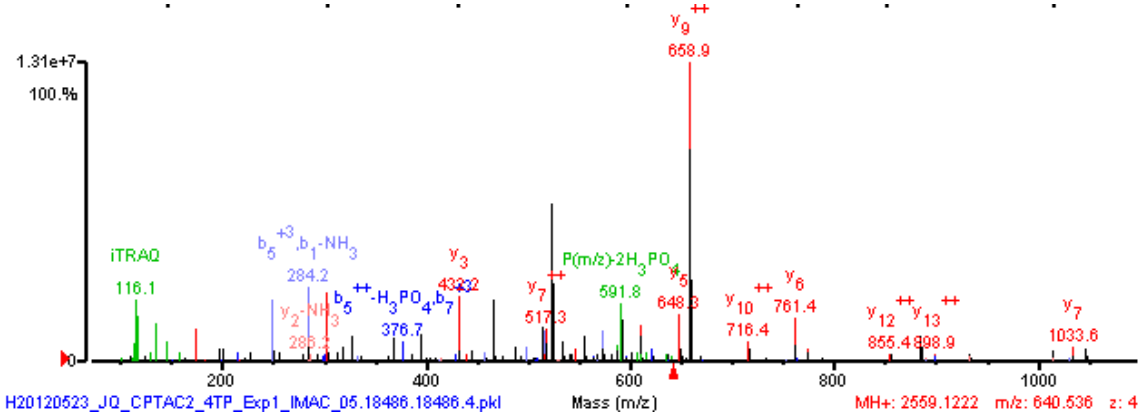

GI-number	Protein name	Gene name	Phosphosite	Sequence
82659109	E3 ubiquitin-protein ligase UBR4	UBR4	S362	T*Gs*TSSKEDDYESDAATIVQK

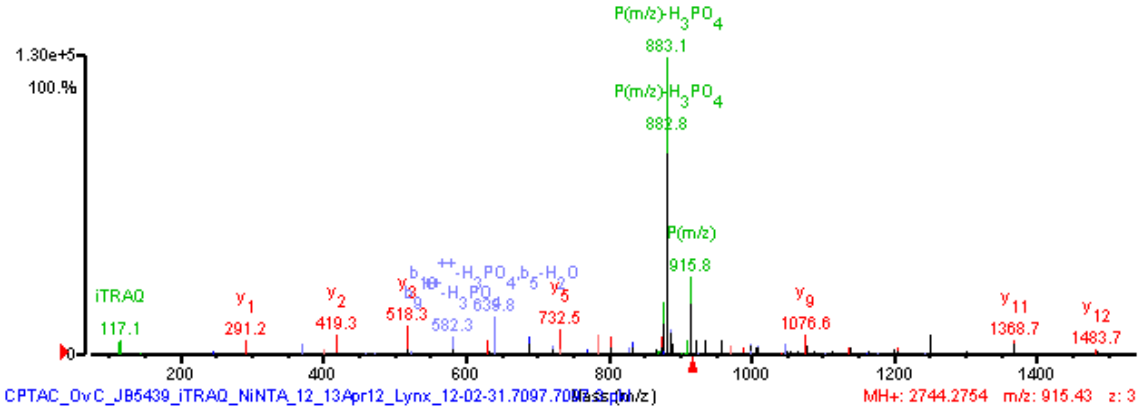

GI-number	Protein name	Gene name	Phosphosite	Sequence
4504517	Heat shock protein beta-1	HSPBL2	S82	QLsSGVSEIR

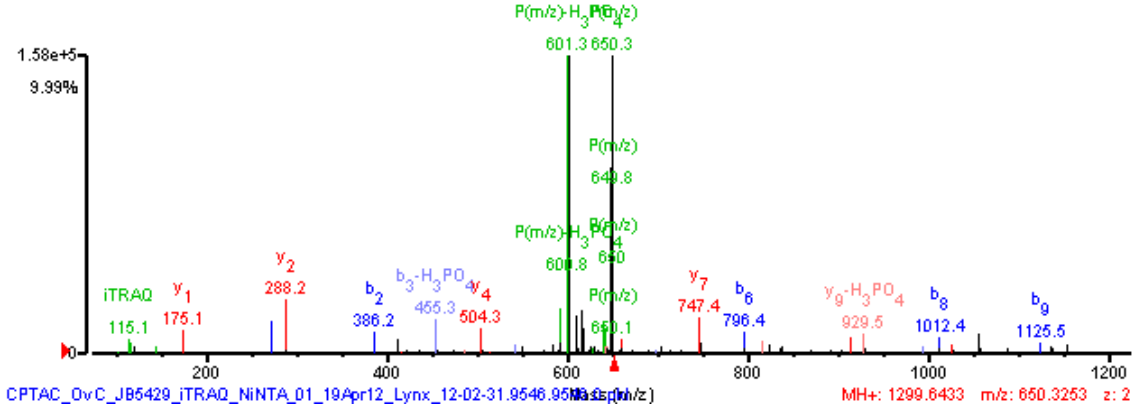

GI-number	Protein name	Gene name	Phosphosite	Sequence
42716280	Vigilin	HDLBP	S645	ILsIQK

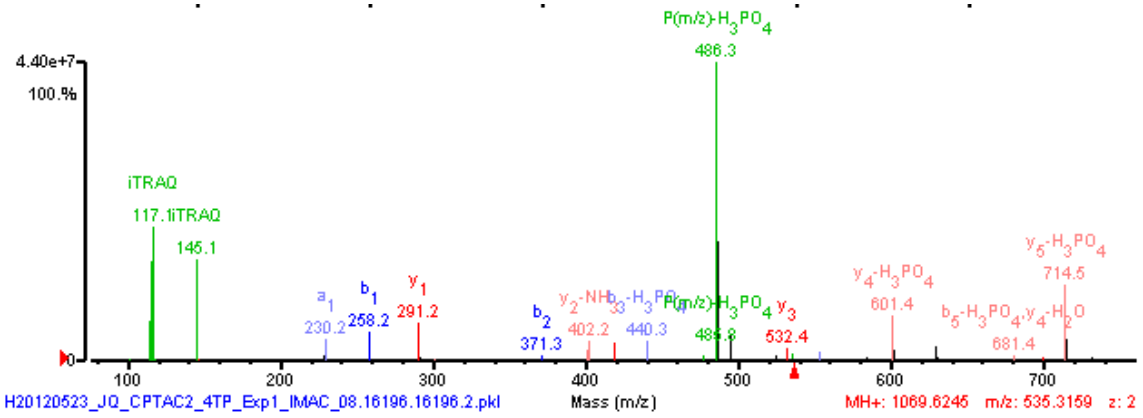

GI-number	Protein name	Gene name	Phosphosite	Sequence
14043072	Heterogeneous nuclear ribonucleoproteins A2/B1 isoform B1	HNRNPA2B1	S212	GGNFGFGDsR

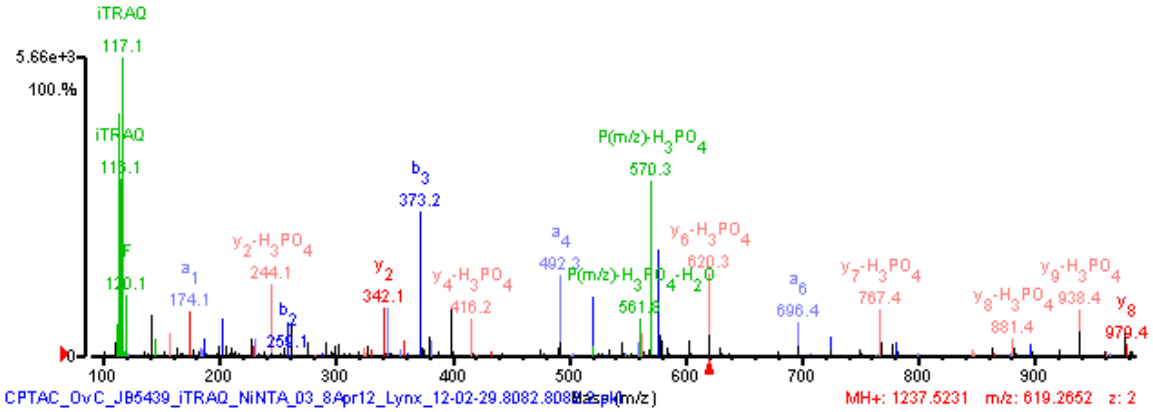

GI-number	Protein name	Gene name	Phosphosite	Sequence
148596984	Golgin subfamily B member 1	GOLGB1	S3010	QAsPETSASPDGSQNLVYETELLR

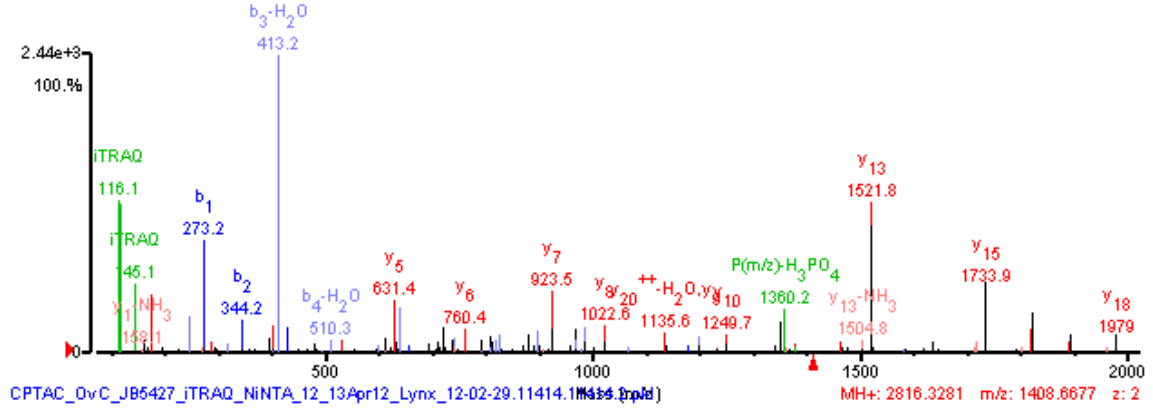

GI-number	Protein name	Gene name	Phosphosite	Sequence
51173720	Peregrin isoform 1	BRPF1	T896	Rt*S*VLFSK

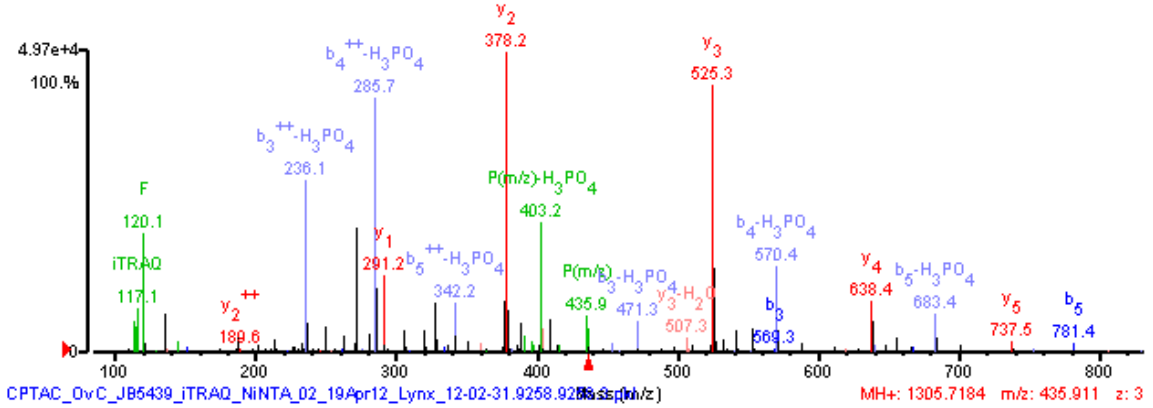

GI-number	Protein name	Gene name	Phosphosite	Sequence
223890147	Kinetochore-associated protein DSN1 homolog isoform 1	DSN1	S109	RKsLHPIHQGITELSR

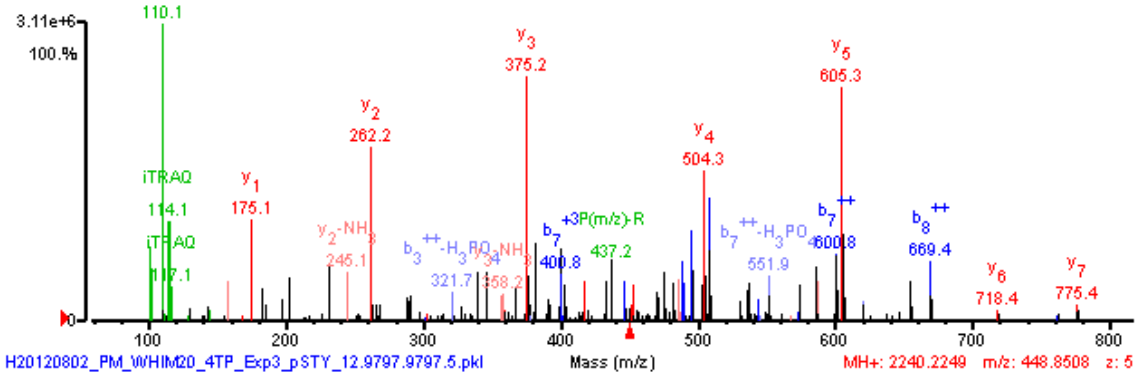

GI-number	Protein name	Gene name	Phosphosite	Sequence
116256352	Tuberin isoform 1	TSC2	S1364	VVsSEGGRPSVDLSFQPSQPLSK

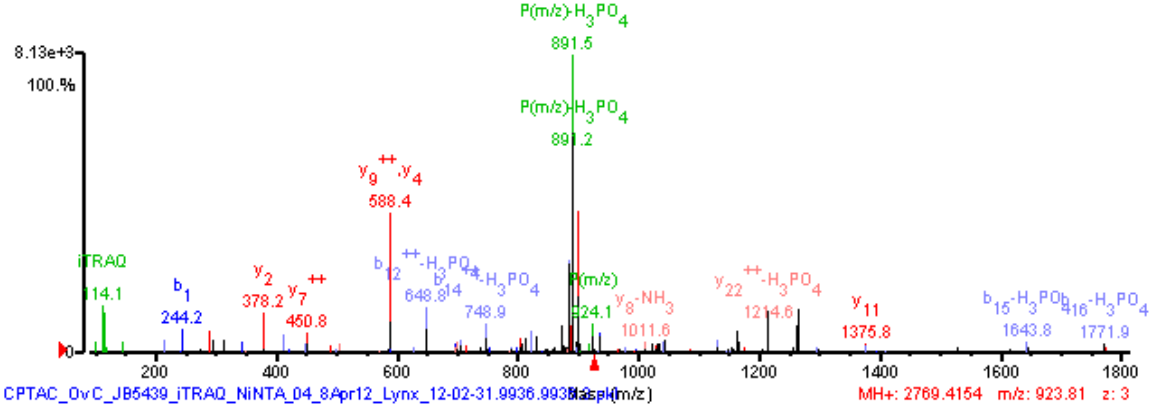

GI-number	Protein name	Gene name	Phosphosite	Sequence
61743954	Neuroblast differentiation-associated protein AHNAK	AHNAK	S5186	VKTPs*FGIS*APQVSIP DVNVNLKGPK

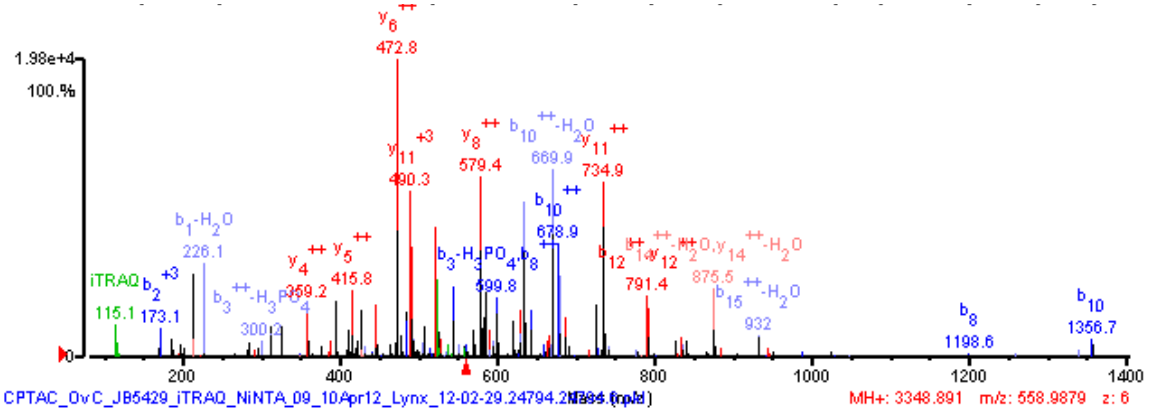

GI-number	Protein name	Gene name	Phosphosite	Sequence
4505611	Poly(A)-specific ribonuclease PARN isoform 1	PARN	S557	NNsFTAPSTVGKR

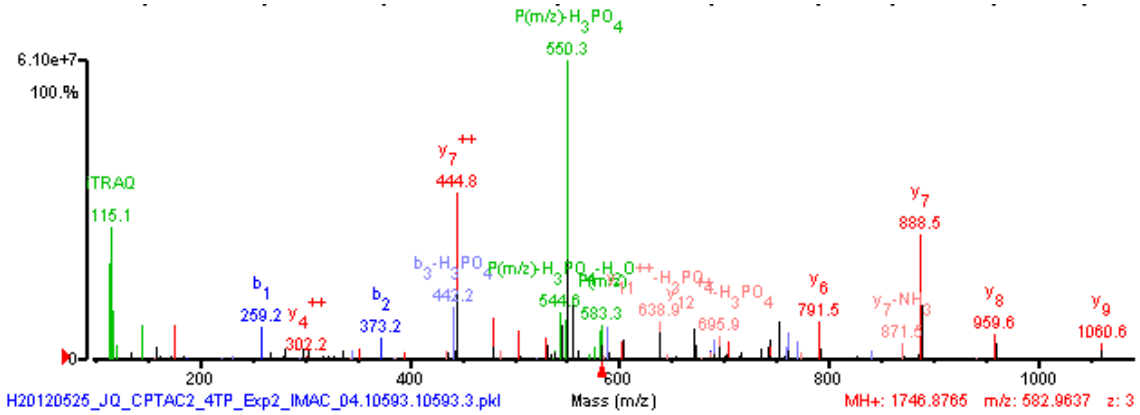

GI-number	Protein name	Gene name	Phosphosite	Sequence
24371248	FUN14 domain-containing protein 2	FUNDC2	S151	IRKsNQIPTEVR

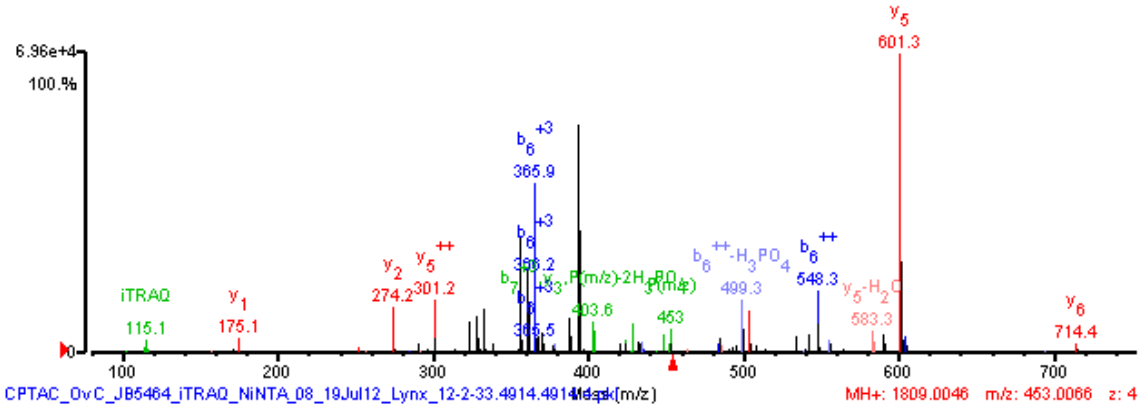

GI-number	Protein name	Gene name	Phosphosite	Sequence
116256352	Tuberin isoform 1	TSC2	S1254	SLsVPAASTAKPPPLPR

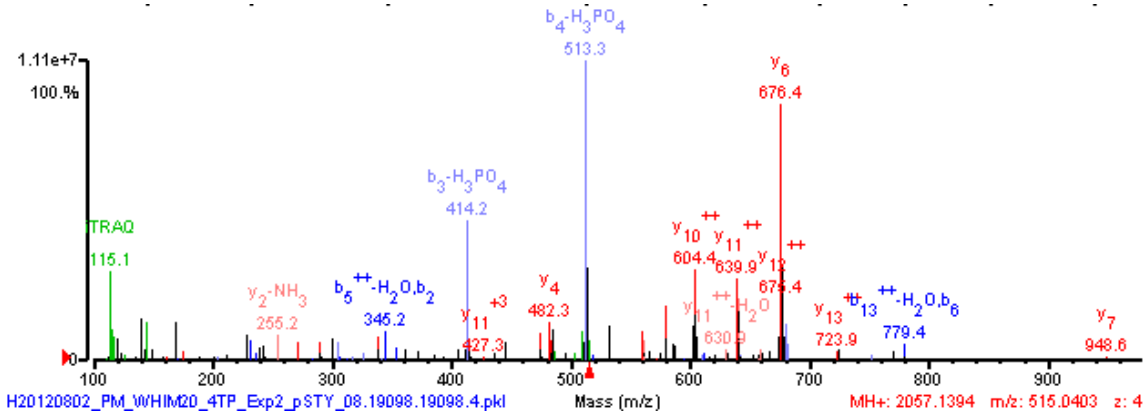

GI-number	Protein name	Gene name	Phosphosite	Sequence
20986531	Mitogen-activated protein kinase 1	MAPK1	T185 Y187	VADPDHDHTGFLtEyVATR

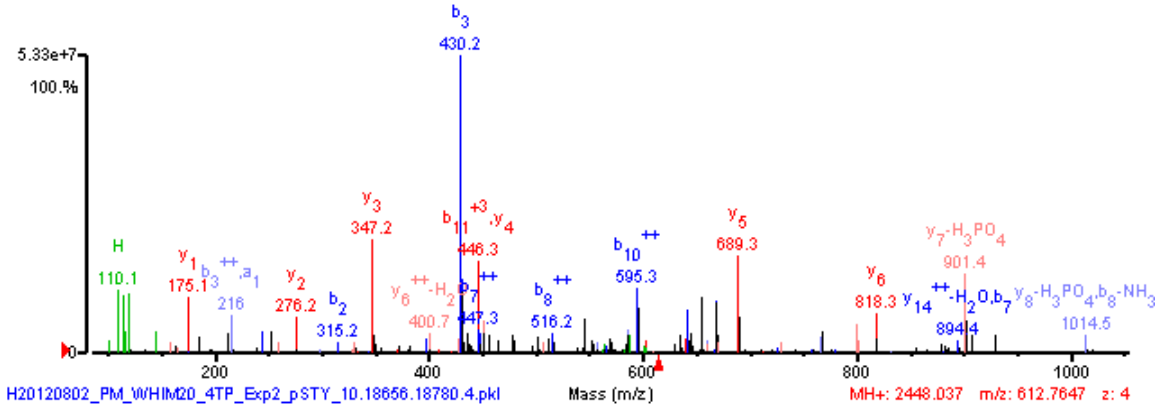

GI-number	Protein name	Gene name	Phosphosite	Sequence
262359929	Protein ELYS	AHCTF1	S1241	IsFVEEDVHPK

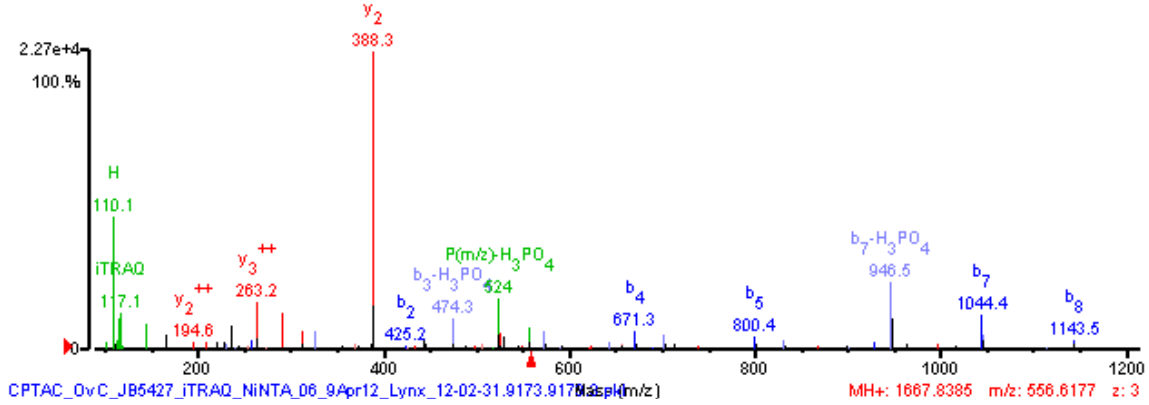

GI-number	Protein name	Gene name	Phosphosite	Sequence
27597090	Transcription elongation factor SPT6	SUPT6H	S91	KRT*s*FDDRLEDDDFDLIEENLGVK

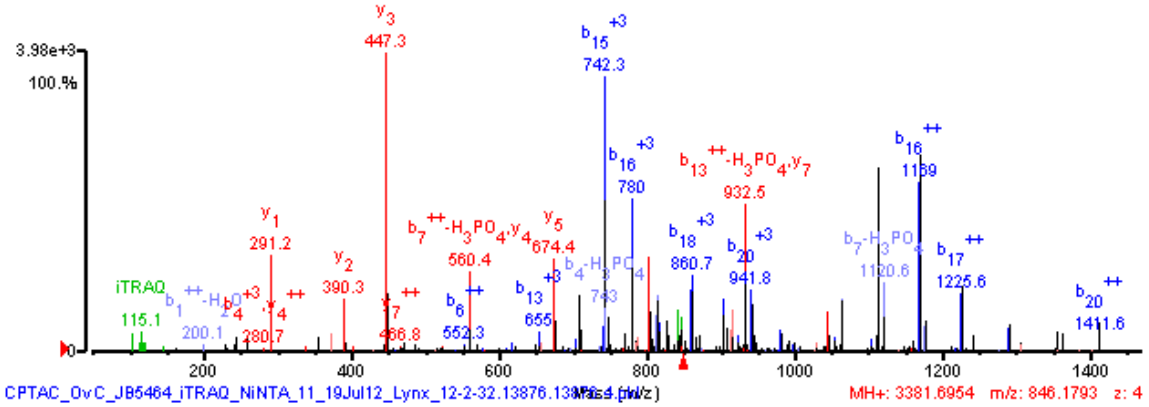

GI-number	Protein name	Gene name	Phosphosite	Sequence
13786127	Cdc42 effector protein 4	CDC42EP4	S174	NGAAGPHsPDPLL DEQAFGDLTDLPVVPK

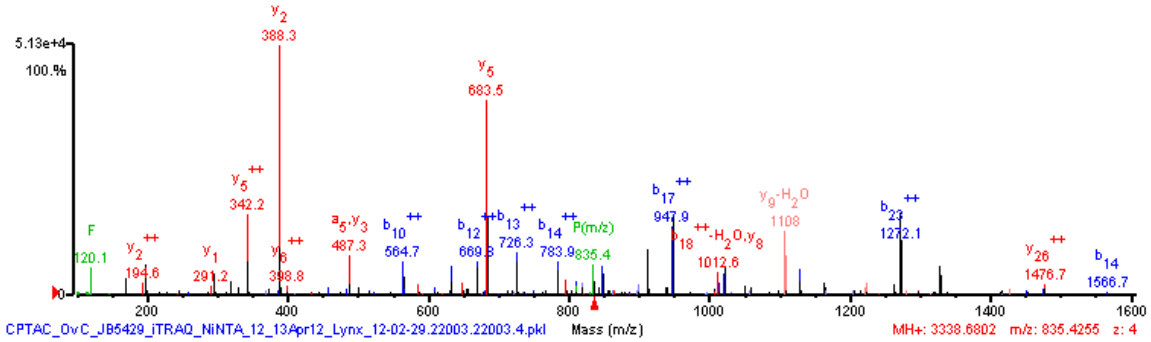

GI-number	Protein name	Gene name	Phosphosite	Sequence
21361891	SH2 domain-containing protein 4A isoform a	SH2D4A	S315	TLsSSAQEDIIR

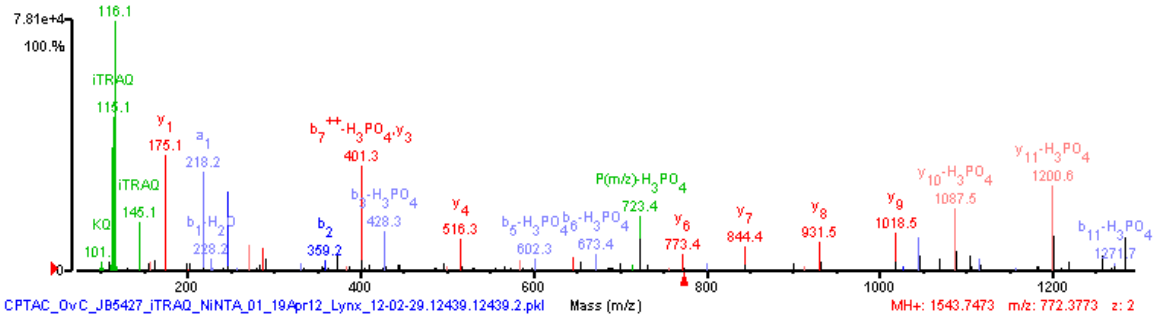

GI-number	Protein name	Gene name	Phosphosite	Sequence
117553584	AP-3 complex subunit delta-1 isoform 1	AP3D1	S567	HRPsEADEEELAR

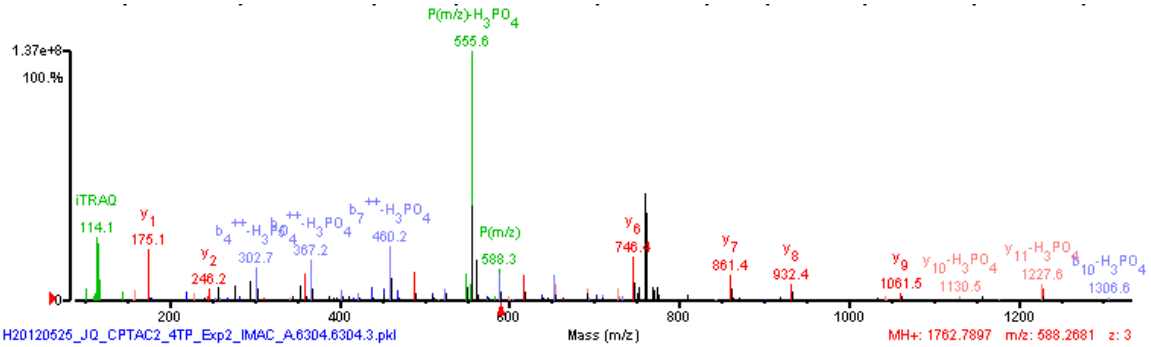

GI-number	Protein name	Gene name	Phosphosite	Sequence
208022661	Nck-associated protein 5-like	NCKAP5L	S767	VDLEPVsPR

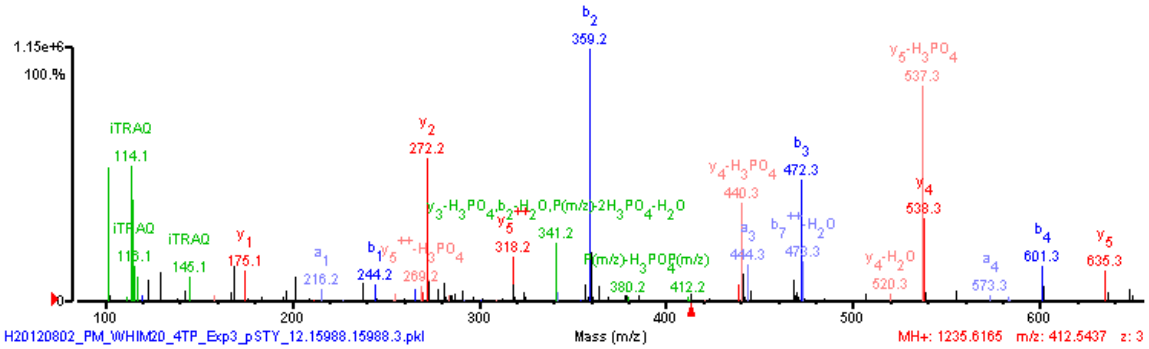

GI-number	Protein name	Gene name	Phosphosite	Sequence
31377562	HAUS augmin-like complex subunit 6	HAUS6	T584	NQIPRtPENLITEIR

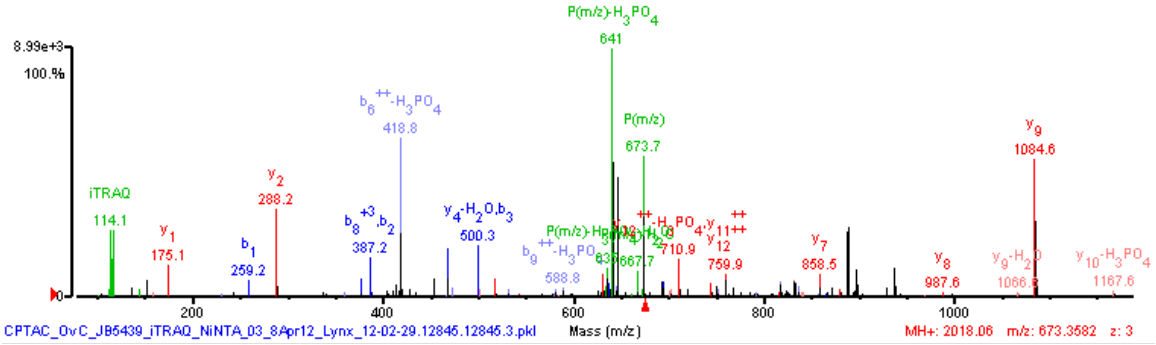

GI-number	Protein name	Gene name	Phosphosite	Sequence
61676188	E3 ubiquitin-protein ligase HUWE1	HUWE1	S3116	LFGHsSTSALSAILR

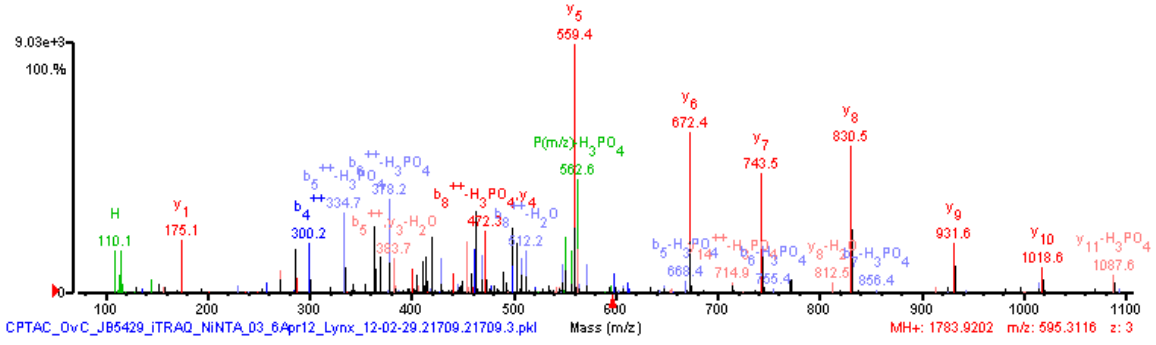

GI-number	Protein name	Gene name	Phosphosite	Sequence
4557896	Myotubularin	MTM1	S588 S590	LSDPPT*s*Ps*S*PSQ mMPHVQTHF

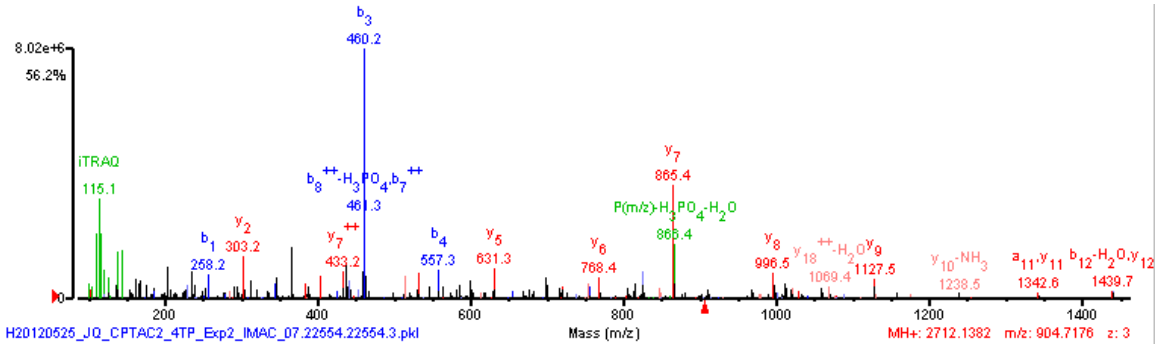

GI-number	Protein name	Gene name	Phosphosite	Sequence
14670268	Negative elongation factor E	RDBP	S131	sLYESFVSSSDRLR

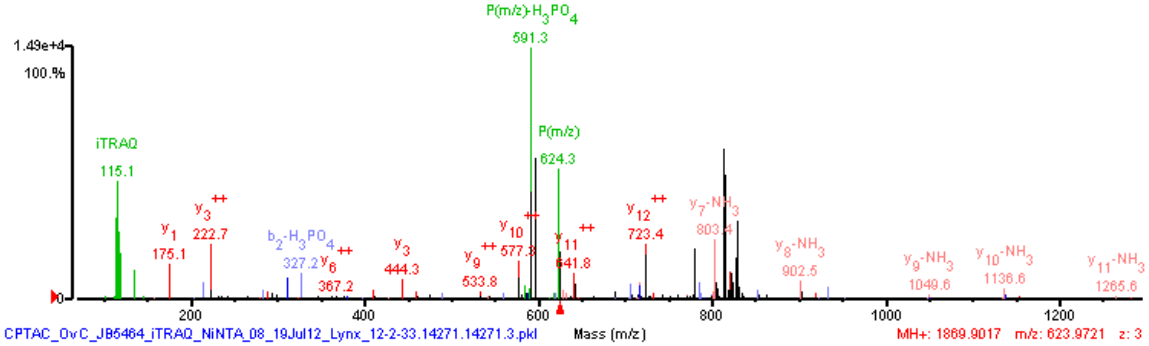

GI-number	Protein name	Gene name	Phosphosite	Sequence
140161500	Ankyrin repeat and SAM domain-containing protein 1A	ANKS1A	S620	AELKLsR

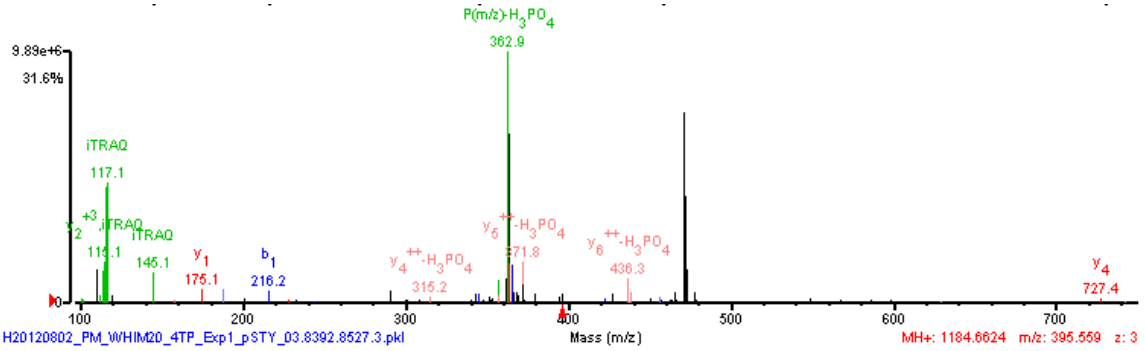

GI-number	Protein name	Gene name	Phosphosite	Sequence
224451142	Stathmin isoform b	STMN1	S25	RASGQAFELILsPR

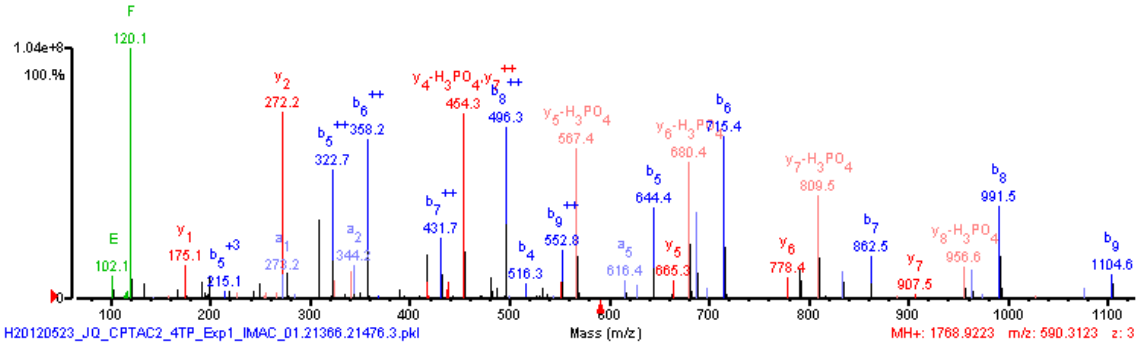

GI-number	Protein name	Gene name	Phosphosite	Sequence
22027612	TNF receptor-associated factor 2	TRAF2	S11	AAASVTPPGsLELLQPGFSK

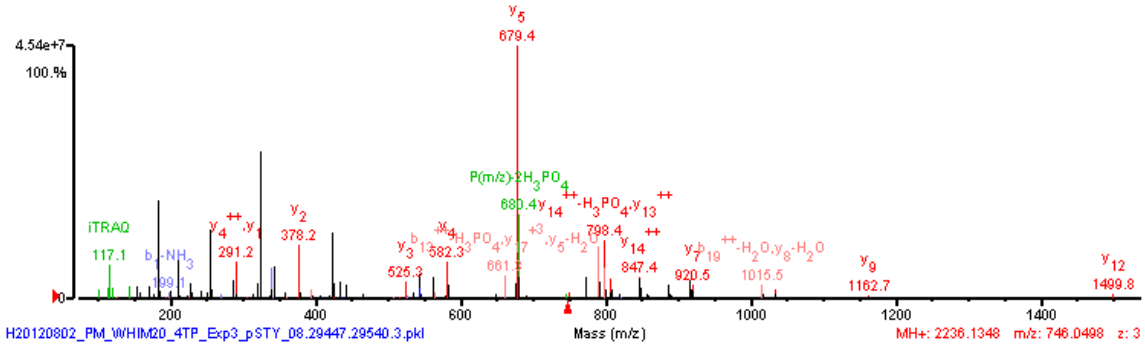

GI-number	Protein name	Gene name	Phosphosite	Sequence
5032179	Transcription intermediary factor 1-beta	TRIM28	S473	sGEGEVSGLMR

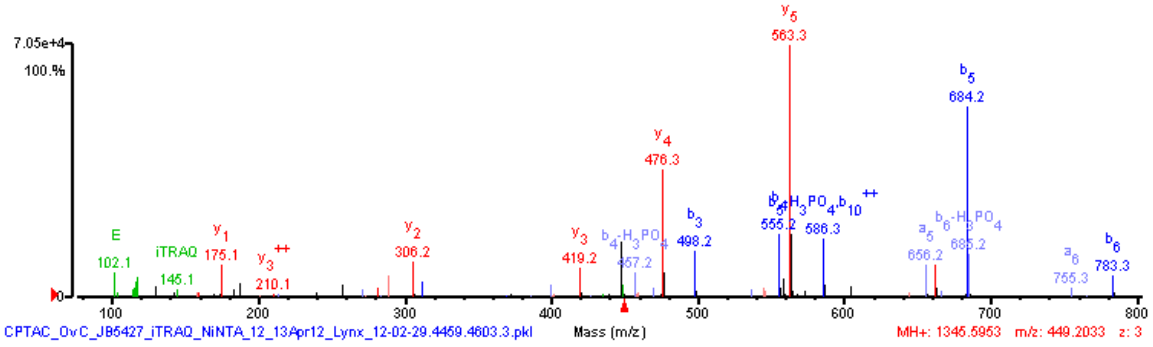

GI-number	Protein name	Gene name	Phosphosite	Sequence
27597059	DnaJ homolog subfamily C member 9	DNAJC9	S109	KIsLEDIQAFEK

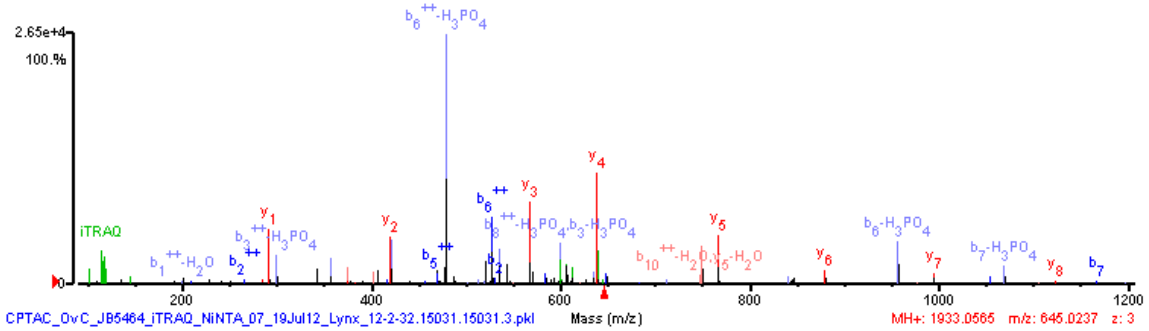

GI-number	Protein name	Gene name	Phosphosite	Sequence
4504919	Keratin, type II cytoskeletal 8	KRT8	S475	LVsESSDVLPK

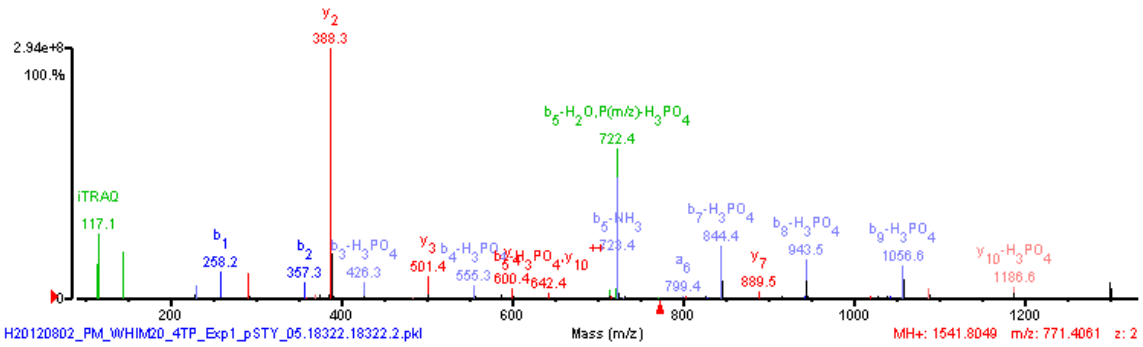

GI-number	Protein name	Gene name	Phosphosite	Sequence
21493029	A-kinase anchor protein 13 isoform 2	AKAP13	S2561	sLSRPSSLIEQEKQR

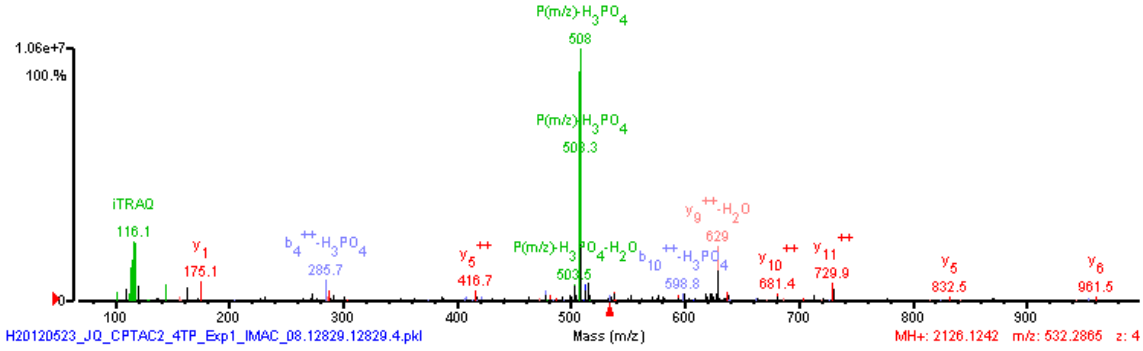

GI-number	Protein name	Gene name	Phosphosite	Sequence
110556636	182 kDa tankyrase-1-binding protein	TNKS1BP1	S1029	GSGGLFsPSTAHVPDGALGQR

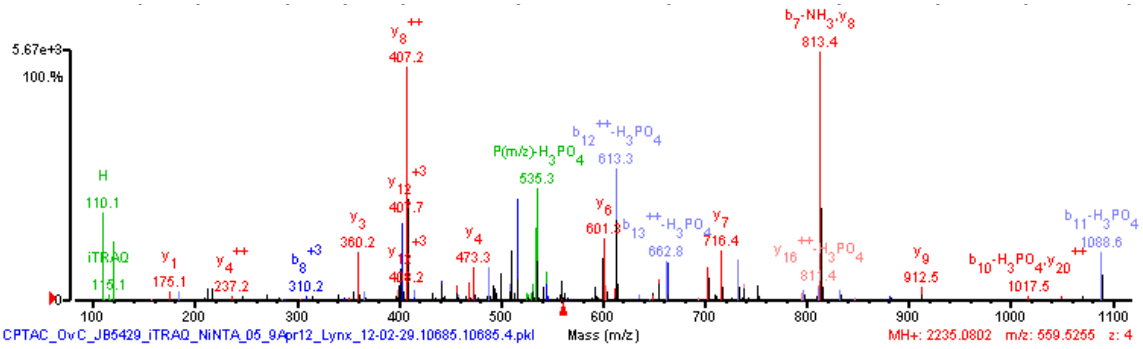

GI-number	Protein name	Gene name	Phosphosite	Sequence
51093863	Niban-like protein 1 isoform 1	FAM129B	S692 S696	AAPEAS*s*PPAsPLQHLLPGK

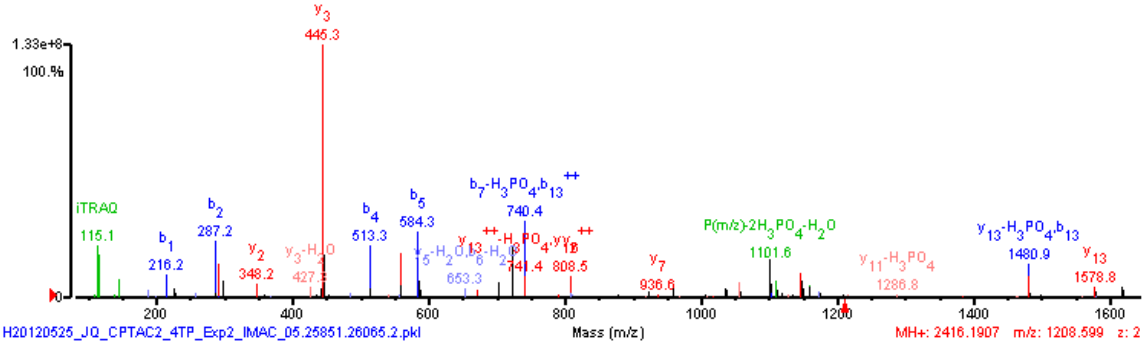

GI-number	Protein name	Gene name	Phosphosite	Sequence
222136641	Serine/threonine-protein kinase Nek9	NEK9	S332	SsTVTEAPIAVVTSR

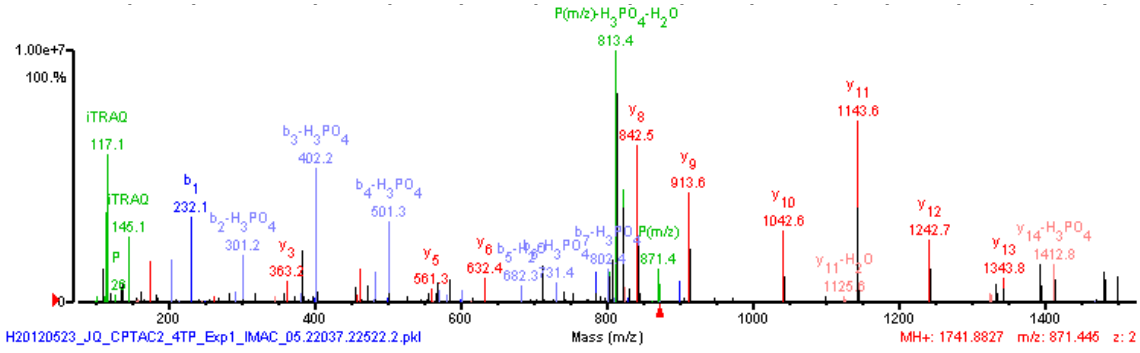

GI-number	Protein name	Gene name	Phosphosite	Sequence
19424132	Serine/threonine-protein kinase Nek7	NEK7	S187	FFSSKtTAAHSL VGTPYYmSPER

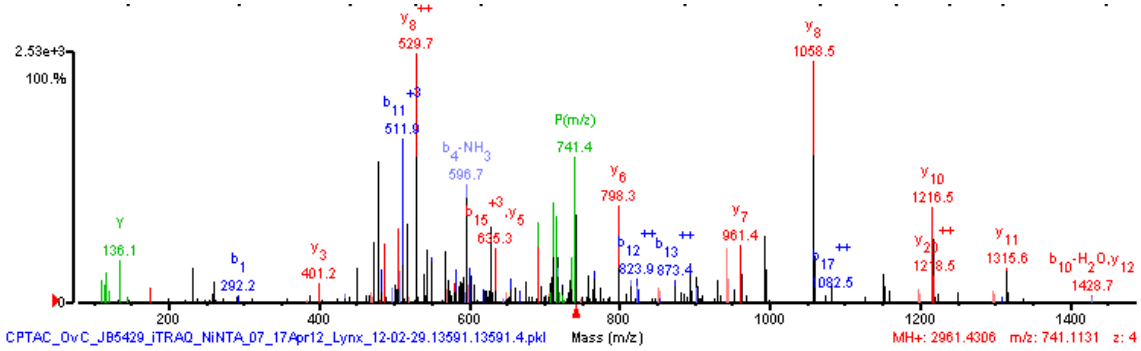

GI-number	Protein name	Gene name	Phosphosite	Sequence
7705373	LIM domain and actin-binding protein 1 isoform b	LIMA1	S604	SRPFTVAASFQS*T*S*VKs*PK

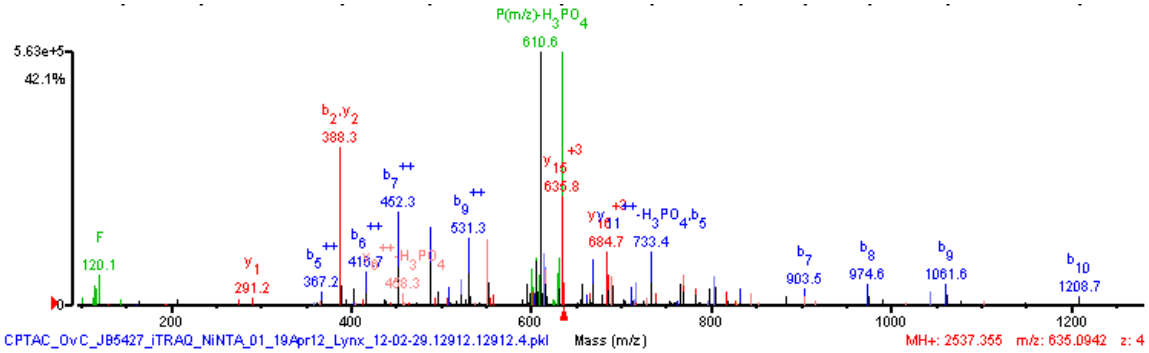

GI-number	Protein name	Gene name	Phosphosite	Sequence
21070984	Peptidyl-glycine alpha-amidating monooxygenase	PAM	S919	GKGsGGLNLGNFFASR

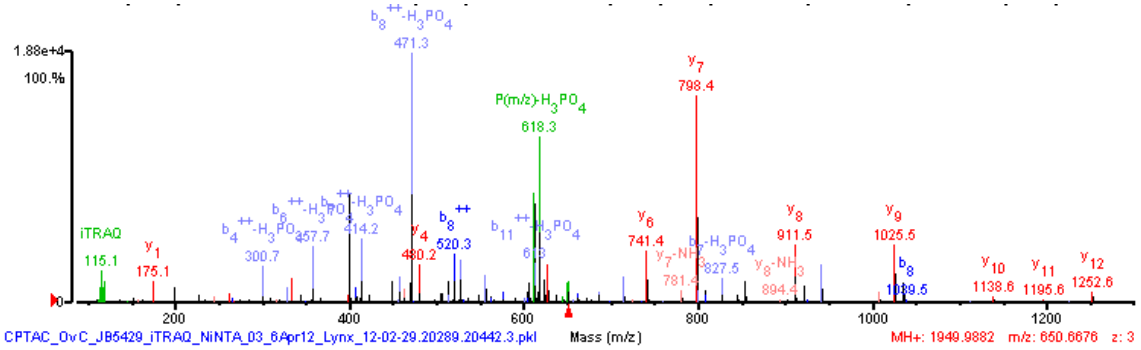

GI-number	Protein name	Gene name	Phosphosite	Sequence
5729858	Nuclear receptor coactivator 2	NCOA2	S771	LERLDSKtDPASNTK

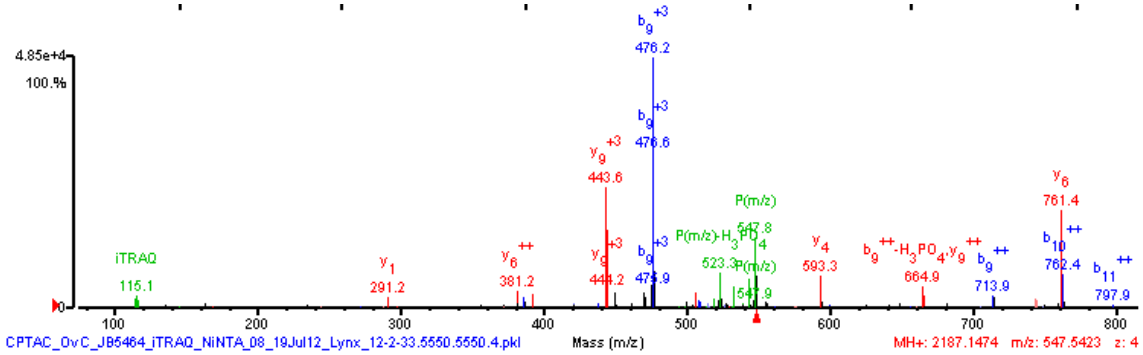

GI-number	Protein name	Gene name	Phosphosite	Sequence
289577098	Protein Shroom1 isoform 1	SHROOM1	S302	LGDAFRPAsR

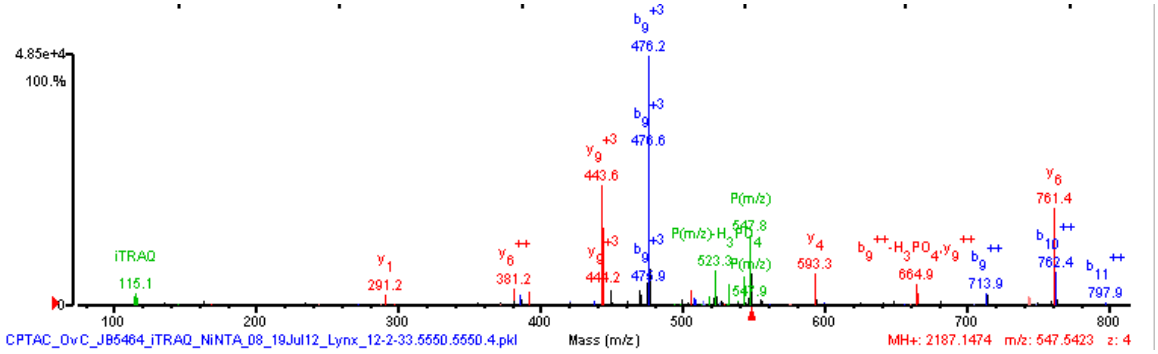

GI-number	Protein name	Gene name	Phosphosite	Sequence
14670268	Negative elongation factor E	RDBP	S115	SIsADDDLQESSR

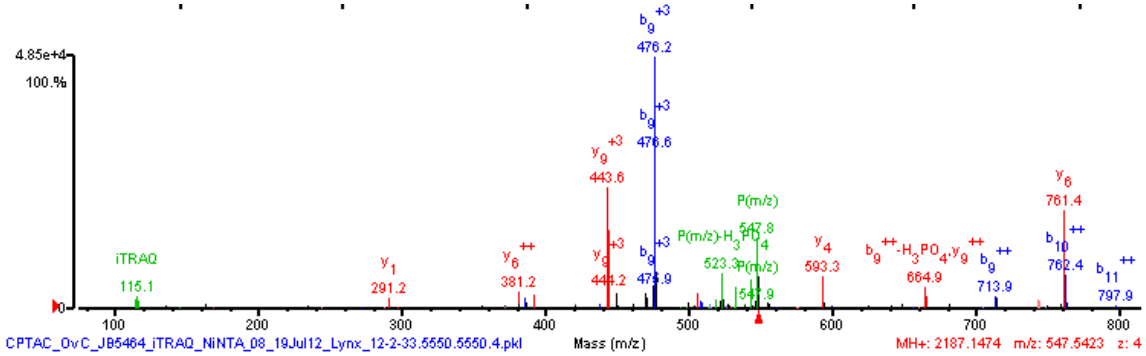

GI-number	Protein name	Gene name	Phosphosite	Sequence
87299628	Biorientation of chromosomes in cell division protein 1-like	BOD1L	S635	RLsESLHVVDENKNESK

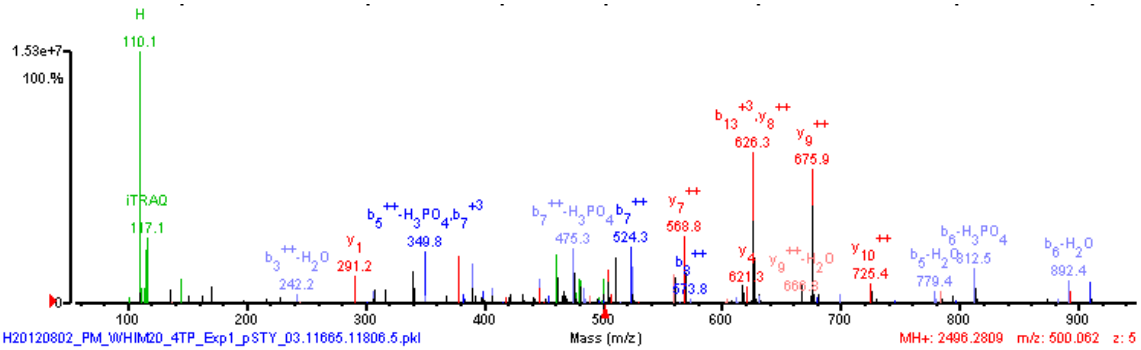

GI-number	Protein name	Gene name	Phosphosite	Sequence
112421108	Protein capicua homolog	CIC	S739	SAAATsPAPHLVAGPLLGTVGK

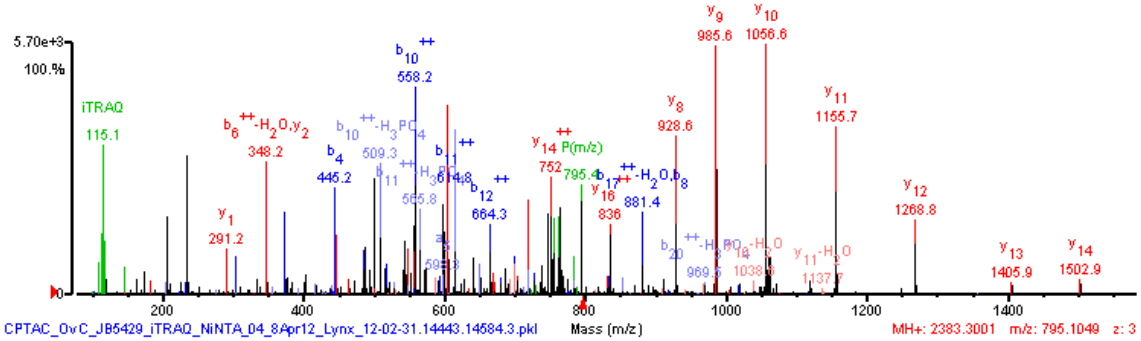

GI-number	Protein name	Gene name	Phosphosite	Sequence
32261324	SHC-transforming protein 1 isoform 2	SHC1	Y318	ELFDDPSyVNVQNLDKAR

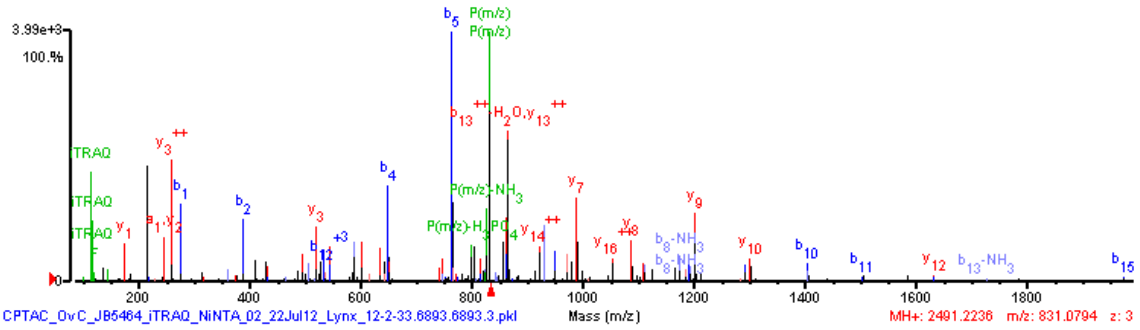

GI-number	Protein name	Gene name	Phosphosite	Sequence
30023820	Hypothetical protein LOC162427	FAM134C	S26	DVsGSWERDQQVEAAQR

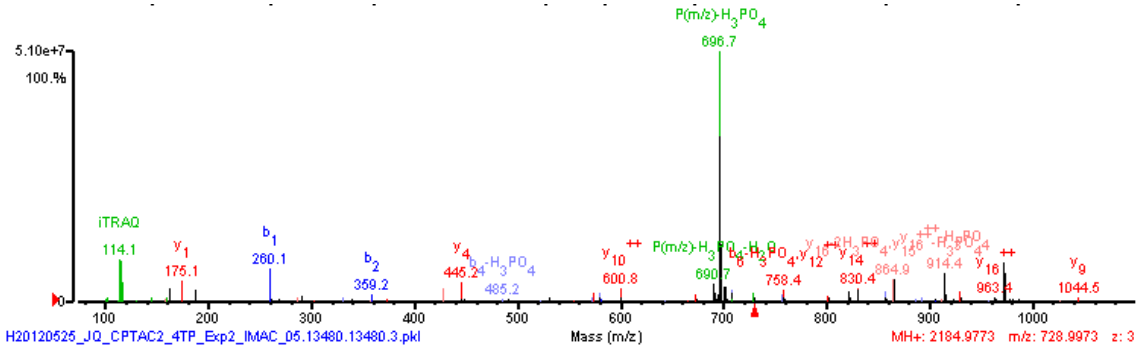

GI-number	Protein name	Gene name	Phosphosite	Sequence
4759050	Ribosomal protein S6 kinase alpha-3	RPS6KA3	T577	AENGLLmtPCYTANFVAPEVLKR

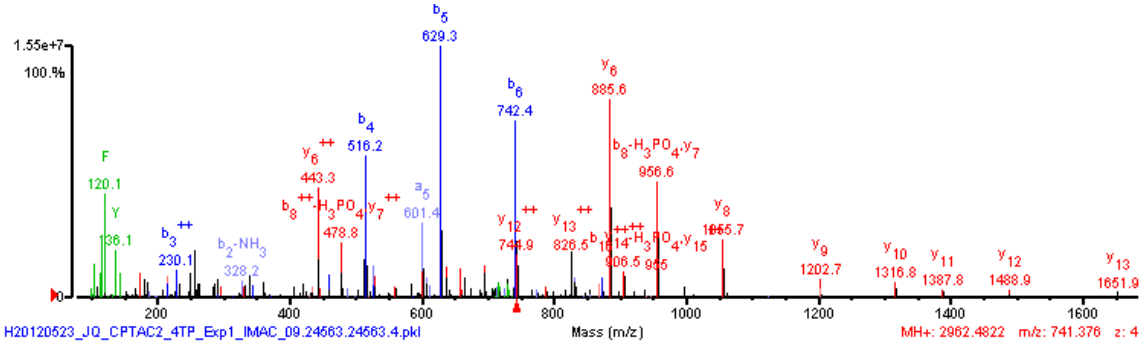

GI-number	Protein name	Gene name	Phosphosite	Sequence
301129165	Death-inducer obliterator 1 isoform c	DIDO1	S1456	RNsVERPAEPVAGAATPSLVEQQK

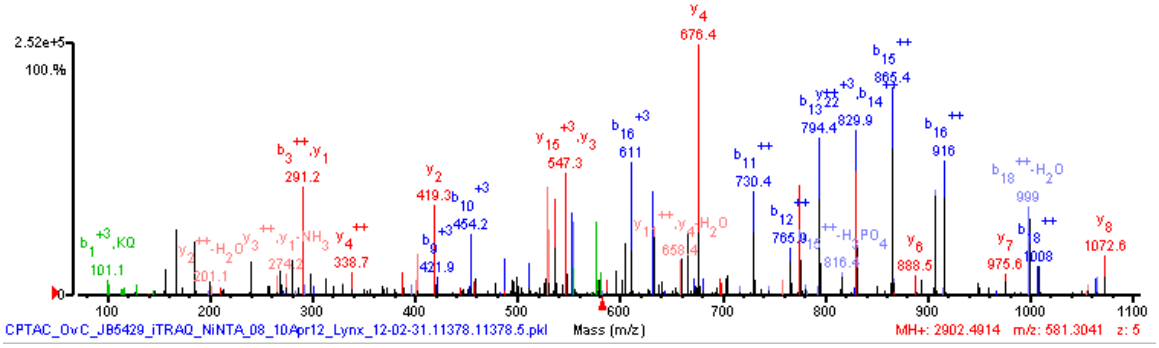

GI-number	Protein name	Gene name	Phosphosite	Sequence
4826730	Serine/threonine-protein kinase mTOR	MTOR	S1261	LHVsTINLQK

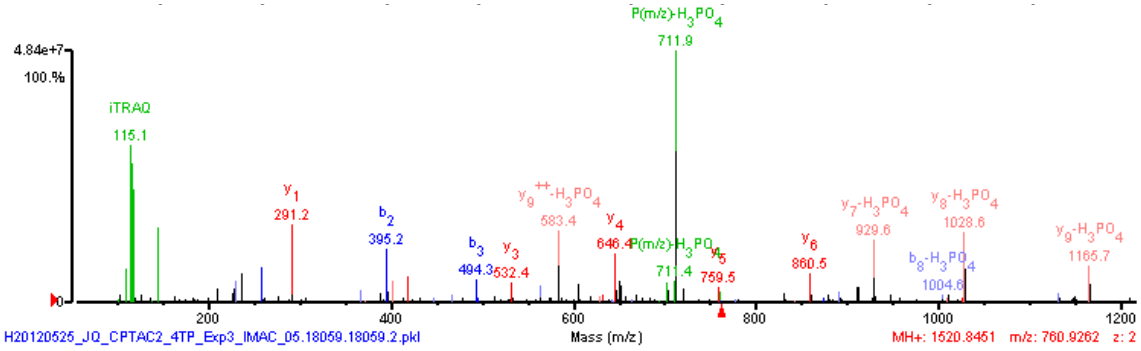

GI-number	Protein name	Gene name	Phosphosite	Sequence
41281496	Mediator of RNA polymerase II transcription subunit 24 isoform 1	MED24	S862	LLsSNEDDANILSSPTDR

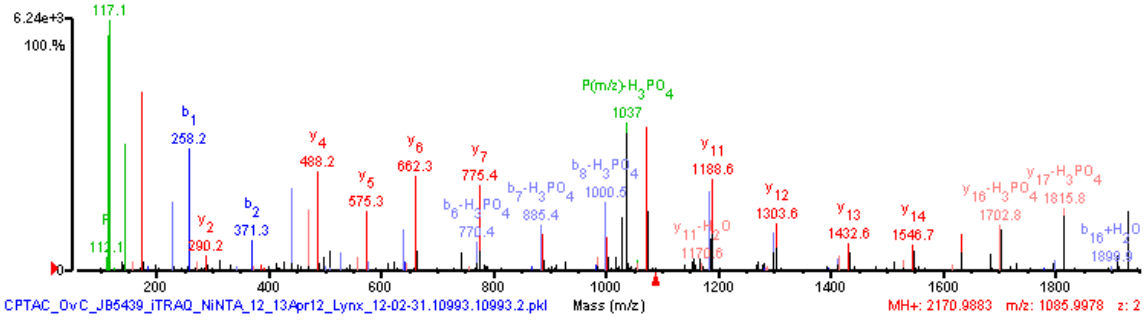

GI-number	Protein name	Gene name	Phosphosite	Sequence
120659782	Serine/threonine-protein kinase D2 isoform A	PRKD2	S214	LGTSEsLPCTAEELSR

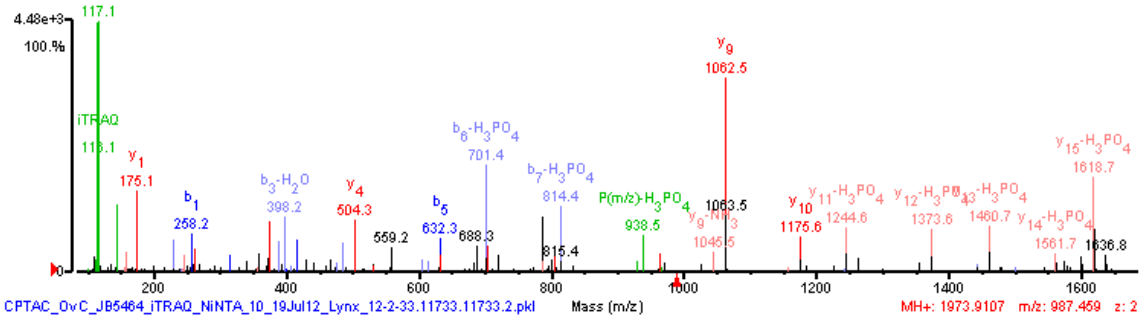

GI-number	Protein name	Gene name	Phosphosite	Sequence
5031689	Serine/threonine-protein kinase D3	PRKD3	S731	IIGEKsFR

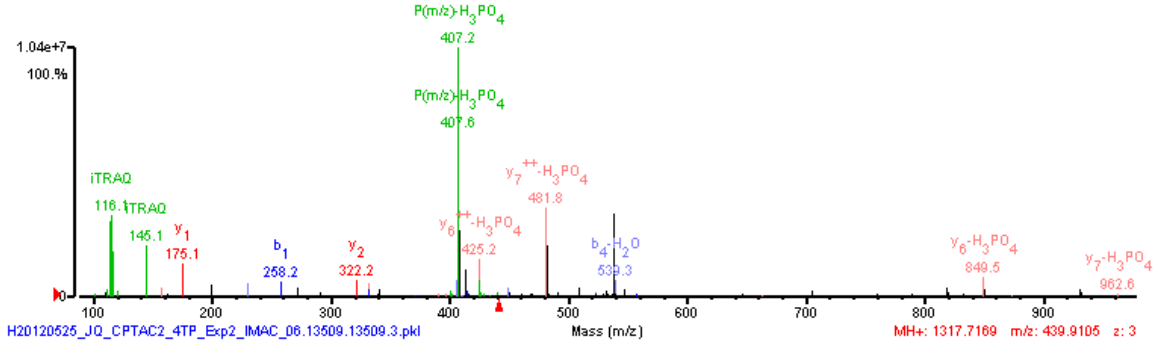

GI-number	Protein name	Gene name	Phosphosite	Sequence
262399371	Transmembrane protein 201 isoform 1	TMEM201	S454	ALsLGTIPSLTR

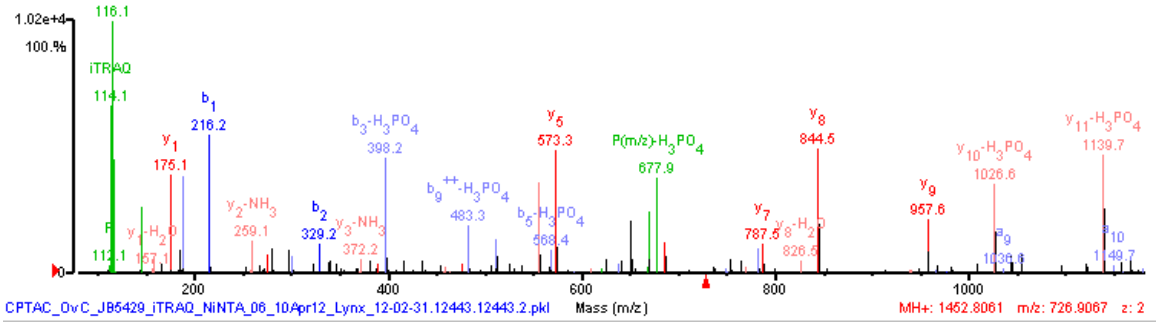

GI-number	Protein name	Gene name	Phosphosite	Sequence
48762920	6-phosphofructokinase, liver type	PFKL	S775	RTLsMDKGF

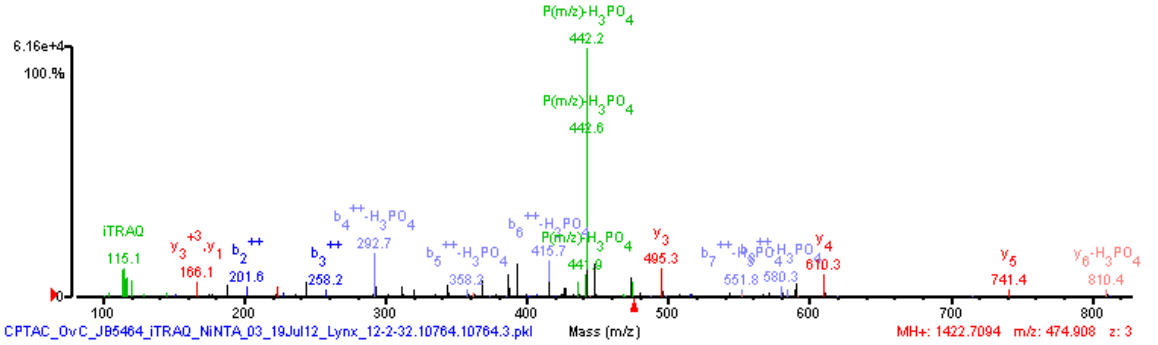

GI-number	Protein name	Gene name	Phosphosite	Sequence
6005884	Translocon-associated protein subunit gamma	SSR3	S105	KLsEADNR

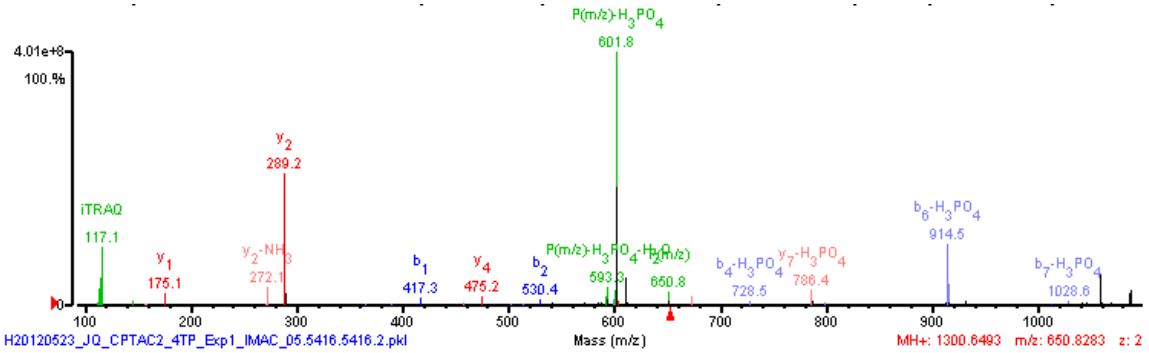

GI-number	Protein name	Gene name	Phosphosite	Sequence
54112429	Dedicator of cytokinesis protein 7	DOCK7	S452	T*T*s*GDDACNLTSFR

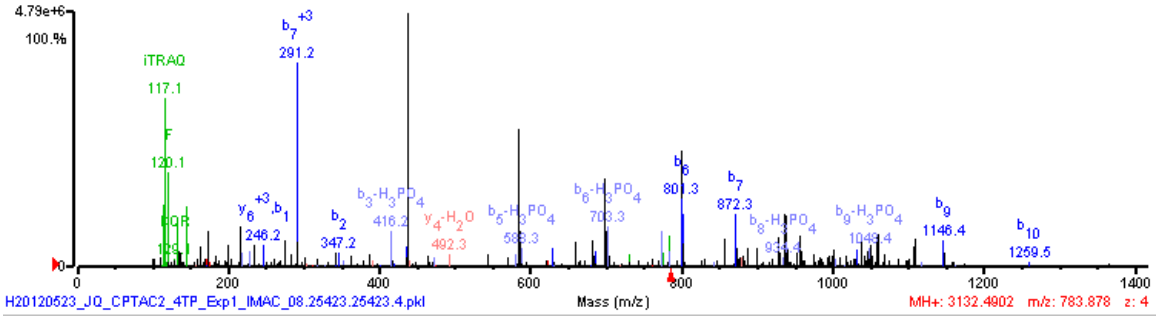

GI-number	Protein name	Gene name	Phosphosite	Sequence
24430146	Nuclear pore complex protein Nup153	NUP153	S516	VQMTsPSSTGSPMFK

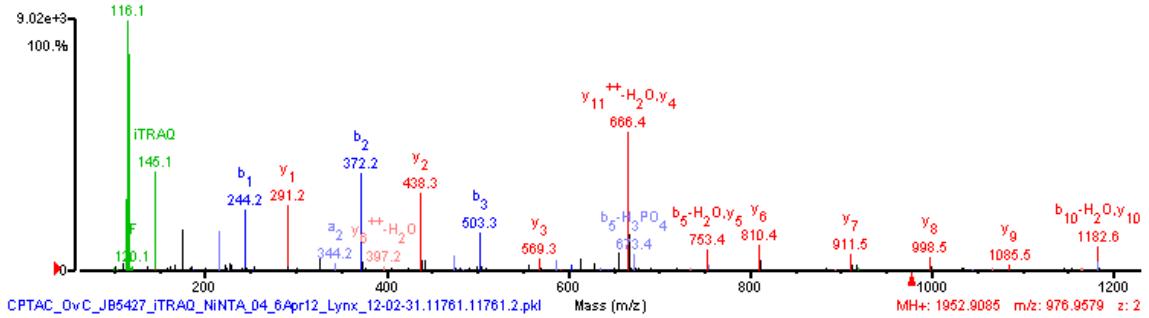

GI-number	Protein name	Gene name	Phosphosite	Sequence
10190682	Chromobox protein homolog 8	CBX8	S256	RQDsDLVQCGVTSPSSAEATGK

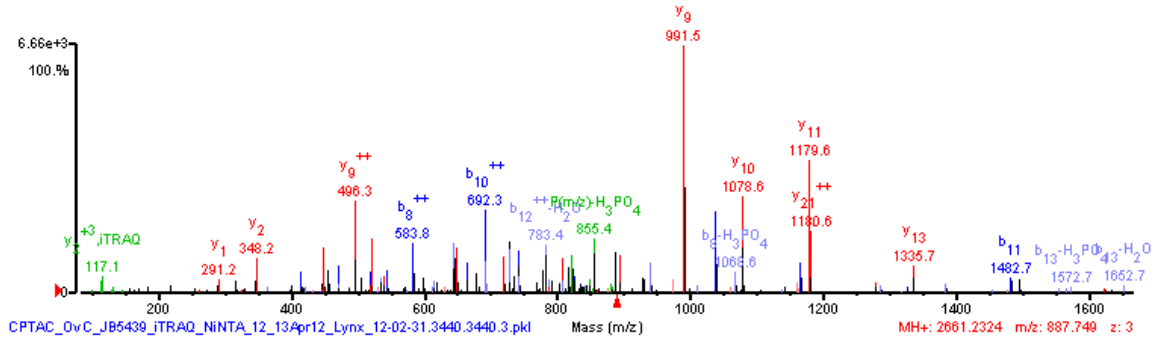

GI-number	Protein name	Gene name	Phosphosite	Sequence
61743954	Neuroblast differentiation-associated protein AHNAK	AHNAK	S135	LKsEDGVEGDLGETQSR

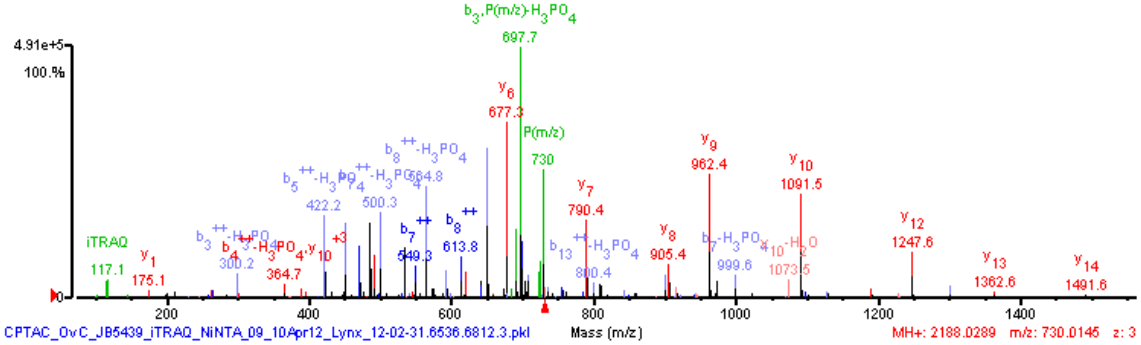

GI-number	Protein name	Gene name	Phosphosite	Sequence
166795297	Cytoplasmic dynein 1 light intermediate chain 1	DYNC1LI1	S516	KPVTVSPTTPT*s*PTEGEAS

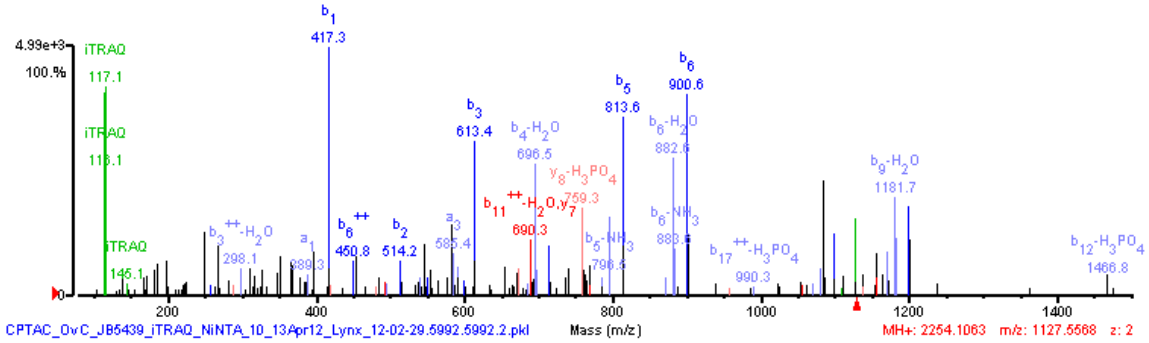

GI-number	Protein name	Gene name	Phosphosite	Sequence
98986457	Host cell factor 1	HCFC1	S666	TITLVKsPISVPGGSALISNLGK

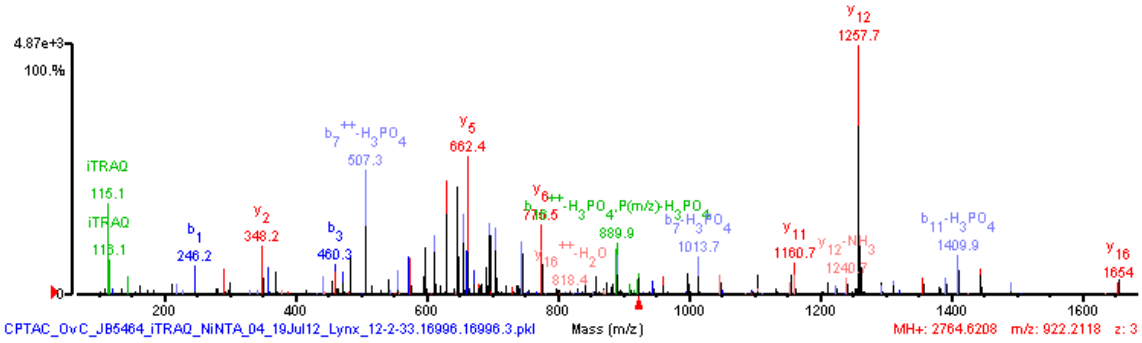

GI-number	Protein name	Gene name	Phosphosite	Sequence
33946327	Nuclear pore complex protein Nup214	NUP214	S1023	TPsIQPSLLPHAAPFAK

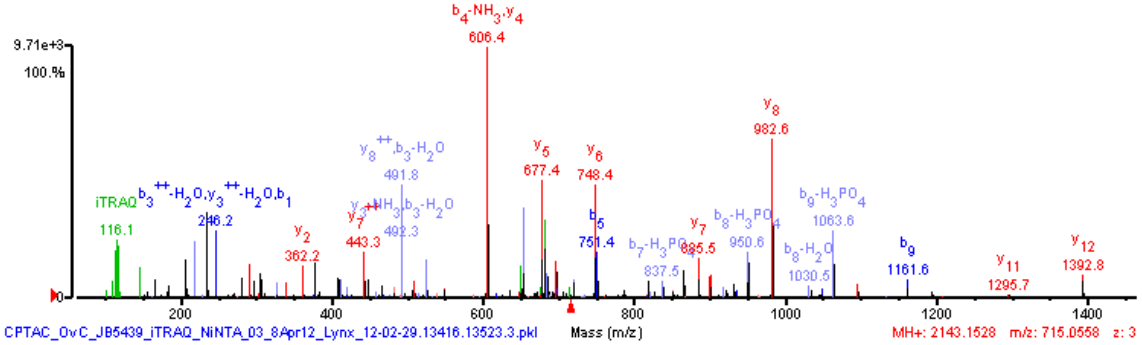

GI-number	Protein name	Gene name	Phosphosite	Sequence
38569480	MKL/myocardin-like protein 2	MKL2	S882	SGEISLPIKEEPsPISK

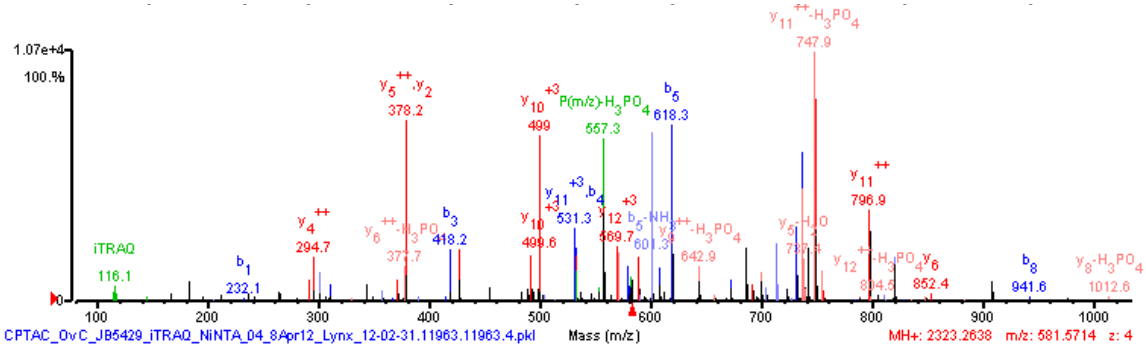

GI-number	Protein name	Gene name	Phosphosite	Sequence
7662647	Phosphatidylserine synthase 1	PTDSS1	S11	TLsKDDVNYK

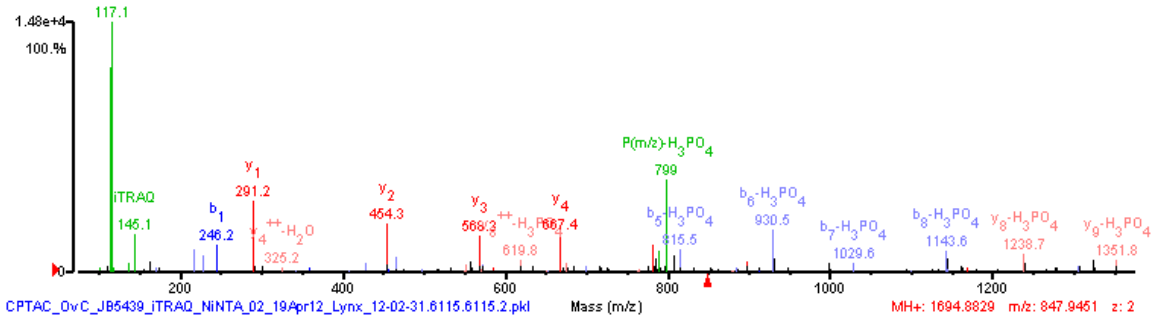

GI-number	Protein name	Gene name	Phosphosite	Sequence
13899253	Uridine-cytidine kinase 1 isoform a	UCK1	S253	TFsEPGDHPGmLTSGKR

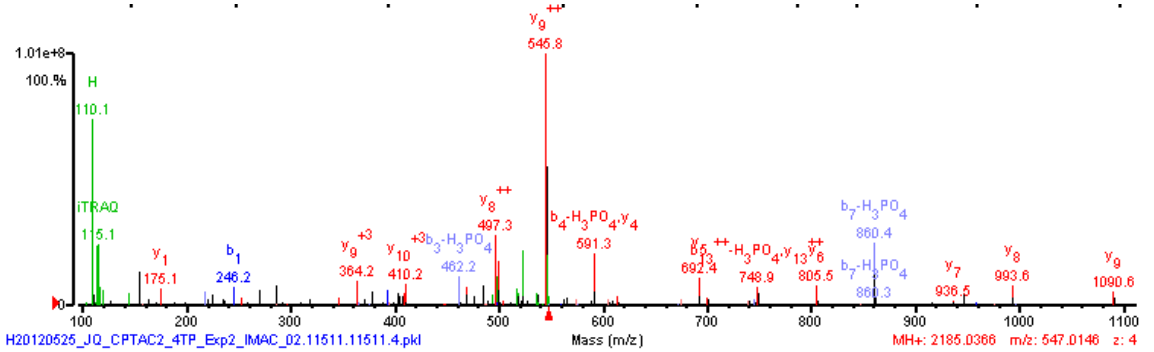

GI-number	Protein name	Gene name	Phosphosite	Sequence
269847874	Probable ATP-dependent RNA helicase YTHDC2	YTHDC2	S1201	Ks*S*ADTEFSDECTTAER

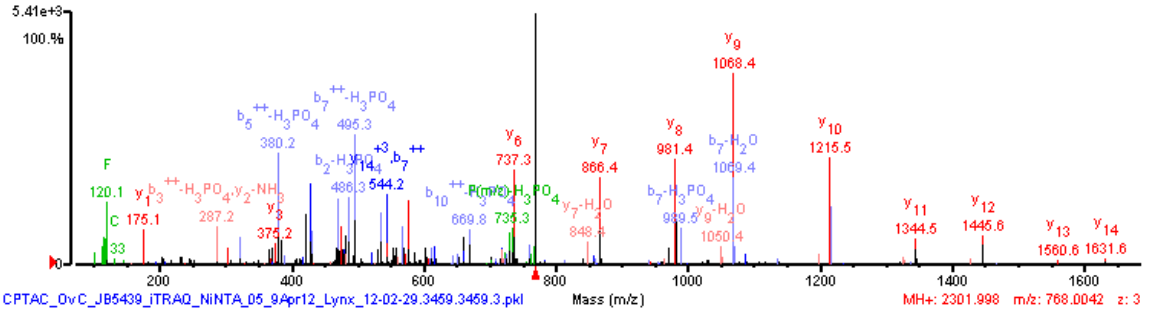

GI-number	Protein name	Gene name	Phosphosite	Sequence
23346420	Nuclear factor related to kappa-B-binding protein	NFRKB	S323	KGsLAALYDLAVLK

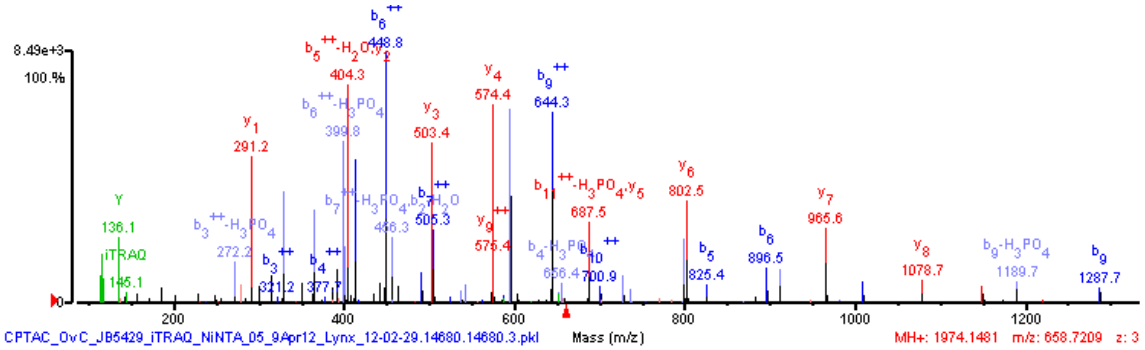

GI-number	Protein name	Gene name	Phosphosite	Sequence
190341074	Pyridoxal-dependent decarboxylase domain-containing protein 1	PDXDC1	S710	sLRGSDALSETSSVSHIEDLEKVER

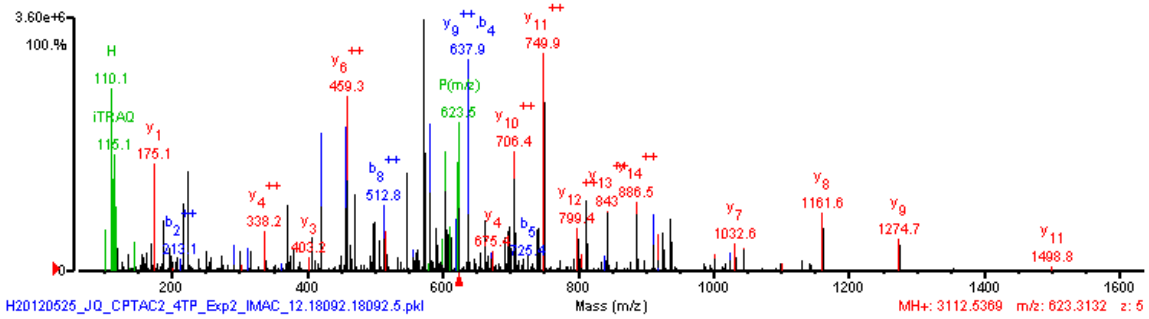

GI-number	Protein name	Gene name	Phosphosite	Sequence
71040094	Arfaptin-1 isoform 1	ARFIP1	S132	KWsLNTYK

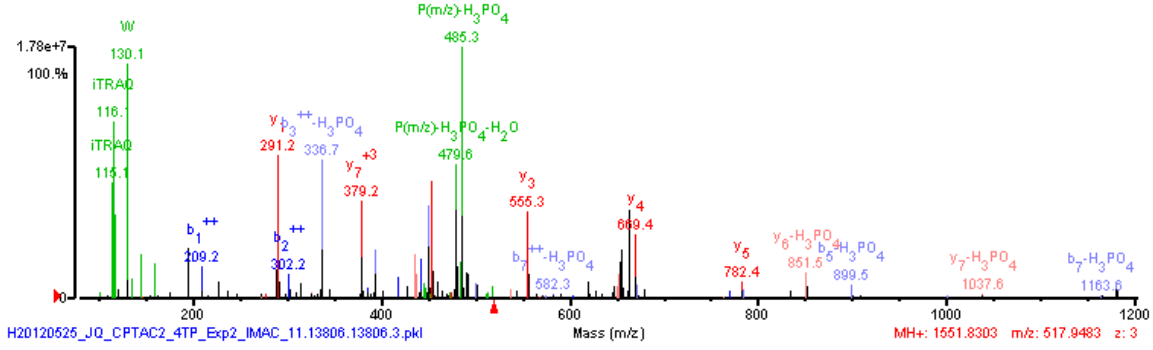

GI-number	Protein name	Gene name	Phosphosite	Sequence
112382252	Spectrin beta chain, brain 1 isoform 2	SPTBN1	S14	TSSISGPLsPAYTGQV PYNYNQLEGR

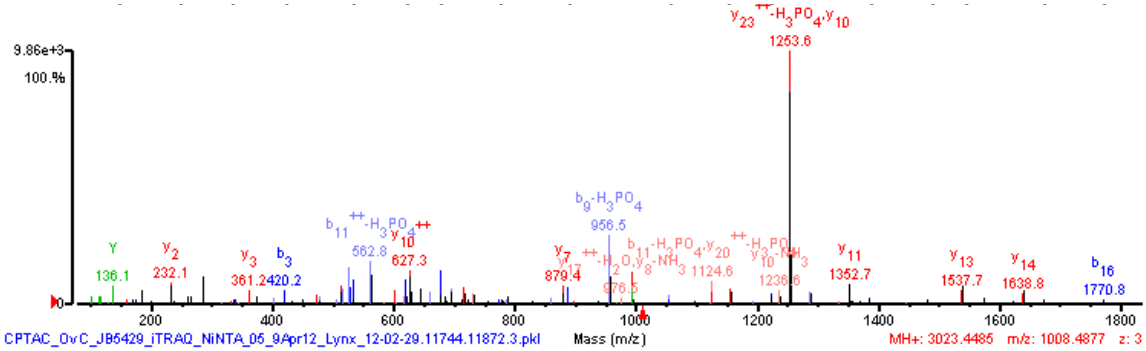

GI-number	Protein name	Gene name	Phosphosite	Sequence
150418007	E3 SUMO-protein ligase RanBP2	RANBP2	S1509	KQsLPATSIPTPASFK

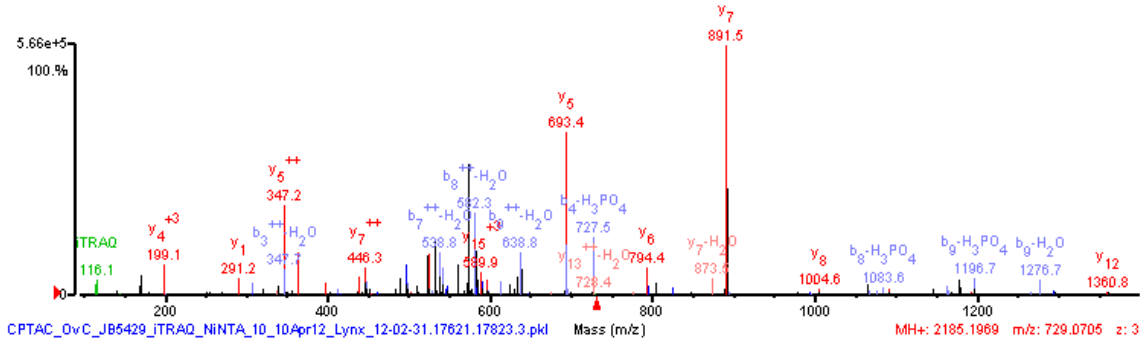

GI-number	Protein name	Gene name	Phosphosite	Sequence
4503579	Band 4.1-like protein 2 isoform a	EPB41L2	S598	sPTKAPHLQLIEGK

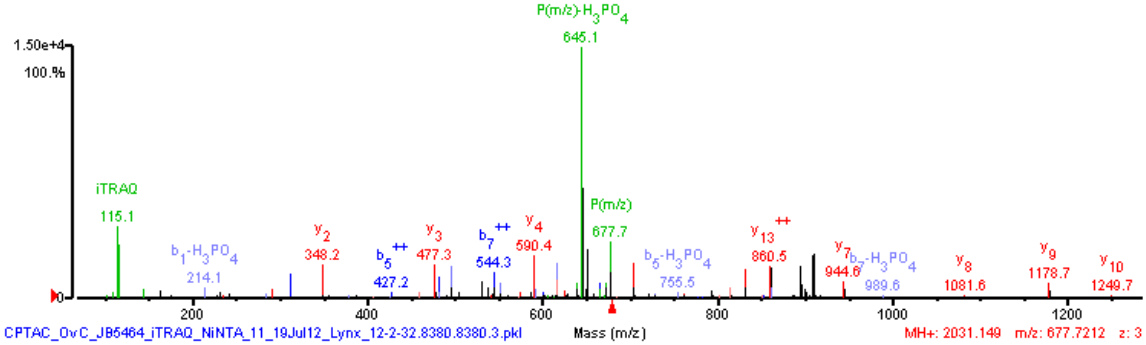

GI-number	Protein name	Gene name	Phosphosite	Sequence
151101292	Thioredoxin-related transmembrane protein 1 precursor	TMX1	S270	QRsLGPSLATDKS

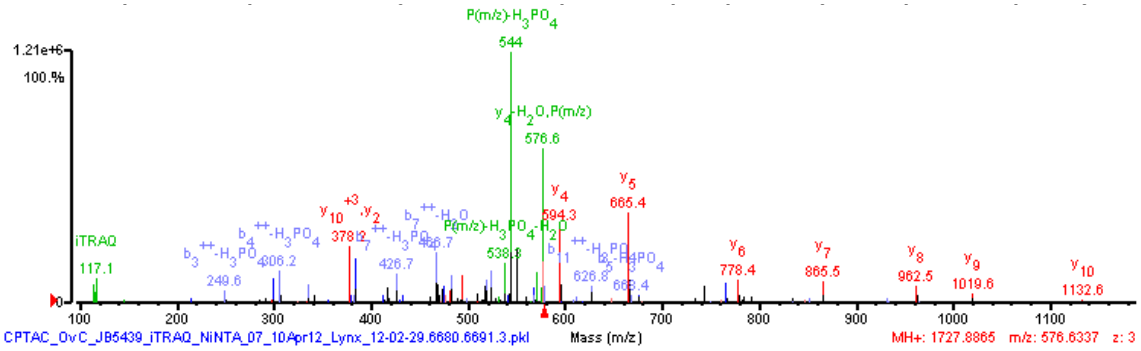

GI-number	Protein name	Gene name	Phosphosite	Sequence
109638745	Transforming growth factor beta-1-induced transcript 1 protein	TGFB1I1	S164	LMAsLSDFR

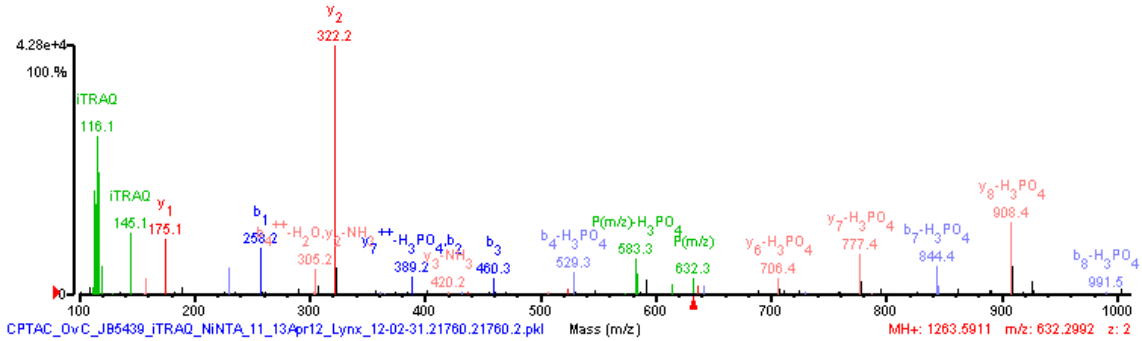

GI-number	Protein name	Gene name	Phosphosite	Sequence
24308171	Zinc finger protein 280C	ZNF280C	S80	SEPHsPGIPEIFR

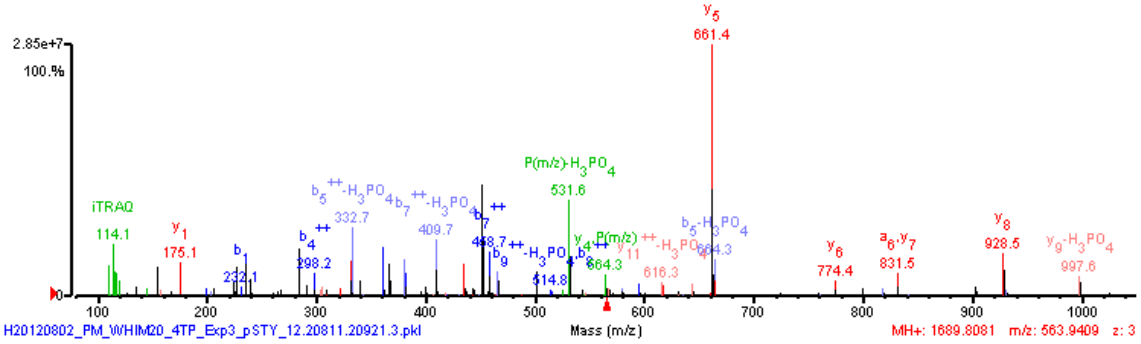

GI-number	Protein name	Gene name	Phosphosite	Sequence
167234419	Thyroid hormone receptor-associated protein 3	THRAP3	S248 S253	ERsPALKsPLQSVVVR

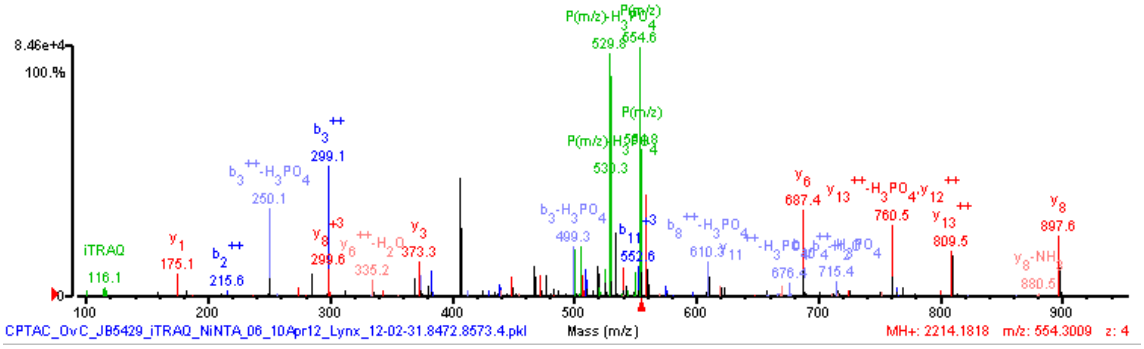

GI-number	Protein name	Gene name	Phosphosite	Sequence
153252201	Zinc transporter ZIP6 isoform 1	SLC39A6	S478	YESQLsTNEEKV DTDDRTEGYLR

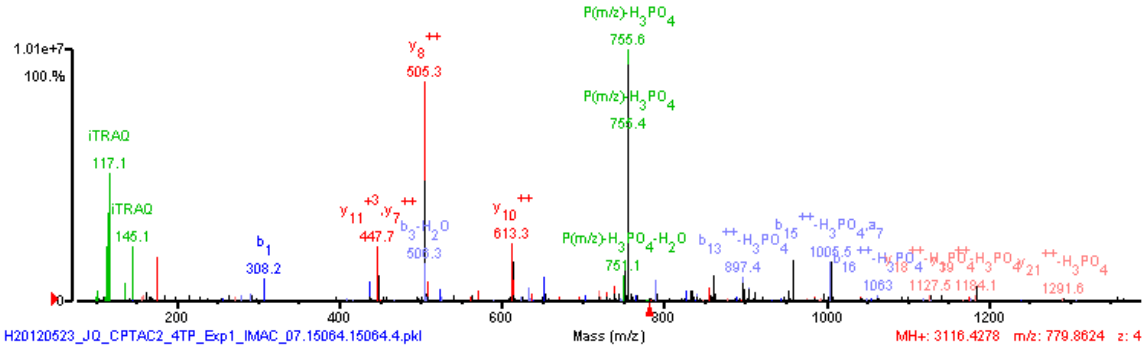

GI-number	Protein name	Gene name	Phosphosite	Sequence
29725609	Epidermal growth factor receptor isoform a precursor	EGFR	T693	ELVEPLtPSGEAPNQALLR

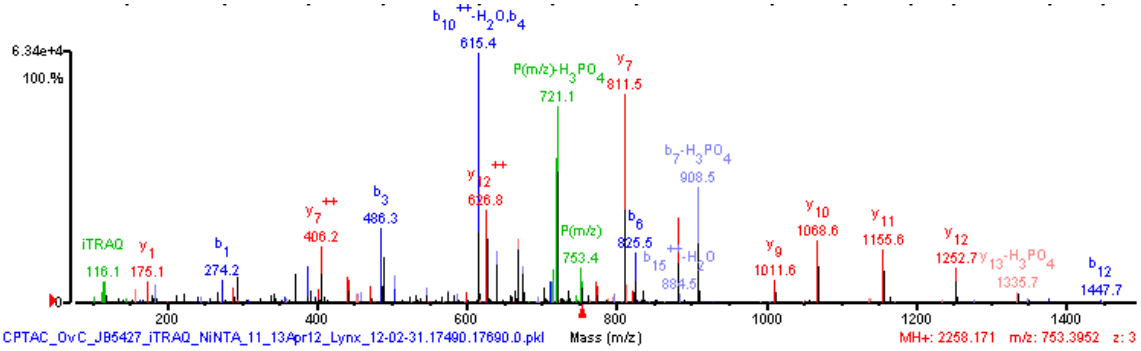

GI-number	Protein name	Gene name	Phosphosite	Sequence
19745184	Cyclic AMP-responsive element-binding protein 1 isoform B	CREB1	S142	ILNDLsSDAPGVPR

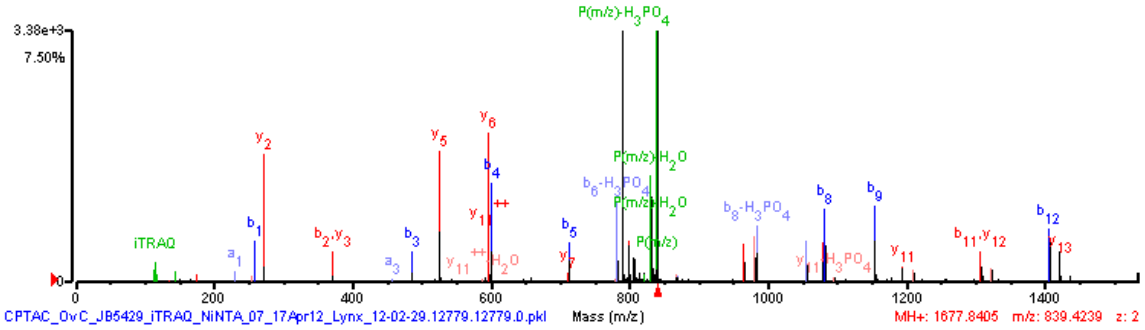

GI-number	Protein name	Gene name	Phosphosite	Sequence
19923723	Ribosomal protein S6 kinase delta-1 isoform a	RPS6KC1	S583	FFPNDDPEAVS*s*PR

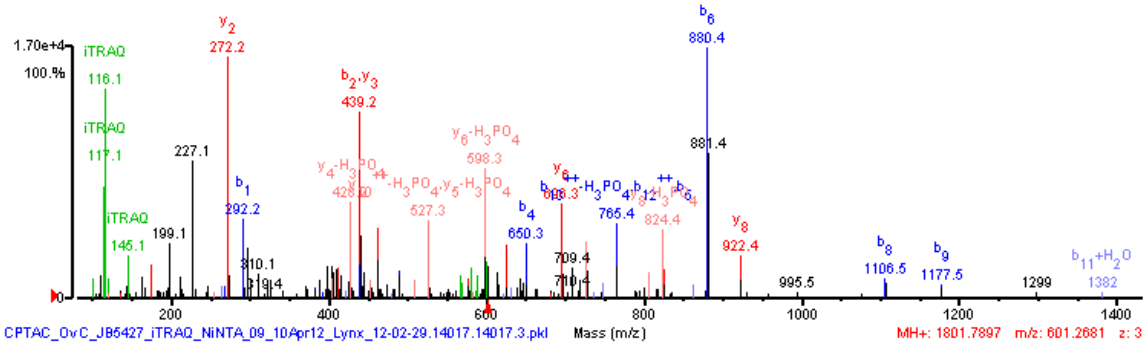

GI-number	Protein name	Gene name	Phosphosite	Sequence
91718899	Mitogen-activated protein kinase 3 isoform 1	MAPK3	Y204	IADPEHDHTGFLTEyVATR

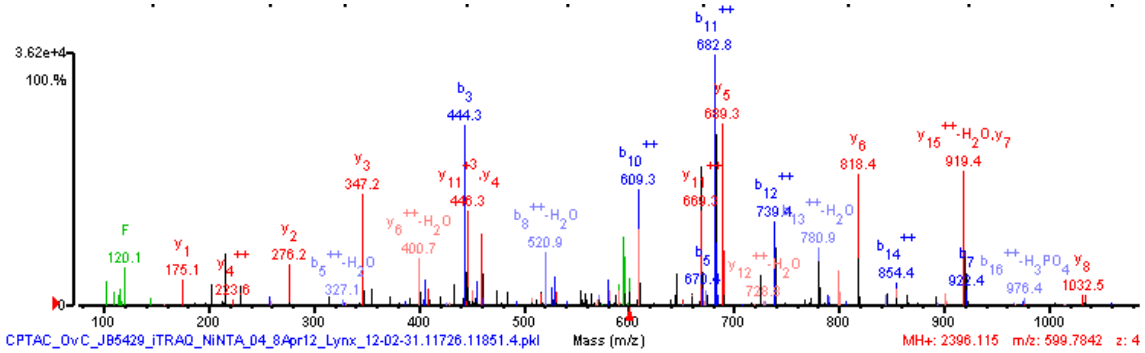

GI-number	Protein name	Gene name	Phosphosite	Sequence
52630440	Peptidyl-prolyl cis-trans isomerase FKBP8	FKBP8	S297	SCsLVLEHQPDNIK

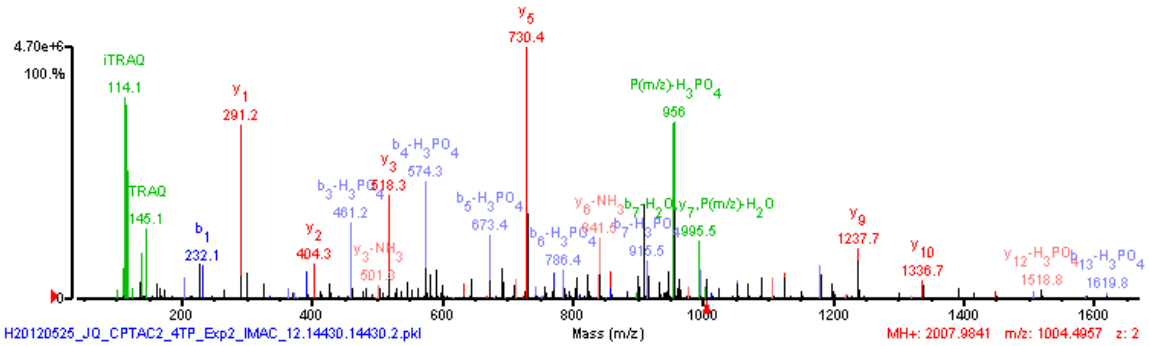

GI-number	Protein name	Gene name	Phosphosite	Sequence
117189975	Heterogeneous nuclear ribonucleoproteins C1/C2 isoform a	HNRNPC	S115	SAAEmYGSVTEHPSPsPLL SSSFDLDYDFQR

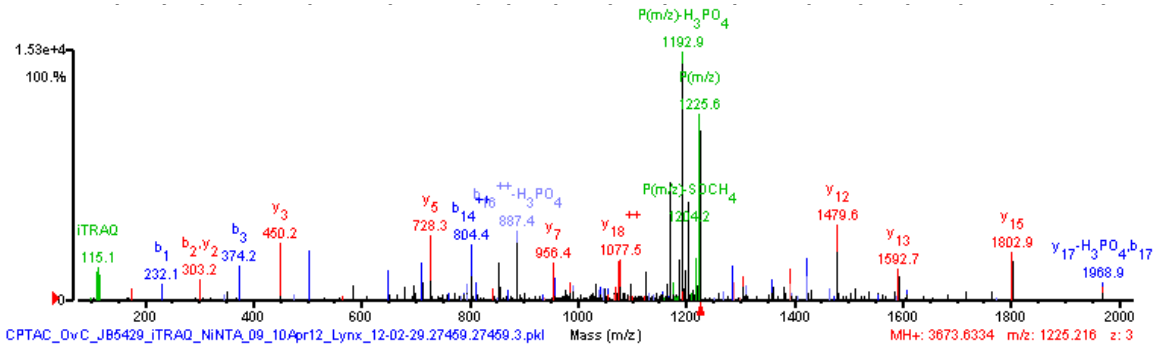

GI-number	Protein name	Gene name	Phosphosite	Sequence
38788260	Nucleosome-remodeling factor subunit BPTF isoform 2	BPTF	S1310	QNsIENDIEEKVSDLASR

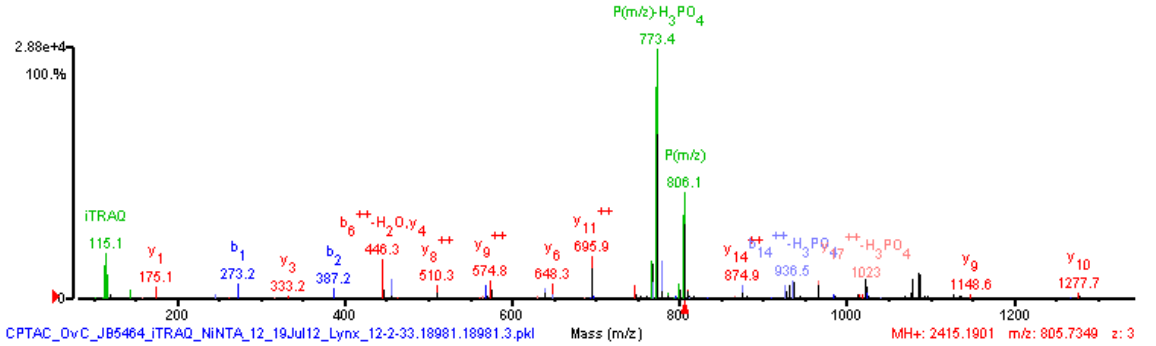

GI-number	Protein name	Gene name	Phosphosite	Sequence
197304775	TBC1 domain family member 5 isoform b	TBC1D5	S522	SEsmPVQLNK

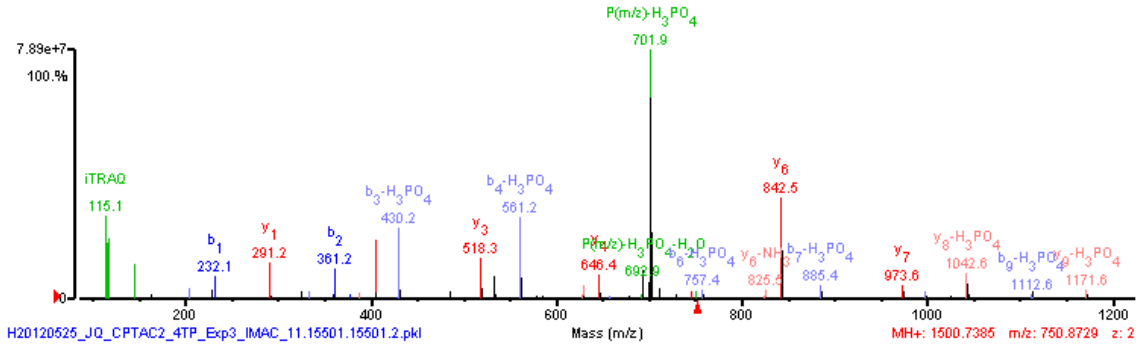

GI-number	Protein name	Gene name	Phosphosite	Sequence
14141152	Heterogeneous nuclear ribonucleoprotein M isoform a	HNRNPM	S637	GNFGGSFAGsFGGAGGHAPGVAR

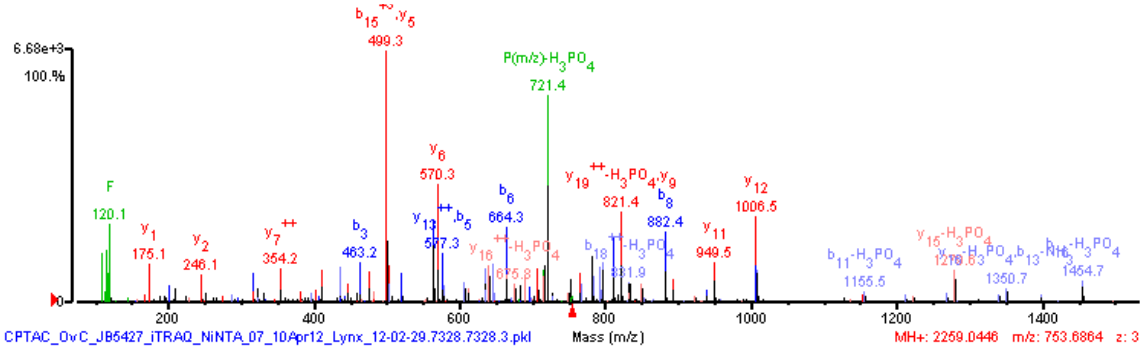

GI-number	Protein name	Gene name	Phosphosite	Sequence
183396804	Regulation of nuclear pre-mRNA domain-containing protein 2	RPRD2	S1099	RmsGEPIQTVESIRVPGK

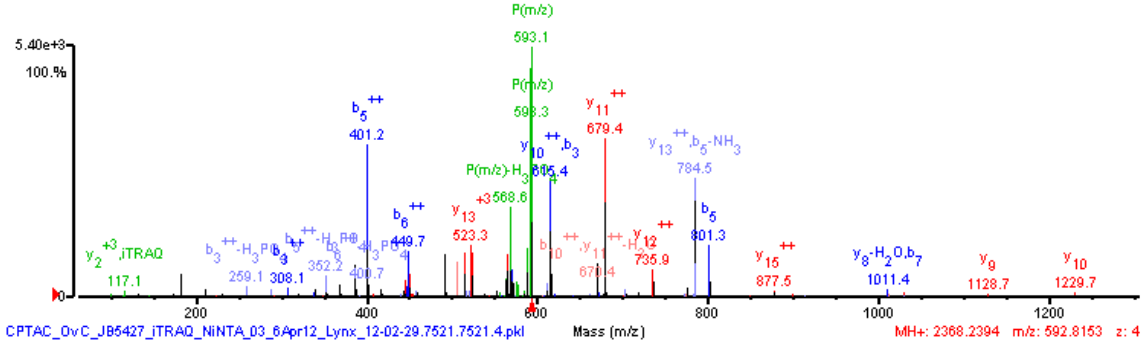

GI-number	Protein name	Gene name	Phosphosite	Sequence
20070205	Ladinin-1	LAD1	S356	LPPVTLQVKIPSKEEADmSsPTQR

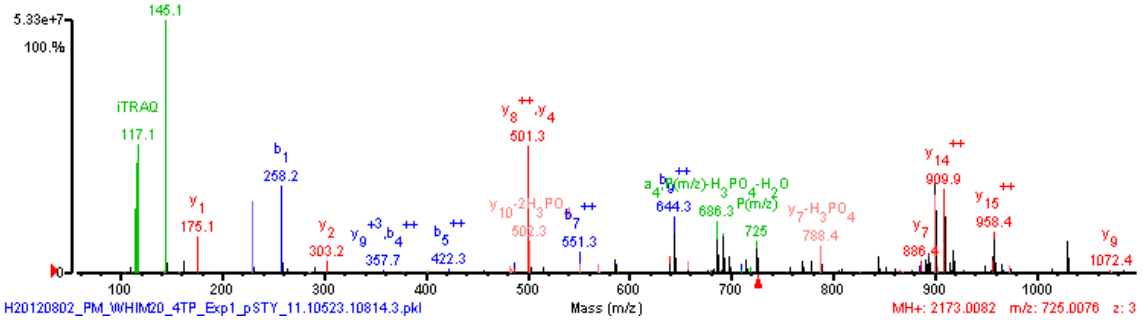

GI-number	Protein name	Gene name	Phosphosite	Sequence
13559514	Phosphatidylinositol 4-kinase type 2-alpha	PI4K2A	S462	SSsESYTQSFQSR

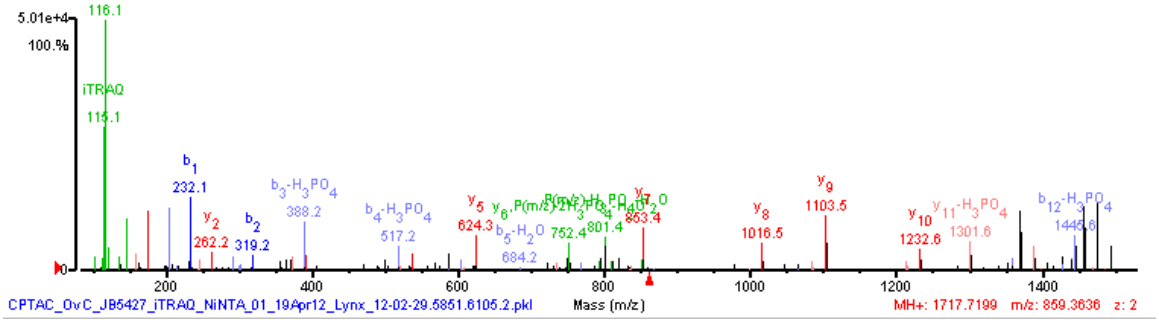

GI-number	Protein name	Gene name	Phosphosite	Sequence
21626466	Matrin-3 isoform a	MATR3	S188	RDsFDDRGPSLNPVLDYDHGSR

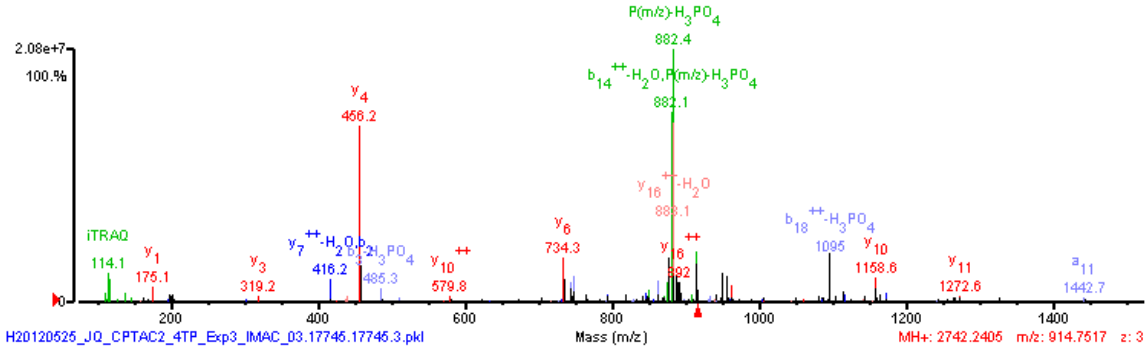

GI-number	Protein name	Gene name	Phosphosite	Sequence
71274144	AT-hook DNA-binding motif-containing protein 1	AHDC1	S1187	ANsEASSSEGQSSLSSLEK

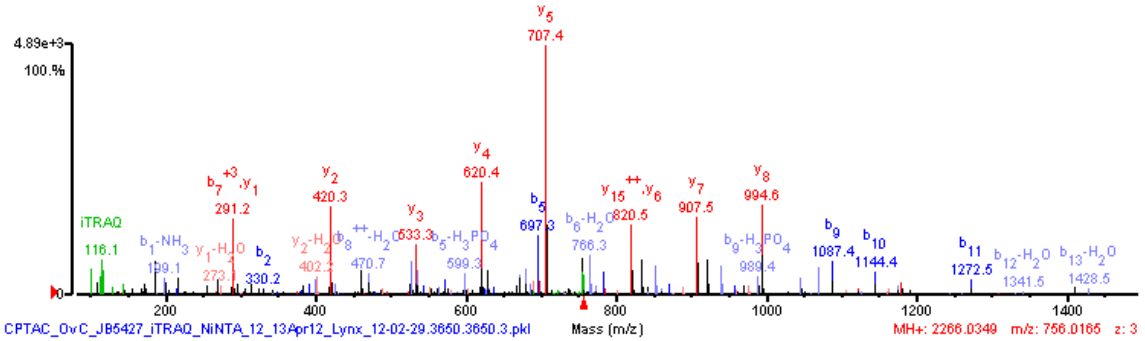

GI-number	Protein name	Gene name	Phosphosite	Sequence
10835069	Bcl2 antagonist of cell death	BAD	S75	HSsYPAGTEDDEGMGEEPSPFR

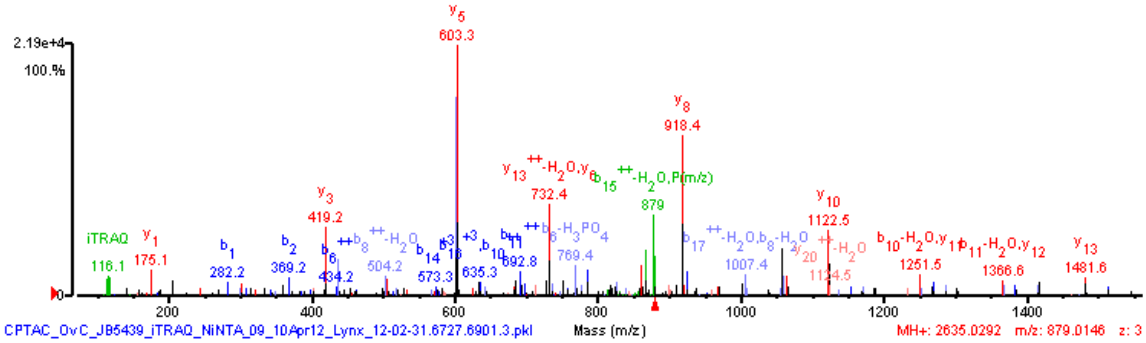

GI-number	Protein name	Gene name	Phosphosite	Sequence
4505581	Interferon-inducible double stranded RNA-dependent protein kinase activator A	PRKRA	S18	EDsGTFSLGK

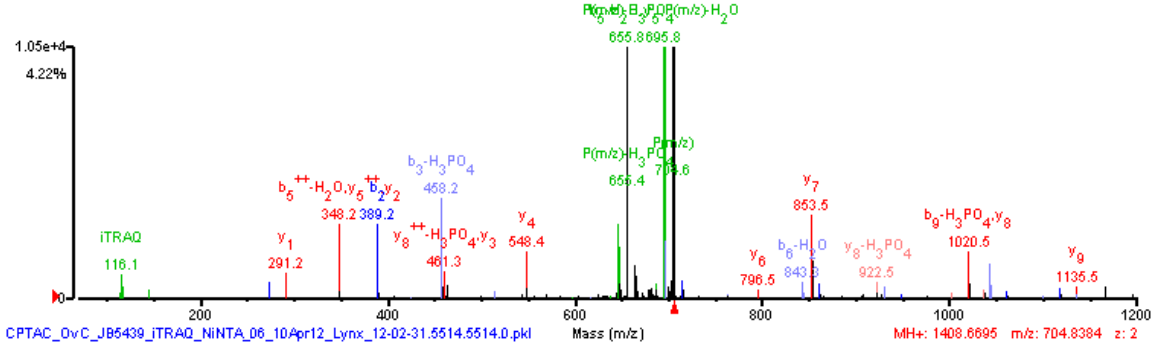

GI-number	Protein name	Gene name	Phosphosite	Sequence
57634536	La-related protein 4B	LARP4B	S568	TLsADASVNTLPVVVSR

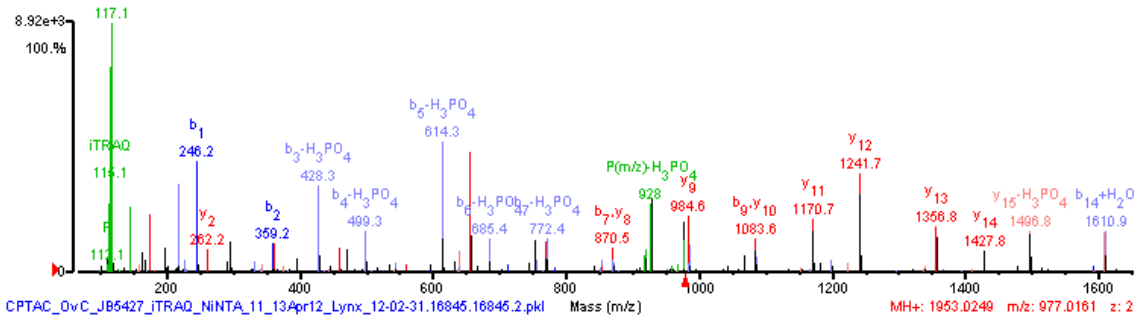

GI-number	Protein name	Gene name	Phosphosite	Sequence
209180457	Target of Myb protein 1 isoform 2	LOC100128526	T164	GLEFPMTDLDMLSPIHtPQR

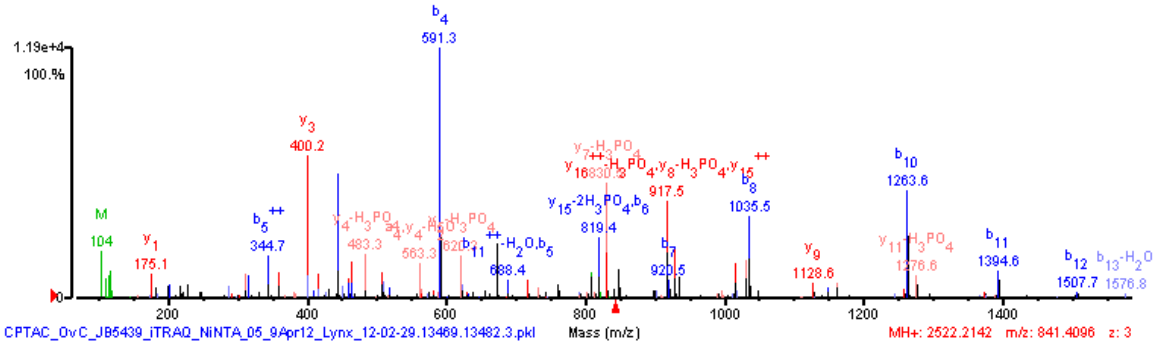

GI-number	Protein name	Gene name	Phosphosite	Sequence
150417986	Brefeldin A-inhibited guanine nucleotide-exchange protein 2	ARFGEF2	S1024	EGsLKGHTLAGEEFM GLGLGNLVSGGVDKR

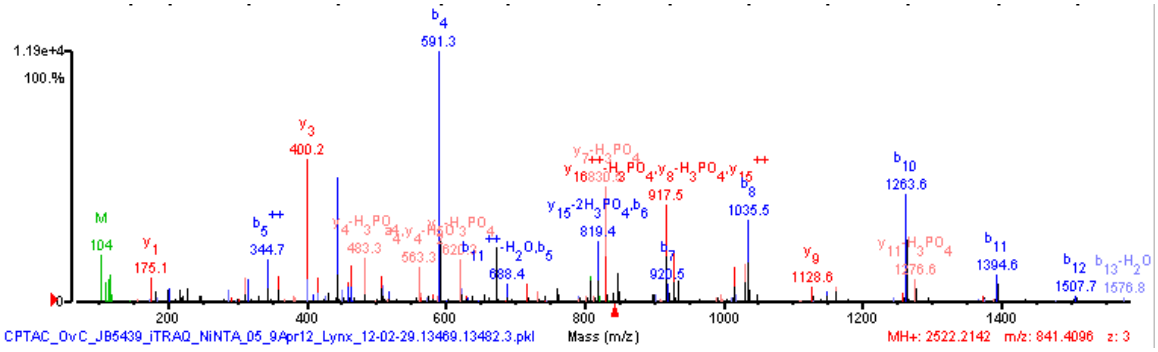

GI-number	Protein name	Gene name	Phosphosite	Sequence
52426745	E3 ubiquitin-protein ligase CBL	CBL	S619	ELTNRHsLPFSLPSQMEPR

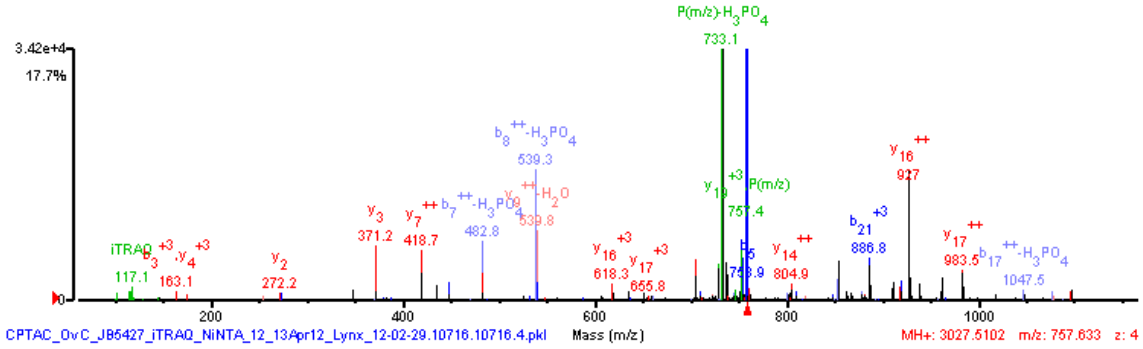

GI-number	Protein name	Gene name	Phosphosite	Sequence
47519639	Microtubule-associated protein 4 isoform 1	MAP4	S825	sPSTLLPK

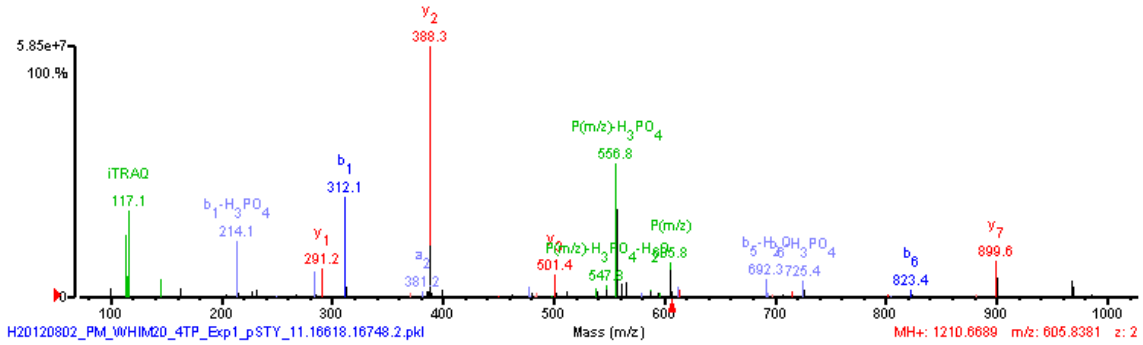

GI-number	Protein name	Gene name	Phosphosite	Sequence
5453710	LIM and SH3 domain protein 1	LASP1	S146	mGPSGGEGmEPERRDsQDGSSYR

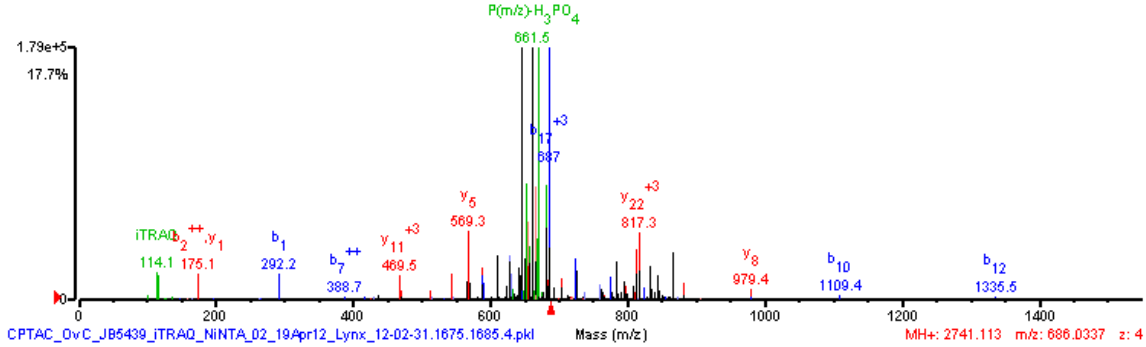

GI-number	Protein name	Gene name	Phosphosite	Sequence
20986531	Mitogen-activated protein kinase 1	MAPK1	Y187	VADPDHDHTGFLTEyVATR

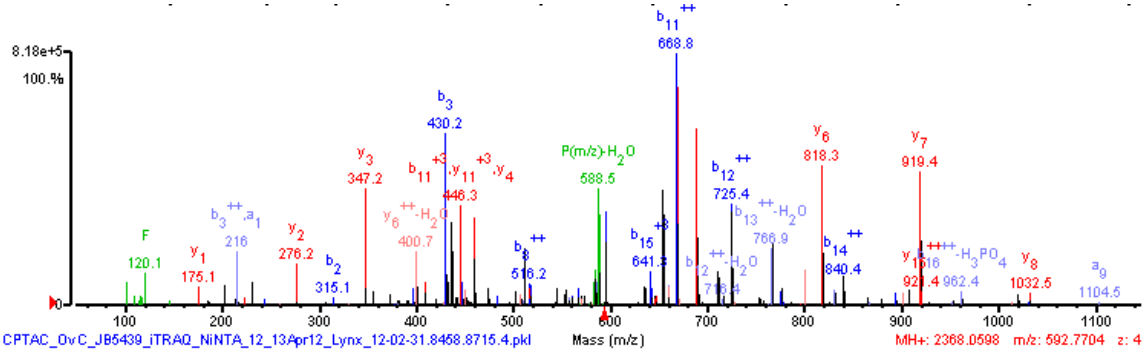

GI-number	Protein name	Gene name	Phosphosite	Sequence
31377782	Protein kinase C delta type	PRKCD	S304	RSDs*AS*SEPVGIYQGFEKK

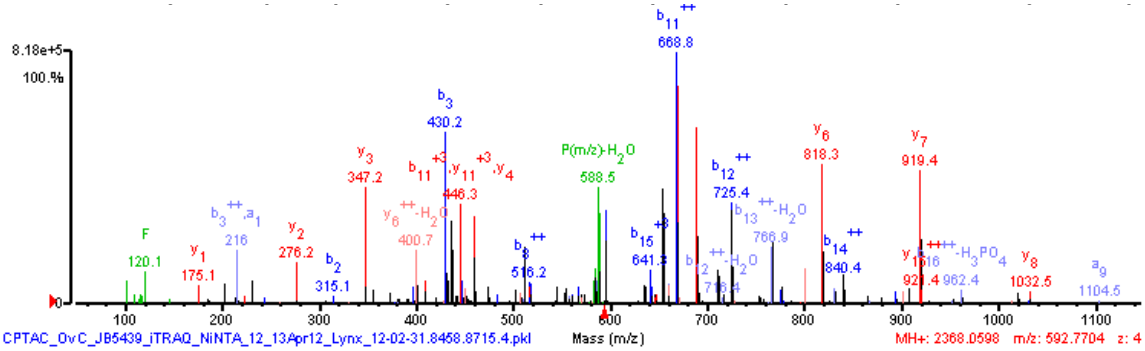

GI-number	Protein name	Gene name	Phosphosite	Sequence
48928019	NEDD4-binding protein 1	N4BP1	S300	KQFsLENVQEGEILHDAK

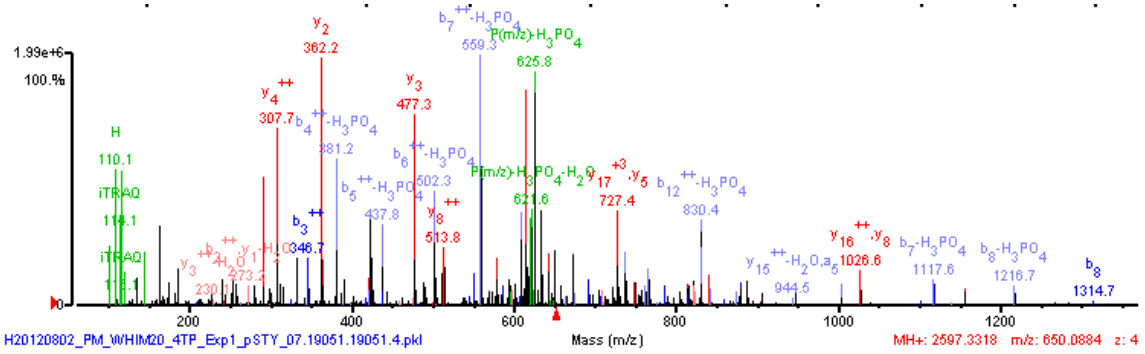

GI-number	Protein name	Gene name	Phosphosite	Sequence
221219024	Pleckstrin homology-like domain family B member 1 isoform a	PHLDB1	S430	TFsDGLATR

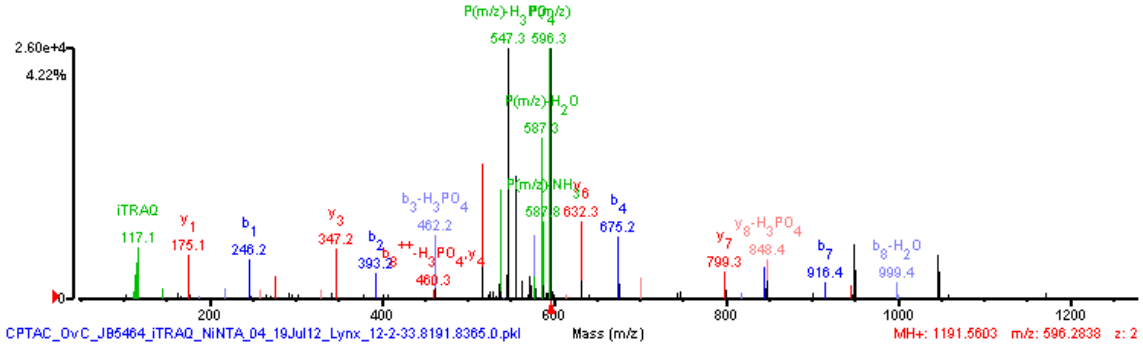

GI-number	Protein name	Gene name	Phosphosite	Sequence
114688046	TBC1 domain family member 4	TBC1D4	S566	sLTSSLENIFSR

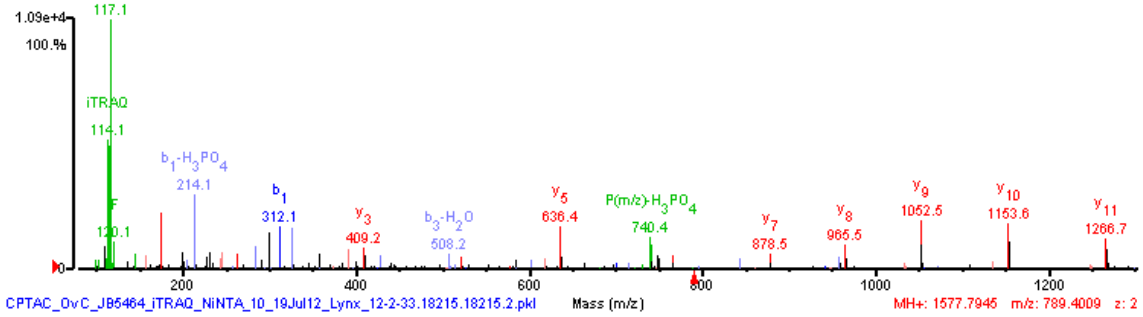

GI-number	Protein name	Gene name	Phosphosite	Sequence
157384982	Transducin-like enhancer protein 3 isoform a	TLE3	T328	NDAPtPGTSTTPGLR

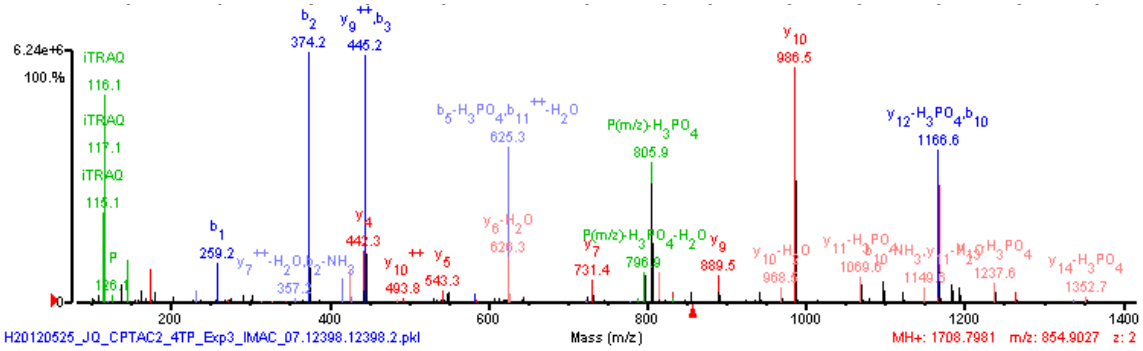

GI-number	Protein name	Gene name	Phosphosite	Sequence
333108224	Afadin isoform 1	MLLT4	S215	TIsNPEVVMK

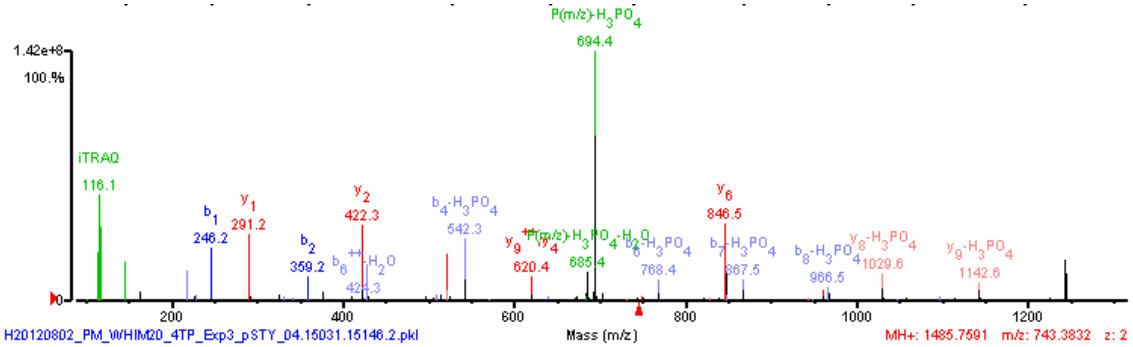

GI-number	Protein name	Gene name	Phosphosite	Sequence
48928019	NEDD4-binding protein 1	N4BP1	T242	NKAGtPVSELTK

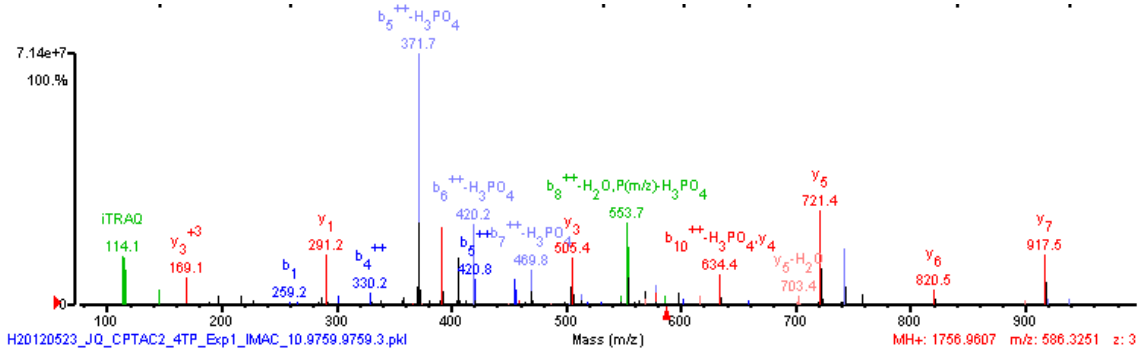

GI-number	Protein name	Gene name	Phosphosite	Sequence
194595509	Spectrin alpha chain, brain isoform 1	SPTAN1	S1029	KLDPAQsASRENL LEEQGSIALR

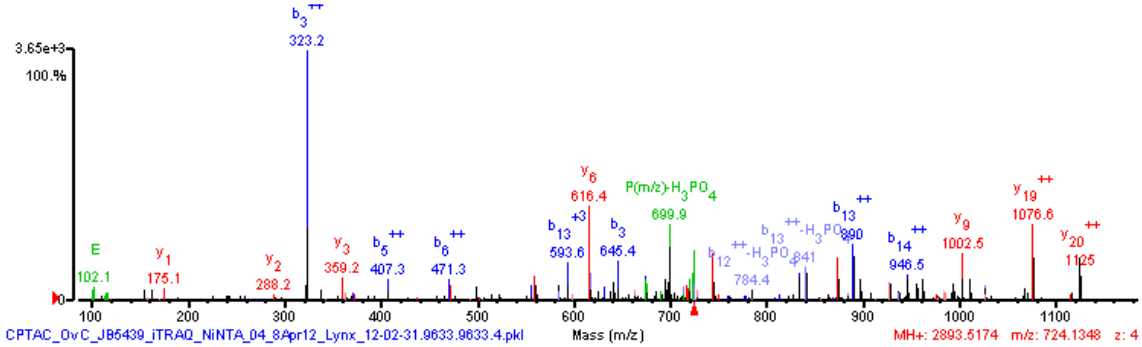

GI-number	Protein name	Gene name	Phosphosite	Sequence
4507641	Tumor protein D53 isoform 1	TPD52L1	S149	NSPTFKsFEERVETTVTSLK

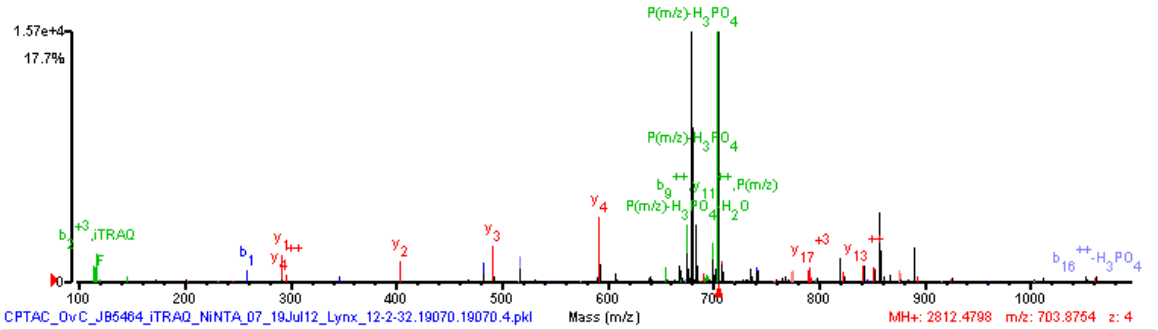

GI-number	Protein name	Gene name	Phosphosite	Sequence
11321634	CD2-associated protein	CD2AP	S458	sVDFDSLTVR

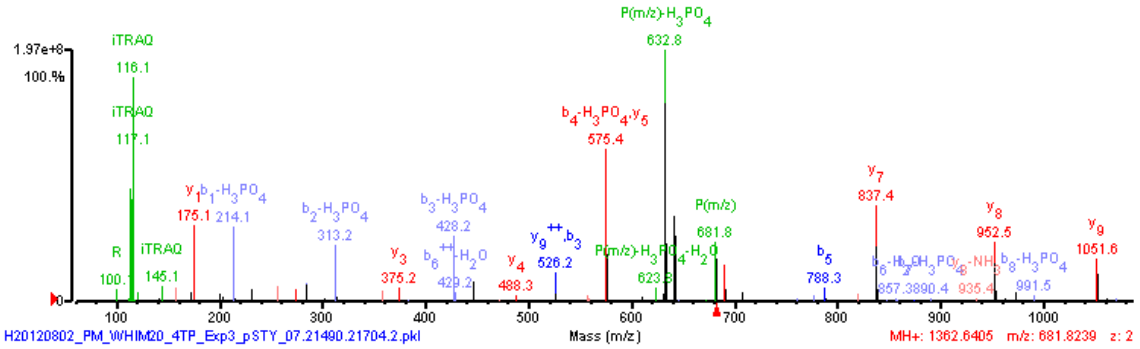

GI-number	Protein name	Gene name	Phosphosite	Sequence
115430211	Phosphatase and actin regulator 4 isoform 1	PHACTR4	S291	NSNPVIAELSQAINS GTLLSKPsPPLPPKR

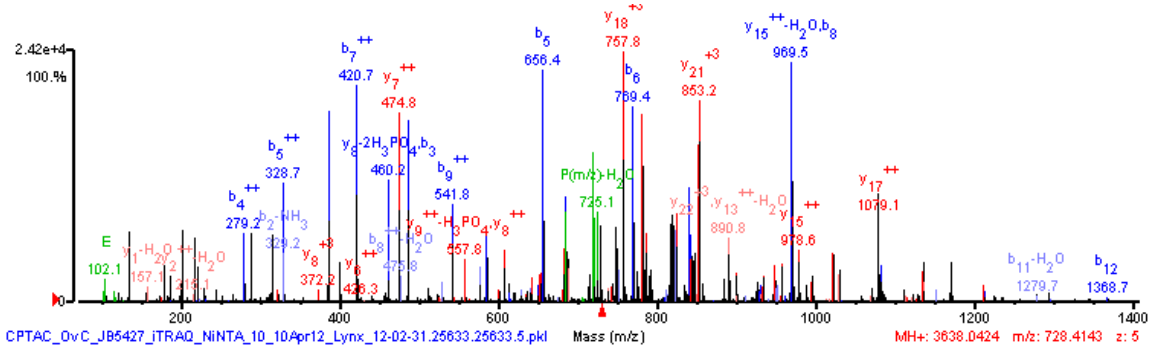

GI-number	Protein name	Gene name	Phosphosite	Sequence
92087055	PERQ amino acid-rich with GYF domain-containing protein 1	GIGYF1	S137	sIEEGDGAFGR

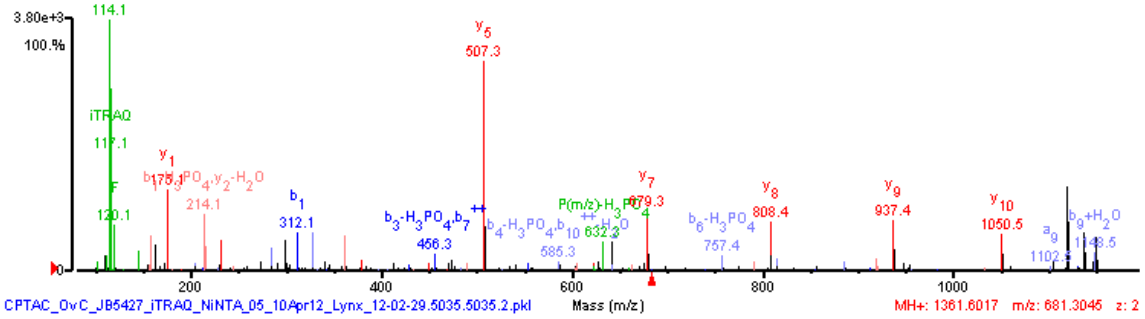

GI-number	Protein name	Gene name	Phosphosite	Sequence
148368962	Pseudopodium-enriched atypical kinase 1	SGK269	S1217	GLDIESYDsLERPLRK

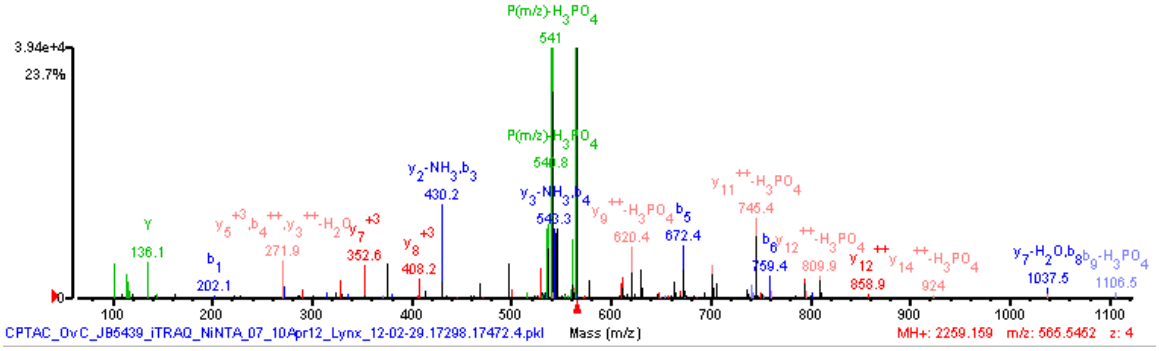

GI-number	Protein name	Gene name	Phosphosite	Sequence
302699245	Eukaryotic translation initiation factor 4 gamma 1 isoform 6	EIF4G1	S1084	ITKPGsIDSNNQLFAPGGR

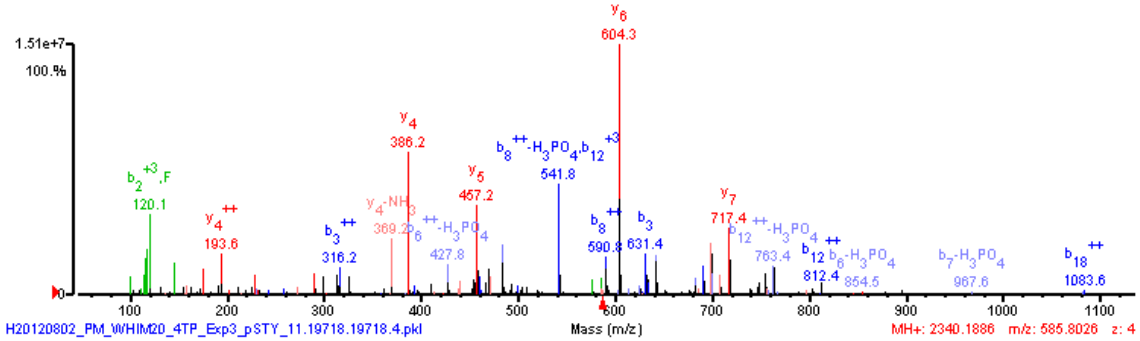

GI-number	Protein name	Gene name	Phosphosite	Sequence
196114951	Tyrosine-protein phosphatase non-receptor type 12 isoform 1	PTPN12	S449	KVPLQEGPKsFDGNTLLNR

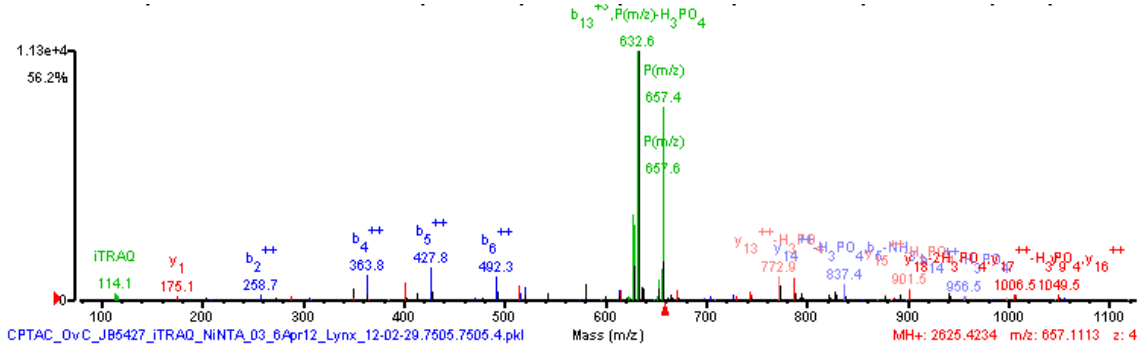

GI-number	Protein name	Gene name	Phosphosite	Sequence
61743954	Neuroblast differentiation-associated protein AHNAK	AHNAK	S379	LKGPQITGPsLEGDLGLK

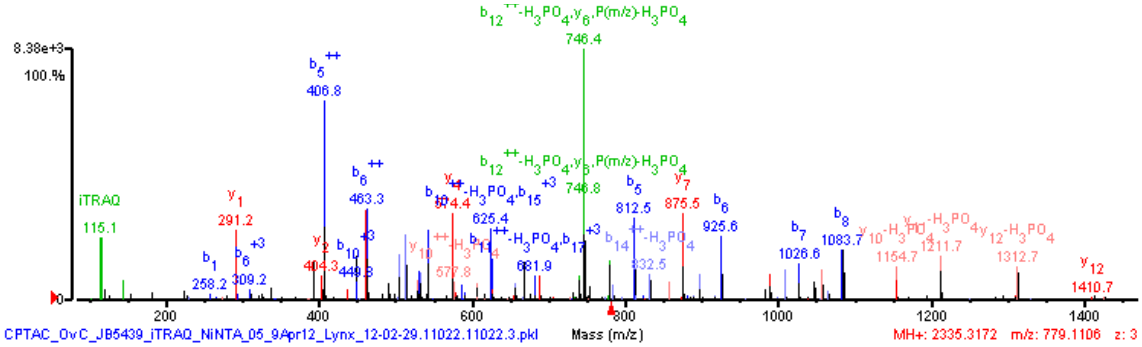

GI-number	Protein name	Gene name	Phosphosite	Sequence
115298682	Protein PRRC2C	BAT2L2	T2673	AFGSGIDIKPGtPPIAGR

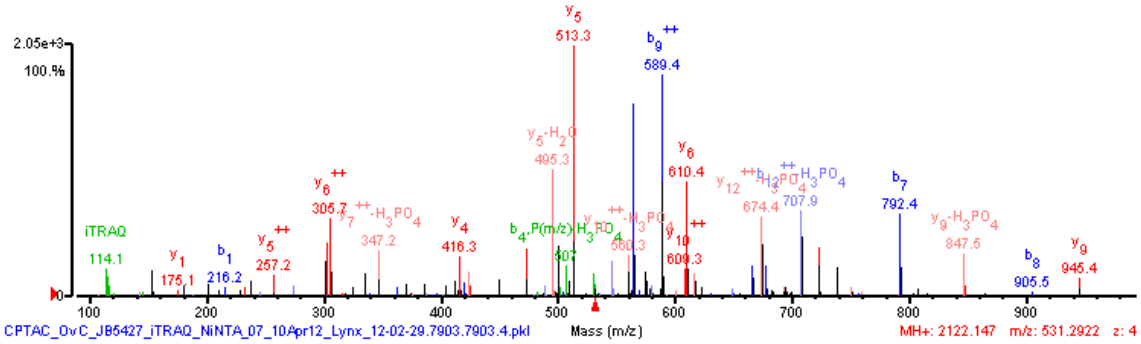

GI-number	Protein name	Gene name	Phosphosite	Sequence
21070997	Stromal interaction molecule 1 precursor	STIM1	S575	LIEGVHPGSLVE KLPDsPALAK

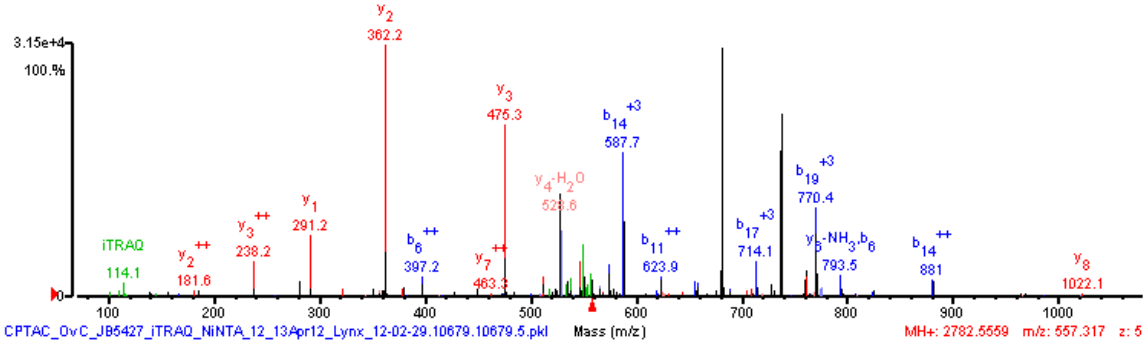

GI-number	Protein name	Gene name	Phosphosite	Sequence
115298682	Protein PRRC2C	BAT2L2	T2682	ST*t*PTSSPFR

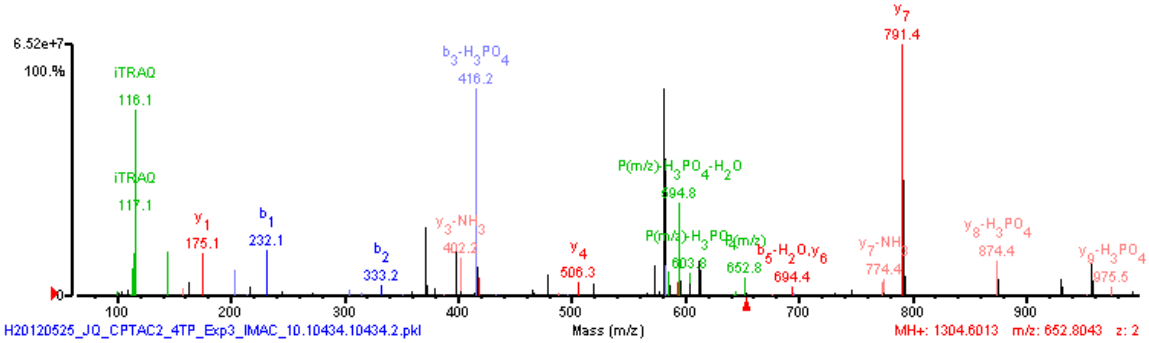

GI-number	Protein name	Gene name	Phosphosite	Sequence
10863895	Thymosin beta-10	TMSB10	T23	TEtQEKNTLPTK

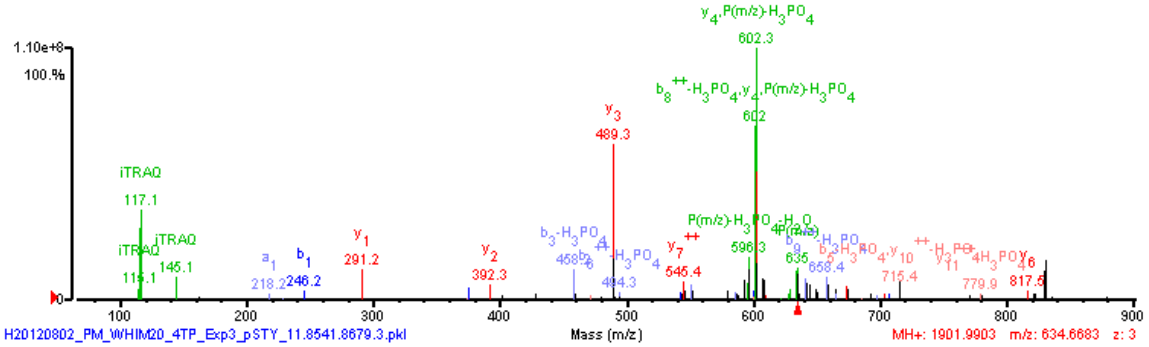

GI-number	Protein name	Gene name	Phosphosite	Sequence
47519639	Microtubule-associated protein 4 isoform 1	MAP4	S941	VGsTENIKHQPGGGR

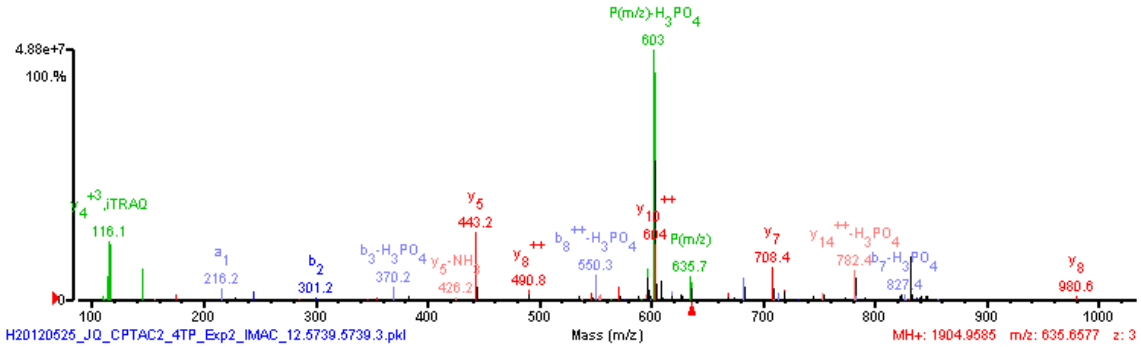

GI-number	Protein name	Gene name	Phosphosite	Sequence
224994221	SH3 domain-binding protein 2 isoform b	SH3BP2	S484	SFsFEKPR

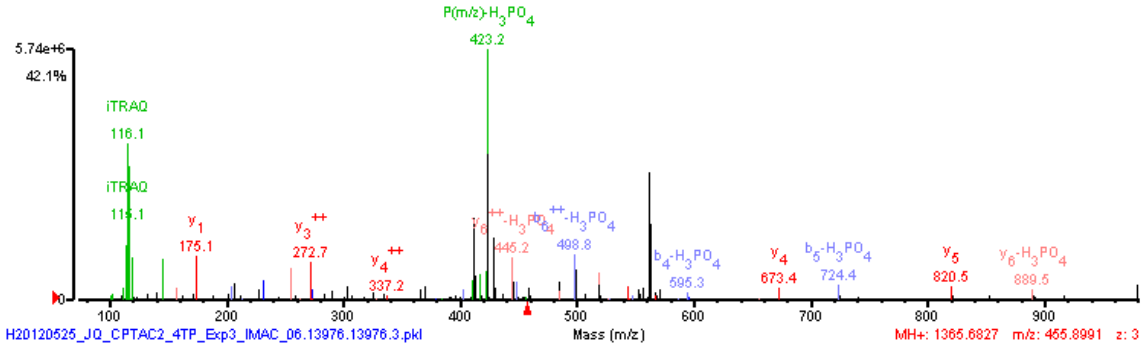

GI-number	Protein name	Gene name	Phosphosite	Sequence
30089916	Phosphofurin acidic cluster sorting protein 1	PACS1	S519	QLsKPLSER

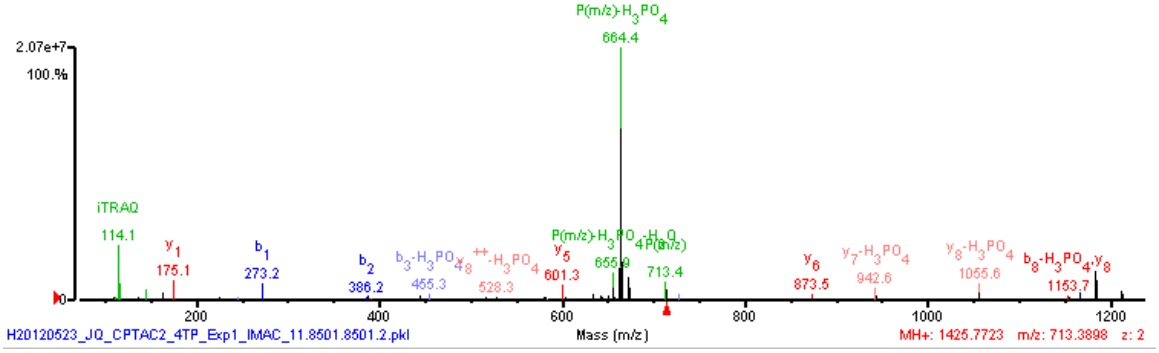

GI-number	Protein name	Gene name	Phosphosite	Sequence
62198235	Drebrin-like protein isoform b	DBNL	T291	QLtQPETHFGREPAAAISRPR

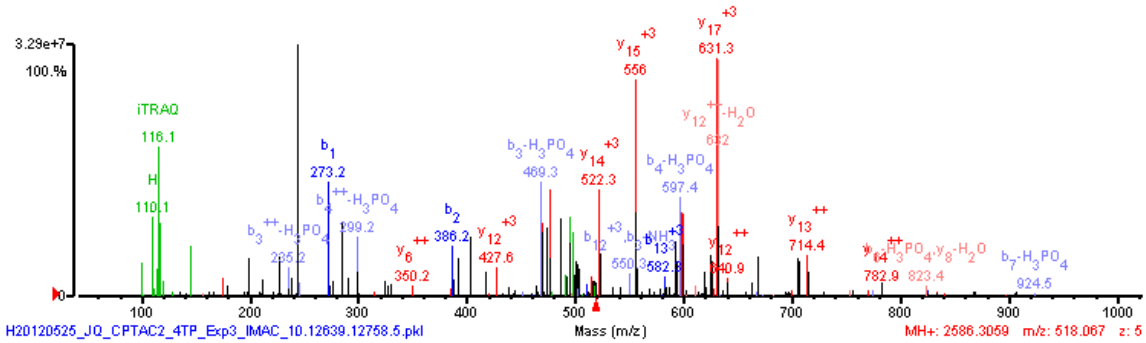

GI-number	Protein name	Gene name	Phosphosite	Sequence
156766050	Protein AHNAK2	AHNAK2	S842	FKMPsFGVSAPGK